An Investigation on Metal Assisted Transformations in Schiff Bases Containing Pyridyl Groups and Transition Metal Chemistry of 4′-(2-Pyridyl)-2,2′:6′,2″-Terpyridine

A Dissertation Submitted
In Partial Fulfillment of the Requirements
For the Degree of
DOCTOR OF PHILOSOPHY

by

Sumanta Kumar Padhi
Roll No. 04612209

Department of Chemistry
Indian Institute of Technology Guwahati
Guwahati – 781 039

June 2008

DEPARTMENT OF CHEMISTRY
INDIAN INSTITUTE OF TECHNOLOGY GUWAHATI

DECLARATION

I hereby declare that the work embodied in this Dissertation entitled ‘‘**An Investigation on Metal Assisted Transformations in Schiff Bases Containing Pyridyl Groups and Transition Metal Chemistry of 4′-(2-Pyridyl)-2,2′:6′,2″-Terpyridine**’’ has been carried out by me in the Department of Chemistry, Indian Institute of Technology Guwahati, under the supervision of Dr. V. Manivannan.

In keeping with the scientific tradition, due acknowledgement has been made, wherever the work done by others has been utilized.

(Sumanta Kumar Padhi)
Roll. No. 04612209
Department of Chemistry
Indian Institute of Technology Guwahati
Guwahati–781039

Date

DEPARTMENT OF CHEMISTRY
INDIAN INSTITUTE OF TECHNOLOGY GUWAHATI

CERTIFICATE

It is certified that the work contained in the Dissertation entitled "**An Investigation on Metal Assisted Transformations in Schiff Bases Containing Pyridyl Groups and Transition Metal Chemistry of 4′-(2-Pyridyl)-2,2′:6′,2″-Terpyridine**" submitted by **Mr. Sumanta Kumar Padhi** to the Indian Institute of Technology Guwahati for the award of the degree of Doctor of Philosophy has been carried out under my supervision in the Department of Chemistry, Indian Institute of Technology Guwahati. This work has not been submitted elsewhere for the award of any other degree.

(Dr. V. Manivannan)

Date

Associate Professor
Department of Chemistry
Indian Institute of Technology Guwahati

DEPARTMENT OF CHEMISTRY
INDIAN INSTITUTE OF TECHNOLOGY GUWAHATI

CERTIFICATE OF COURSE WORK

This is to certify that Mr. Sumanta Kumar Padhi, Roll. No. 04612209 has satisfactorily completed all the course requirements for the degree of Doctor of Philosophy in Chemistry. This course includes:

Semester I (*July-Nov*, 2004)

CH-603: Supramolecules: Concepts and Application
CH-621: New Reagents for Organic Synthesis

Semester II (*Jan-May*, 2005)

CH-601: Physical Methods in Chemistry
CH-632: Advanced Group Theory and Application

(Prof. A. T. Khan)
Head
Department of Chemistry
Indian Institute of Technology Guwahati
Guwahati–781039

(Dr. A. K. Saikia)
DPPC Secretary
Department of Chemistry
Indian Institute of Technology Guwahati
Guwahati–781039

Dedication

A work, which by its utility is dedicated to the furthering of human knowledge or quality of living, to a single person, even more so if that person were a beloved from whose immediate presence the researcher was torn again and again to indulge at the bosom of another muse. Be causative of this, I would like to dedicate the present work to

My

"*Parents and Elder Brothers*"

Whose blessings, relentless effort and sacrifice have allowed taking ever greater steps in exploring the unknown.

Acknowledgement

This Dissertation is the result of about three and half years of work whereby I have been accompanied and supported by many protagonists. It's a pleasant aspect for earning the opportunity to convey my gratitude towards them.

I am extremely grateful to my guide Dr. V. Manivannan for his patient guidance and encouragement throughout the doctoral degree course. As my mentor his insight, observations and suggestions helped me to establish the overall direction of research and contributed immensely to the success of present work. The research hadn't been possible without his brotherly affections, valuable support and advices.

I am very much thankful to my doctoral committee members Dr. Manabendra Ray, Prof. A. T. Khan, Dr. G. Krishnamoorthy and Prof. B. K. Patel for their valuable discussions and cooperation. I am thankful to all the faculty members of Department of Chemistry for providing a comfortable and active environment for pursuing my research.

I am grateful to Dr. S. Ravi for his cordial help for providing the AC susceptibility measurements facility.

I would like to extend my pleasure to SAIF IIT Madras, CDRI Lucknow, IACS Kolkata, CIF IIT Guwahati for providing various facilities and Mr. Babulal Das for collecting the X-ray data of the crystals discussed in this thesis.

My heartiest gratefulness goes towards Rosy for her relentless effort and cooperation during this time span, as well as Sarvanan, Bibhuti, Susanta, Girija, Dipankar, Akshaya, Himansu and Vijendra. I am thankful to my batchmates and departmental friends.

I am grateful to Indian Institute of Technology Guwahati for offering me the opportunity to carry out the present thesis work.

Sumanta Kumar Padhi

Contents

Chapter 1

Introduction

1.1 Schiff bases

Schiff base,[1-3] named after "Hugo Schiff", are the compounds derived from the condensation of primary amine and carbonyl group (aldehyde or ketone), contain an imine or azomethine group (–RC=N–).

This reaction is reversible, progress through a carbinolamine intermediate and often requires the removal of the product water by azeotropic distillation with benzene, to achieve high yields.

1.2 Role of Schiff Bases in Coordination Chemistry

Schiff bases have played an important role in the development of coordination chemistry as they readily form stable complexes with most of the transition metals. The prominent place held in coordination chemistry by metal complexes of Schiff-base ligands has been attested over many years by the large number of publications and by the comprehensive reviews.[4-8] The research field dealing with Schiff base metal complexes has expanded enormously, and embraces very diversified subjects comprising vast areas of organometallics, biochemistry, material science, catalysis, encapsulation, activation, transport and separation phenomena, hydrometallurgy, *etc*.[9-13] In Schiff base metal complexes, the environment at the coordination center can be modified by attaching different substituents to the ligand, which provides a useful range of steric and electronic properties essential for the fine-tuning of structure and reactivity. Therefore, Schiff base ligands are among the most fundamental chelating systems in coordination chemistry[14-15] and complexes of both transition and p-block metals based on these type ligands have been shown to catalyze a wide variety of reactions.[16-18] Many ligands have been designed to mimic the function of natural carriers in recognizing and transporting

specific metal ions, anions or neutral molecules and in understanding and reproducing the catalytic activity of metallo-enzymes and proteins.[19-31]

The studies of Schiff bases have been extensively employed and a large variety of planar macrocyclic and macroacyclic ligands have been synthesized to ascertain correctly the role of the different donor atoms, their relative position, the number and size of the chelating rings formed, the flexibility and the shape of the coordinating moiety on the selective binding of charged or neutral species.[32-38] The evolution of these Schiff bases has produced macro-bicyclic ligands obtained in one-step multiple condensation reactions; the cyclic [2+3] Schiff base condensation represents the extension of the [2+2] macrocyclic coordination systems into the third dimension. In addition to the use in the field of molecular recognition, catalysis and transport, these cage molecules are promising in the stabilization of particular species. The nature and disposition of donor atoms in the rigid cage may enhance the stability of unusual oxidation states in the coordinated transition metal ion, while encapsulation may protect normally labile substrate species. This combination of characteristics will eventually permit moisture sensitive chemistry to be carried out in the protected cavity under room temperature and atmospheric pressure. Pendant arm macrocyclic or macroacyclic ligands and their metal complexes have also attracted attention.[39-42] Arms bearing additional potential ligating groups have been introduced at both carbon and nitrogen atoms of macrocycles generally based on polyaza- or polyoxa-donor sets, in order to have modified complexation properties with transition metals relative to the corresponding simple macrocyclic or macroacyclic precursors.[43-47]

At the beginning of 1960's the chemistry of metal template cyclization to form Schiff-base macrocyclic ligands was developed with the aim to obtain not only unsaturated macrocycles but also open systems which would not readily obtained in the absence of metal ions have been formed as unsaturated multidentate ligands. The nature of the obtained ligands has been controlled by choosing appropriate organic precursors

and by the metal ion as template. Mononuclear and polynuclear complexes containing different donor groups along with imine function and with various shapes can be obtained.[48-58]

Since, the focus of a major part of the thesis is on the chemistry of Schiff base containing pyridyl ring and considering the presence large quantum of research reports on Schiff base metal complexes, a restriction is made to cover the literature reports on the chemistry of Schiff base ligands with at least one pyridyl ring attached to it.

1.3 Pyridyl Group Containing Schiff Bases

The general mechanistic scheme for the formation of the Schiff bases is given below.

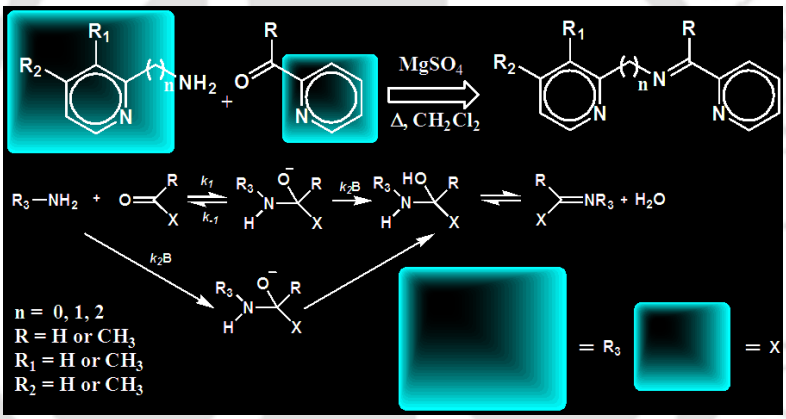

1.3.1 Imines Having an Active Methylene Group and Aldimine/Methylketimine Groups

The 2-pyridyl Schiff base (**SB1a**) and (**SB1b**) were utilized as copper-based catalysts for the 1,3-dipolar cycloaddition of azides and alkynes and found to exhibit significant ligand-accelerated catalysis.[59] The [60]fullerene reacts with azomethine ylides generated from 2- and 4-picolylamines in 1,2-dichlorobenzene to form corresponding fullero-pyrrolidines (*cis*-1,3-di(2-pyridyl)[60]fullereno[1,2-c]pyrrolidine) bearing pyridyl substituents.[60] The azomethine ylides generated from RCH=N–ZH, possessing a range of ZH groups (Z=CHCOPh, CHCOSR, CHCONHR, $CHP(O)(OEt)_2$, 2-CH pyridyl, 2-CH-thiazolyl, and 9-fluorenyl), undergo cycloaddition reactions with dipolarophiles either via an *endo*-transition state or via both *endo*- and *exo*-transition states to give polyfunctional pyrrolidines.[61] These ligands along with metal are useful catalysts for the synthesis of a copolymer derived from the living radical polymerization of one or more acrylic monomers in the presence of the initiator containing a halogen containing polymer or copolymer having at least one initiator.[62] A controlled polymerization of certain monomers with an expanded range of transition metals as the function of counterion and these imines are useful for the preparation of novel polymeric materials.[63] Well-controlled polymerization were obtained for styrene, methyl acrylate and methyl methacrylate using this ligand in copper-mediated ATRP.[64] **SB1a** is also useful as a synthon for the synthesis of 2,4,6-trisubstituted pyridines. This involves deprotonation of **SB1a** with LDA, [3+3] annulation with 2-azaallyl anion generated from 1, 3 dipolar iodosilane leading to a piperazine derivative and its oxidation with mercuric acetate in acetic acid.[65] The synthesis of a unique redox asymmetric dinuclear Rh(-I,I) complex of **SB1a** and its reaction with O_2 leading to O atom transfer to a benzylic group ligand has been reported recently.[66]

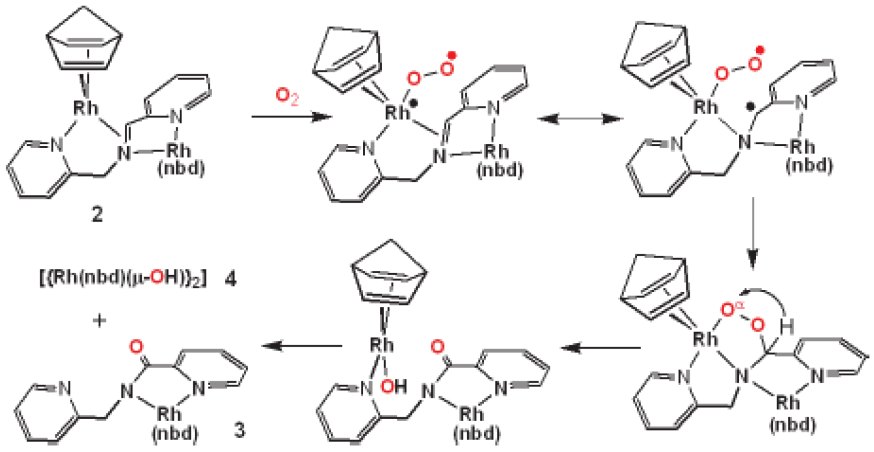

The iron(II) and cobalt(II) chemistry of **SB1a** have been studied along with other tridentate nitrogeneous ligands.[67] The structural and NMR studies on the hexa-coordinated platinum(IV) complexes of **SB1a** and **SB1b** having the composition, [Pt(I)Me$_3$(**SB1a**)] and [Pt(I)Me$_3$(**SB1b**)] were found to have the bidentate coordination nature of the Schiff bases. The imine-N and the N-atom of the pyridine attached to the imine function are bound to the Pt(IV) ion.[68]

The imines **SB1a**–**SB1o** was synthesized by hydrogenation of 3-cyanopyridine and amines in the presence of a Rh-loaded catalyst.[69]

The synthesis of the Schiff bases (**SB1l–SB1m**) and their functions as a tridentate ligand with Cu salts were studied and substituents adjacent to the donor N-atom sequence are found to lower their capacity to coordinate with Fe salts.[70] The Schiff base ligands (**SB1n-SB1q**) made by condensing either 2-acetylpyridine, 2-or 8-quinolinecarboxaldehyde, or o-methylthiobenzaldehyde with either N,N'-dimethyl-1,3-diaminopropane, 2-aminomethylpyridine, or 2-(2-aminoethyl)pyridine, gave ionic Pt(IV)Me_3 complexes containing tridentate NNN- or SNN-bonded ligands.[71] The Zn^{II} and Cd^{II} complexes of **SB1a** and **SB1p** containing nitrate ions as coligands were synthesized and characterized by structural and thermogravimetric studies.[72]

Iminopyridines (**SB1i**) act as efficient bidentate ligands for the palladium(II)-catalyzed cyclization of (*Z*)-4'-acetoxy-2'-butenyl 2-alkynoates in acetic acid to afford the α-(*Z*)-acetoxyalkylidene-β-vinyl-γ-butyrolactones. The iminopyridine ligands could not only inhibit β-hydride elimination but also stabilize the vinyl-palladium intermediate in acetic acid in the reaction.[73] The insertion reaction of acetonitrile on aryl nickel complexes stabilized by this type of bidentate N,N'-chelating ligands were also reported.[74] (2-pyridyl-phenylmethyl)imine (**SB1i**) acts as bidentate Schiff-base ligand and its Cu as well as Mn complexes containing chloride bridging is reported.[75] Multidentate ligands can also be prepared from the corresponding reduced amine through an efficient microwave heating method.[76]

In the metal-catalyzed cross-coupling scenario, Sonogashira reaction and oxidative dimerization of terminal alkynes, are the most relevant and attractive C–C bond forming transformations. The homocoupling reactions of substituted acetylenic derivatives are concomitant to the Sonogashira pathway and time-consuming optimization procedures are required in order to reach satisfactory levels of selectivity. The potential of a class of Pd complexes of 2-pyridylphenylcarbaldimine (**SB1i**) (loaded to mesoporous silica gel promotes the Sonogashira reaction between arylacetylenes and iodoarenes is underlined.[77]

2-pyridylphenylcarbaldimine (**SB1i**) was used to prepare α-aminoamide by its reaction with carbamoylsilane, in the presence of BF_3 etherate,[78] and indium-mediated Barbier-type allylation of **SB1i** is useful for the preparation of homoallylic amines in

alcoholic solvents.[79] Appropriate mixtures of Br-TMS and tri-methylphosphite or tri-ethyl phosphite are effective reagents for phosphorylation of aldimine (**SB1i**) and generates aminophosphonic acids, or corresponding dialkyl or monoalkyl esters, respectively.[80] The Schiff bases derived from RCHO (R = 2-, 3-, 4-pyridyl) and $PhCH_2NH_2$ on reaction with phosphonates, $HP(O)(OR')_2$ (R' = Ph, $PhCH_2$), form corresponding heterocyclic aminophosphonates, e.g., $RCH[P(O)(OR')_2]NHCH_2Ph$.[81] Imines like (**SB1a** and **SB1i**) are used for the preparation of chelating resins containing an α-aminopyridylphosphonic acid.[82] A few of these imines are also used for synthesis of five-membered heterocycles containing a nitrogen-oxygen bond *via* O-acylation of aliphatic nitro compounds.[83] The transposition of the imine function was achieved by treatment with excess $LiN(CHMe_2)_2$ and subsequent acidification using oxalic acid in aqueous MeOH.[84] Ketones were prepared by the oxidative deamination of amines through, condensation of the amines with 2-pyridinecarboxaldehyde, oxidation of the resulting imines with *m*-CPBA to oxaziridines and ring opening of the oxaziridines with KOH.[85]

Synthesis, spectroscopic and magnetic characterization of the mixed-tris chelates of Ru(II) and Ru(III) with **SB1i** are reported.[86] The facial and meridional isomers of $[Mo(CO)_3\{P(OEt)_3\}\{C_5H_4NCH=NCH(Me)Ph\}]$ has been characterized by ^{1}H, ^{13}C, ^{31}P, ^{95}Mo NMR spectroscopy.[87] Copper complexes of Schiff base ligands derived from pyridine- 2-carboxaldehyde and 6-methylpyridine-2-carboxaldehyde with benzylamine has been prepared and characterized by spectroscopic methods.[88] The effects of a polymer matrix on the substitution reactions of $Mo(CO)_6$ with chelating ligand N-phenylpyridinaldimine, under photochemical conditions are reported.[89] The LaPorte forbidden spectra, in Ni(II) octahedral complexes of **SB1i** is interpreted in terms of ligand

field theory.[90] Transfer hydrogenation of imines to the corresponding amines by Et_2CHONa catalyzed by the mono-coordinate Ni(0)/N-heterocyclic carbene species has also been studied.[91] In presence of phase-transfer catalyst, Bu_4NBr, the anion derived from the imine **SB1j** reacted with alkyl halide, to form alkylated products **SB1j(2)** (R = CH_2Ph, $CH_2C_6H_4OMe$-4, $CH_2C_6H_4Cl$-4, Bu, allyl), the hydrolysis of **SB1j(2)** gave α-alkyl-2-pyridylmethylamines **SB1j(3)**.[92]

The reaction of the bidentate ligands, (**SB1r-SB1t**; R = H / Me) with Zeise's salt were studied and the products were characterized by spectroscopic and diffraction studies.[93]

The reaction of $[RuCp(\mathbf{L})(CH_3CN)_2]PF_6$ (**L** = CH_3CN, PMe_3, $SbPh_3$) with 1 equivalent of py-N:CHR [R = Ph, Fc (ferrocenyl), Np (naphthyl)] afforded the cyclic aminocarbene complexes $[RuCp(\mathbf{L})(:C(R)NH\text{-}py)]PF_6$, whereas when L = PPh_3, $PiPr_3$, and CO the reaction stopped at the stage of the imine complex $[RuCp(L)(\mathbf{SB1u})]PF_6$.[94]

The effect of (**SB1u**) on the stability of regular gasoline, with respect to their oxidative degradation hydrocarbons by traces of metals, is examined.[95] The inter- and

intramolecular coupling of a variety of imines (including **SB1v**) to *syn* and *anti* 1,2-diamines, promoted by samarium diiodide and Lewis acids or by Zn/MsOH was studied. The metal complexes of these 1,2-diamines are useful in asymmetric catalysis.[96]

1.3.2 Schiff Bases Having an Ethylene Group and Imine Function

Methylpalladium compounds, [Pd(**SB2a**)(Me)(Y)], [Pd(**SB2b**)(Me)(Y)] and [Pd(**SB2c**)(Me)(**Y**)] (**Y** = Cl^-, $CF_3SO_3^-$, 4-$MeC_6H_4SO_3^-$) were synthesized and characterized by spectroscopic methods. The CO insertion across the Pd–CH_3 bond to a Pd–$C(O)CH_3$ and olefin insertion across the Pd–C(O) bond in Pd–$C(O)CH_3$, in all the above noted compounds were described.[97] The Pd(II) compounds of **SB2a** and **SB2b**, have been synthesized by reacting them with [Pd(COD)(CH_3)(Cl)]. The structural and NMR studies of the complexes were also reported.[98]

The compounds of the formula, [Cu(**SB2a**)Cl](PF_6)·nH_2O [n = 0 and 1] and [Cu(**SB2a**)Br](PF_6), were synthesized and the crystal structures determined. The chloro complexes are reported to exhibit weak antiferromagnetic interactions, while the bromo one is ferromagnetic.[99] The *homo* and *hetero* metal-metal bonded compounds of the type, *fac*-$(CO)_5MM'(CO)_3$(**SB2a**) (M, M' = Mn, Re) in which **SB2a** bidentately (N,N) coordinated to the metal center M' were synthesized and their photochemical reactivity were described.[100] Low-spin [Fe(**SB2b**)$_2$]$(ClO_4)_2$·3H_2O was prepared and are reported to have a higher Fe^{III}/Fe^{II} reduction potential compared to that of the $[Fe(\mathbf{bpy})_3]^{2+}$ ion.[101] The powder diffraction studies on [Cu(**SB2d**)XY]·nH_2O; X = I^-, N_3^-; Y = I^-, NO_3^-, PF_6^-; n = 0, 1; are reported.[102] Compounds of **SB2e** are used as seizure-preventing agents and can be coated on a fixed head-type magnetic record-reproducing apparatus, having magnetoresistive-type heads and/or induction-type thin-film heads, magnetic recording media and/or cleaning tapes.[103]

New phosphonate mono-Me esters (**SB2f**) which are designed to have properties intermediate between the acid and the diesters and thus able to form discrete metal complexes with enhanced solubility in water, were synthesized using (**SB2g**) as starting reagent.[104] The Mg^{2+} catalyzed reduction of the imines by 3,5-diethoxycarbonyl-2,6-dimethyl-1,4-dihydropyridine, has been studied as an NAD(P)H model.[105]

Copper complexes of Schiff base ligands derived from pyridine- 2-carboxaldehyde and 6-methylpyridine-2-carboxaldehyde with 2-phenylethylamine has been prepared and characterized by spectroscopic methods.[88] Complexes of Hg(II), Sn(II), Pb(II) and Zn(II) with 1,2-glyoxilidine-bis-2-aminoethylpyridine were synthesized and characterized by physicochemical methods.[106] Cr(III), Co(II), Ni(II), Cu(II) and Cd(II) were also

synthesized with **SB2i**. An octahedral geometry is proposed for the Cr(III) and Ni(II) complexes and tetrahedral geometry for the rest.[107]

Cu(I) complexes having the formula $\{[Cu_2(\mathbf{SB2j})(PPh_3)_2]BF_4\}_n$, $[Cu_2(\mathbf{SB2l})(PPh_3)_4I_2]$, and $[Cu_2(\mathbf{SB2k})(PPh_3)_2I_2]$ were prepared by reactions of Schiff base ligands with PPh_3 and Cu(I) salt and the first two complexes are reported to exhibit photoluminescence in the solid state at room temperature.[108]

A triphenylphosphine reagent linked to linear polystyrene, has the reactivity superior to that of the phosphine bound to cross-linked polystyrene, reacted very rapidly with azides to generate iminophosphoranes which could then react with aldehydes to generate these imines in good yields and high purities.[109] The crystal structure of the complex, $[Cu_2I_2(\mathbf{SB2i})((C_6H_5)_3P)_2]\cdot 2MeCN$ contain two Cu(I) ions are bridged by one **SB2i**.[110] $[Ag_2(\mathbf{SB2i})_2](ClO_4)_2$, was also synthesized and structurally characterized by single-crystal X-ray diffraction and contain the **SB2i** ligand coordinating *via* four N atoms to two silver(I) centers. The complex has a double-helical structure with the two silver ions in distorted square pyramidal environments.[111] Syntheses and crystallographic characterization of $\{[Cd_2(\mu\text{-}\mathbf{TP})_2(\mathbf{SB2n})_2]\cdot 9H_2O\}$ and $\{Cd(H_2O)(\mathbf{SB2o})\}_2(\mu\text{-}\mathbf{TP})](\mathbf{TP})\cdot 10H_2O$; **TP** = benzene-1,4-dicarboxylate and that of the $[Cd(\mathbf{SB2o})(NCS)_2]$ were reported. [112-113] The synthesis brown colored bis-chelate complexes $[Ni(\mathbf{SB2o})](ClO_4)_2$ along with their magnetic as well as redox properties were known.[114]

The reactions of $Mn(NO_3)_2\cdot 6H_2O$ with the tetradentate Schiff bases N,N'-bis[1-(pyridin-2-yl)ethylidene]ethane-1,2-diamine and N,N'-bis[1-(pyridin-2-yl)benzylidene]ethane-1,2-diamine affords the eight-coordinate complexes $[Mn(NO_3)_2(L)]$ which were characterized by x-ray crystallographically.[115]

The structural studies on $[Pr(NO_3)_3(\mathbf{SB2o})]$, revealed the presence of a deca-coordinated Pr(III) and the Gd(III) analog was characterized by spectroscopic methods.[116] $[Zn(\mathbf{SB2o})Cl_2]$ and $[Zn(\mathbf{SB2o})Br_2]$ were also synthesized and their structures are reported.[117] Spectroscopic characterization of $[Cu(\mathbf{SB2o})(ONO_2)(H_2O)](NO_3)$ are also known.[118] The use of **SB2o** and its analogs, N,N'-bis(2-pyridylmethylidene)-1,2-diiminoethane and

N,N'-bis(2-pyridylmethylidene)-trans-1,2-diiminocyclohexane, as complexation reagents for ion-pair extraction of divalent transition metal cations into nitrobenzene with picrate anion, as well as, in the treatment of hypertension in animals, has been investigated.[119-121]

1.3.3 Schiff Bases Having an Imine Function Only

The formation of the Schiff base product of 2-, 3-, 4-pyridinealdehydes and 6-methylpyridine-2-aldehyde with 2-aminopyridine and its 3-, 4-, and 6-Me derivatives, in benzene in the presence of molecular sieves was studied.[122] The ^{1}H, ^{13}C and ^{15}N NMR analyses for a series of diaryl-aldimines containing Ph, pyridyl, pyrazolone and furanyl moieties are described.[123]

Addition of compounds with a P–H bond to Schiff bases of both simple and macrocyclic compounds are also described.[124] Synthesis and characterization of [Ga(**SBa**)$(CH_3)_2$] complexes are reported.[125] The synthesis of aminopyridin-2-ylmethylphosphonic acids and their di-ethyl, starting from the corresponding Schiff base as precursors, were studied.[126] Benzaldimines **SB(i)** (R = Ph, ClC_6H_4, HOC_6H_4, $O_2NC_6H_4$, $Me_2NC_6H_4$) were converted to thiazolidinones **SB(ii)**, which are useful as anticonvulsants and local anesthetics.[127]

The electro-reduction of $R_1HC{=}NR_2$ [R_1 = 2-, 3-pyridyl, R_2 = 2-pyridyl] in CO_2-saturated DMF-Bu_4NI at potentials markedly more positive than CO_2 give $R_1CH(CO_2Et)NHR_2$ and traces of $R_1CH_2NR_2CO_2Et$.[128] The use of 2-(2-pyridylmethyleneamino)phenol, as a reagent for spectrophotometric determination of scandium is described.[129] The formation of heterocyclic thioamides from alkylpyridines, heteroaromatic amines and sulfur was investigated.[130] Reduction of the azo- and other

unsaturated linkages by hydrogenase from *Azotobacter vinelandii* and *Desulfovibrio desulfuricans*, was studied.[131] *Syn* and *anti* isomers of **SBa** are studied by IR and NMR spectroscopy.[132] The inhibiting effect of Schiff bases containing pyridyl group, 2-((1*E*)-1-aza-2-(2-pyridyl)vinyl)benzene-1-thiol, (1*E*)-1-aza-1,2-di(2-pyridyl)ethene, [((1*Z*)-1-aza-2-(2-pyridyl)vinyl)amino]benzene-1-thione and 2-((1*E*)-1-aza-2-(2-pyridyl)vinyl)benzo-thiazole, was studied on the corrosion of low C steel in 0.1M HCl solution under various conditions by potentiodynamic polarization method and impedance measurements.[133] Chemical reactivity of radicals generated from pyrolysis of thermally labile diaryltriazene 1-oxides with thiophene was reported.[134] The addition of hydrosilanes ($HSiEt_3$, $HSiMe_2Ph$, H_2SiPh_2) to the CH=N bond of heterocyclic azomethines has been studied in the presence of monovalent complexes of rhodium and palladium.[135] The electronic absorption spectra of some heterocyclic compounds consisting of two rings joined through an imino group have also been investigated.[136] **SBu** complexes of Al^{3+}, Ga^{3+}, In^{3+}, Sc^{3+}, Cd^{2+}, Be^{2+}, Zn^{2+}, Zr^{3+}, etc., are evaluated as agents for converting UV light of 280-400 nm, into blue light of 400-500 nm.[137] Neutral P(II) complexes of **SBm** synthesized and structure is proposed from chemical analysis, electrical conductivity and IR studies.[138]

The Co(II), Ni(II), Cu(II) complexes of **SBu** and two other related ligands were prepared and characterized by IR spectroscopy.[139] The clay montmorillonite K10 has been used as a reusable co-catalyst in the synthesis of **SBv** and **SBw** from the respective aldehydes

and amines, which are then transformed into the ketone through the hydroiminoacylation reaction, in the presence of $[Rh(PPh_3)_3Cl]$.[140] Reactions of haloketenes ($Cl_2C=CO$; IClC=CO) with different 2-arylideneaminopyridines (**I**), was employed to prepare the products **II–V**.[141]

The spectroscopic (IR, UV, NMR, and mass) and thermal properties of **SBy** (R = 4-Me, 6-Me; R_1 = H, OH) were examined, the relation of their acidity constants to their stereochemistry were reported.[142]

A compound comprising iron, **SBj** and an activator is used as a single-site olefin polymerization catalyst.[143] The synthesis and absorption spectra of many of the ligands (**SBa-SBz**) are also discussed.[144] Rhodium(I)-catalyzed Heck-type coupling reaction involving carbon-heteroatom double bonds between aryl halides with N-pyrazyl aldimines is reported.[145] The synthesis of **SBz(i)** by the coupling of (α-chloroalkyl)oxazolinyllithium compounds with diheteroaryl imines was investigated.[146]

The Pt(II) complex of **SB(O)** and its reactivity of the complex with acetone was elucidated with spectroscopic and structural studies.[147] Two ternary copper(II) complexes [Cu(pyp)X] with the tridentate Schiff base 2-(picolinylideneamino)phenol (Hpyp) and halide (X = Cl^-, Br^-) were synthesized and characterized by single-crystal x-ray diffraction.[148] Mono-, tri- and dinuclear neutral complexes [Ni(**SB(OH)**)(**SB(O)**)]$(ClO_4)\cdot 0.16H_2O$, [Zn**(SB(O))**$Zn(OOCCH_3)_4$Zn**(SB(O))**] and [Cd_2**(SB(O))**$_2(CH_3\ CO_2)_2(H_2O)_2$] were obtained from the reaction between the **(SB(O))** with Ni, Zn or Cd salts, respectively.[149] Tetranuclear Mn(II) compound, [Mn_4**(SB(O))**$_6$]$(ClO_4)_2$ was synthesized and characterized structurally and magnetically.[150] The synthesis of homoallylic amines, **SB(O)1** was achieved from **SB(O)** when reacted with allyltrichlorosilanes, in the presence of DMF, HMPA, or pyridine N-oxide as a neutral coordinate-organocatalyst.[151]

Heterocycles **SB(O)2** (R = H, Me, Me_3C; pyridyl ring attached at the 2-, 3-, or 4-position) were prepared in excellent yields by oxidative cyclization of phenolic Schiff

bases with thianthrene cation radical perchlorate in the presence of 2,6-di-tert-butyl-4-methylpyridine.[152]

[Cr(**SB(O)a**)(bipy)(Cl)] and [Cr(III)(**SB(O)b**)(bipy)(Cl)]$^{+}$ complexes were prepared and characterized by physico-chemical methods. The complexes were used as catalysts in the oxidation of both saturated and unsaturated hydrocarbons using ^{t}Bu hydroperoxide.[153] Single site catalyst systems based on pyridine-iminophenol, pyridine-iminoalcohols or pyridine-iminoamine complexes are suitable for oligomerizing or homo- or co-polymerizing ethylene and alpha-olefins.[154] A series of neutral and cationic methylplatinum(II) hemi-labile complexes with 2-pyridinecarbaldimine, N-oxyalkyl- and N-oxyaryl-2-pyridinecarbaldimine ligands has been prepared.[155]

$TiCl_4$(**SB(O)c**) and related compounds were prepared and IR, ^{1}H NMR data were used to assign structures for them.[156] The Co(III) complex, [Co(**SB(S)**)$_2$]Cl (1), was synthesized and characterized by x-ray crystallography.[157] Monobasic bidentate benzothiazolines, prepared by reaction of 2-mercaptoaniline with heterocyclic aldehydes, were found to have fungicidal activity.[158]

1.4 4′-(Pyridyl)-2,2′:6′,2″-Terpyridine and its Transition Metal Chemistry

1.4.1 A General View About Terpyridine

Polypyridyls are the bases in which two or more pyridine rings are linked (but not fused) together. Terpyridine (tpy) has three linked pyridine rings and became one of the most important tridentate ligands in coordination chemistry since the report of its synthesis[159–160] and subsequently substituted analogs have been reported.[161] Metal complexes of terpyridines have versatile applications, *viz.*, DNA binding ability,[162] cytostatic activity,[163] topoisomerase I inhibitory activity,[164] supramolecular chemistry,[165–166] enantioselective synthesis,[167–169] fluorophores,[170] photo-induced light harvesting.[171–172] Reviews describing the syntheses of terpyridine, its higher homologues and its derivatives having aromatic and aliphatic ring substituents have appeared.[173–174] The transition metal chemistry of terpyridine itself is vast and the details are not described further.

1.4.2 4′-(Pyridyl)-2,2′:6′,2″-Terpyridine

The substitution at the 4′ position of terpyridine with different groups could lead to new multidentate ligands. The synthesis of 4′-(pyridyl)-2,2′:6′,2″-terpyridine was first reported by Kröhnke.[175] The method involves the condensation of 2-acetylpyridine and appropriate aldehyde, Michael addition of the condensation product with another molecule of 2-acetylpyridine forming a diketone, followed by the ring closure reaction of the diketone with ammonium acetate and acetic acid.

Recently a green method of Kröhnke procedure in poly(ethyleneglycol) has been reported.[176] The metal chemistry of 4′-(pyridyl)-2,2′:6′,2″-terpyridine has been studied by various groups and are detailed below.

1.4.3 4′-(2-Pyridyl)-2,2′:6′,2″-Terpyridine (L3)

Complex of the type [Pt(**L3**)(4-picoline)]$^{2+}$ are reported to be irreversible inhibitors of trypanothione reductase from *Trypanosoma cruzi*, the causative agent of Chagas' disease.[163] **L3** itself is shown to have antitumor cytotoxicity against several human cell lines and topoisomerase I inhibitory activity.[164]

Mixed-valent rectangular grid-type coordination polymers based on Cu(I)/Cu(II) and **L3** are structurally characterized.[177] The homoleptic complex [Ir(**L3**)$_2$]$^{3+}$, display structured emission with luminescence lifetimes of about 1 μs.[178] The coordination compounds with different nuclearity, has been made in the hydrothermal conditions using Cu(I) reagent and **L3**.[179] Supramolecular copper complexes of **L3**, stabilized through C–H···O, C–H···N, C–H···O and O–H···O interactions as well as π–π stacking are reported.[180] Cadmium complexes of composition, [Cd$_2$(**L3**)$_2$(N$_3$)$_4$] and [Cd$_2$(**L3**)$_2$(SCN)$_4$] have been synthesized and characterized by luminescent spectroscopy as well as structural studies.[181] The syntheses and structures of [Cu(NCS)(**L3**)]SCN and [Ag$_2$(**L3**)$_2$](PF$_6$)$_2$ were reported and in [Cu(NCS)(**L3**)]SCN, the Cu atom is

four-coordinated by a tridentate chelating **L3** ligand and one isothiocyanate group in a square-planar coordination geometry.[182–183] The mononuclear complexes [Cr(**L3**)Cl_3]·DMF, [Cr(**L3**)$(N_3)_3$]·CH_3CN and and [Cr(**L3**)$(NCS)_3$]·DMF were synthesized from $CrCl_3.6H_2O$ and in presence of catalytic amount of zinc powder and were characterized by IR, UV-Vis, fluorescence, EPR spectroscopic and X-ray crystallographic studies.[184]

1.4.4 4′-(3-Pyridyl)-2,2′:6′,2″-Terpyridine (L3′)

An alternative, solvent free grinding method of synthesis of **L3**, **L3′** and **L3″**, as well as other related ligands was devised by Raston.[185-186] Coordination polymers of cadmium complexes of **L3′**, $\{[Cd_3(\mathbf{L3'})_2(SCN)_6](THF)_2\}_n$ and $[Cd_2(\mathbf{L3'})(CH_3OH)Cl_4]_n$ have been synthesized and characterized by luminescent spectroscopy as well as structural studies.[181] Reaction **L3′** with MeI in acetonitrile results in the *N*-methylation of the 4′-(3-pyridyl) group and the Ir(III) mixed ligand complex (shown below) is reported to display long-lived luminescence in solution and is

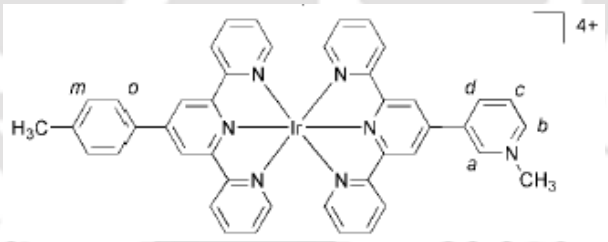

quenched by the chloride ions.[187] The synthesis and structural characterization of metallotecton of the formula [Ru(4′-(3-pyridyl)-2,2′:6′,2″-terpyridine)$_2$]$^{2+}$ is reported.[188]

1.4.5 4′-(4-Pyridyl)-2,2′:6′,2″-Terpyridine (L3″)

L3″ is a versatile member of 4′-(pyridyl)-2,2′:6′,2″-terpyridines, in which the N atom of 4′-(4-pyridyl) is suitably positioned and can be utilized for further coordination or linking. Therefore, the metal chemistry of **L3″** has been investigated more extensively. A one-pot procedure for the synthesis of 4'-(4-pyridyl)-terpyridine using poly(ethyleneglycol) (PEG) as a benign reaction medium is reported.[176] The spectroelectrochemistry of **L3″** were studied.[189] An alternative method for the synthesis of **L3″**, using morpholine enamines derived from α-pyridyl ketones, on reaction with aromatic pyridine-4-carboxaldehyde leading to the formation of a 1,5-diketone intermediate which in turn provides **L3″** was reported.[190] Other methods for the preparation of **L3″**, were also reported.[191–193]

Medicine

The **L3″**, terpyridine and its derivatives are effective in promoting the production of nerve growth factors and neurotrophic factor activity. Hence they can be used as an ameliorant or remedy for the symptoms and diseases accompanying peripheral nerve degeneration which is idiopathic or caused by trauma, chemicals such as alcohol or anticancer drug, inflammation, or metabolites, senile dementia of Alzheimer type, cerebrovascular dementia, Down's syndrome, Parkinson's disease or Hantington's chorea, mental and motor function incompetences caused by cerebral ischemia, cerebral infarction, cerebral hemorrhage or head injury, spinal neuroparalysis, and so forth.[194]

Transition Metal Chemistry

Iron

The one-dimensional coordination polymer $\{(H_2O)(NO_3)_2CuFe(\mathbf{L3''})_2\}_2(NO_3)_4\cdot 2.15\ MeCN\cdot 5.85H_2O]_n$ is assembled when the N-atom of the pendant (4-pyridyl) in $[Fe(\mathbf{L3''})_2]^{2+}$ linked through the $Cu(NO_3)_2(H_2O)$ moiety. In this case, the (4-pyridyl) ring in the $[Fe(\mathbf{L3''})_2]^{2+}$ exemplify as an expanded 4,4′-bipyridine ligand. In the solid

state, the polymer chains are threaded through hydrogen-bonded macrocycles comprising coordinated and non-coordinated water molecules and nitrate ions, the macrocycles being motifs within interconnected sheets in the structure.[195] The protonation of $[Fe(\mathbf{L3''})_2]^{2+}$, generates a trication which forms a one-dimensional, hydrogen-bonded polymer. The structures of the trication $[Fe(\mathbf{L3''})(\mathbf{HL3''})]^{3+}$ were reported with $[Fe(NCS)_6]^{3-}$ and $[ClO_4]^-$ as counter anions. The packing reveals the presence of $\{[Fe(\mathbf{L3''})(\mathbf{HL3''})]^{3+}\}_n$ chains in the solid state in which the conjugate acid of $[Fe(\mathbf{L3''})(\mathbf{HL3''})]^{3+}$ units acts as a self-complementary hydrogen-bonded building blocks.[196]

New terpyridines containing end-functionalized poly(ε-caprolactone)s and poly(L-lactide)s, have been synthesized via Sn(II)-catalyzed ring-opening polymerization of hydroxy- and amino-functionalized Kröhnke-type terpyridines. These form a set of metallo-supramolecules of AA type homopolymers by complexation with Fe(II) ions.[197]

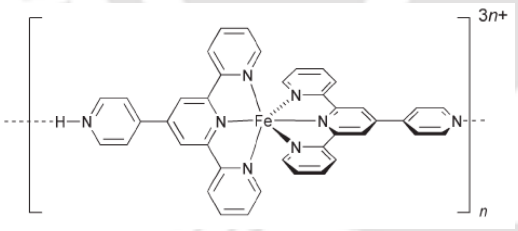

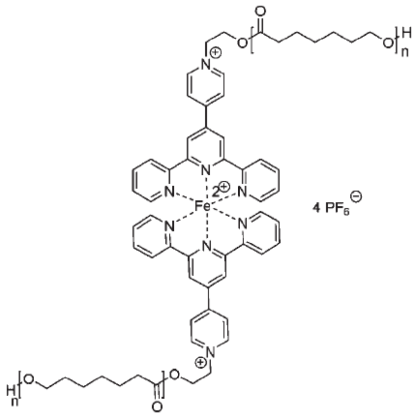

The N-atom of 4'-(4-pyridyl) group of **L3″** is known to react readily with alkylbromides resulting in the formation of a pyridinium ion. This reaction has been utilized in the incorporation of the cationic (dipyridinium)ethane axle into the terpyridine moiety and a self-assembly synthesis is used to create three [2]rotaxanes using 24-membered crown ether wheels: 24-crown-8, dibenzo-24-crown-8 and dinaphtho-24-crown-8 ether. These rotaxanes act as ligands and the bis(tpy) chelate complexes of Fe(II),*viz.,* $Fe([2]rotaxane)_2(triflate)_8$ has been synthesized and characterized by UV-visible absorption spectroscopy of the Fe(II) complexes.[198]

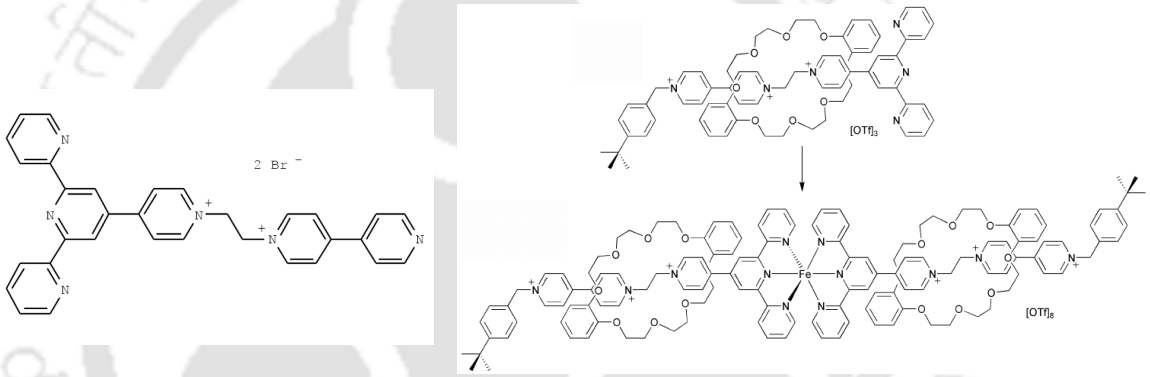

Similarly, the many *N*-alkylated derivatives of **L3″** and its Fe(II) complexes were synthesized. Ferramacrocycles has been prepared in two steps by first reacting bis[4-(bromomethyl)phenyl]methane or 4,4' bis(bromomethyl)biphenyl with two equivalents of **L3″**, and then treating the resulting bis(*N*-alkylated) product with Fe(II) salts. And a dinuclear octacationic box was also assembled.[199-201]

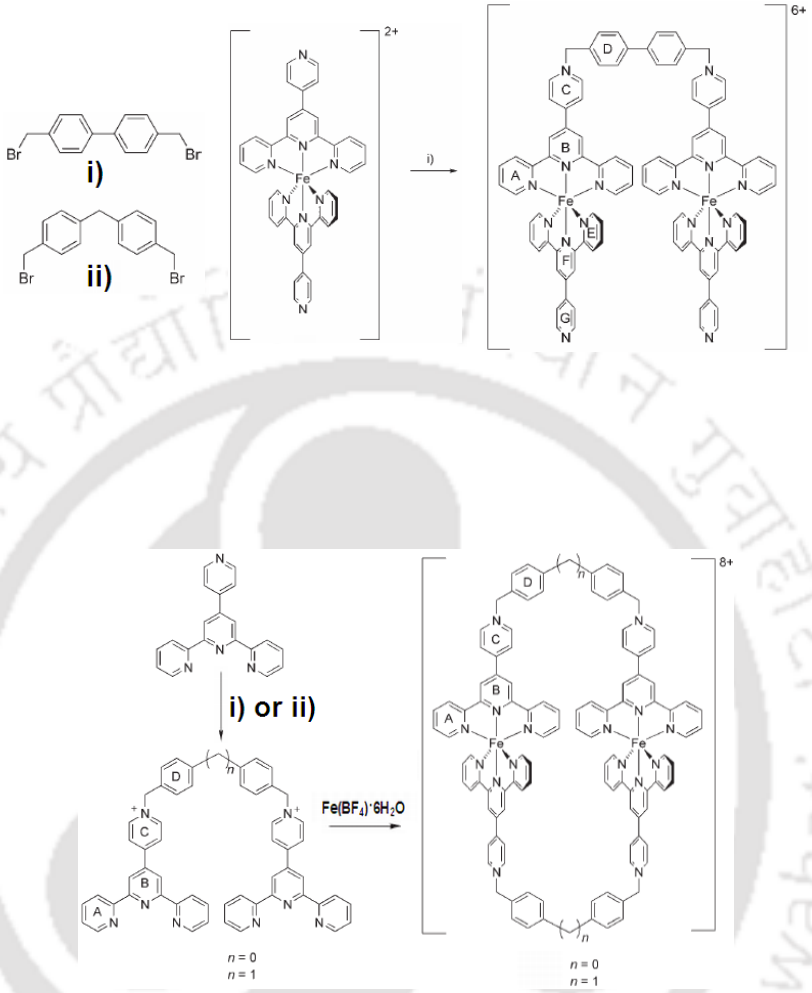

The related ligand, 4'-(4-pyridyl-N-oxide)-2,2':6',2"-terpyridine, in which the 4'-(4-pyridyl) of **L3″** is replaced by a 4'-(4-pyridyl-N-oxide) and its homoleptic Fe(II) bis-complex have been synthesized and structurally characterized.[202]

Ruthenium

The donor properties of **L3″** towards Fe(II), Ru(II) and Os(II) ions and the reactivity of the non-coordinated pyridyl group towards a range of electrophiles that leads to

complexes containing the cationic ligand **HL3″** and 4'-(4-methylpyridino)-2,2':6',2"-terpyridine (mpytpy) were studied.[203] A comparative structural and spectroscopic investigation of the complexes, $[M(\mathbf{L3})_2]^{2+}$, $[M(\mathbf{L3'})_2]^{2+}$ and $[M(\mathbf{L3''})_2]^{2+}$ in which M = Fe or Ru, were reported. The ruthenium complexes are reported undergo mono- and bis-N-methylation.[204] Two trinuclear Ru complexes containing the star-shaped ligands 1,3,5-tris{[4'-(2,2':6',2"-terpyridinyl)-1-pyridiniumyl]methylphenyl}benzene and 2,4,6-tris{[4'-(2,2':6',2"-terpyridinyl)-1-pyridiniumyl]methyl}mesitylene, respectively are synthesized and characterized by NMR, Mass and electrochemical methods.[205]

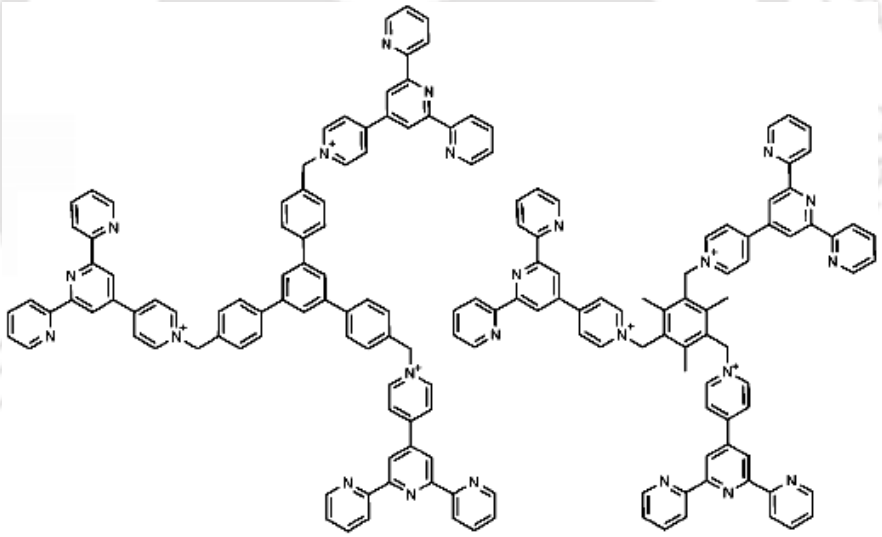

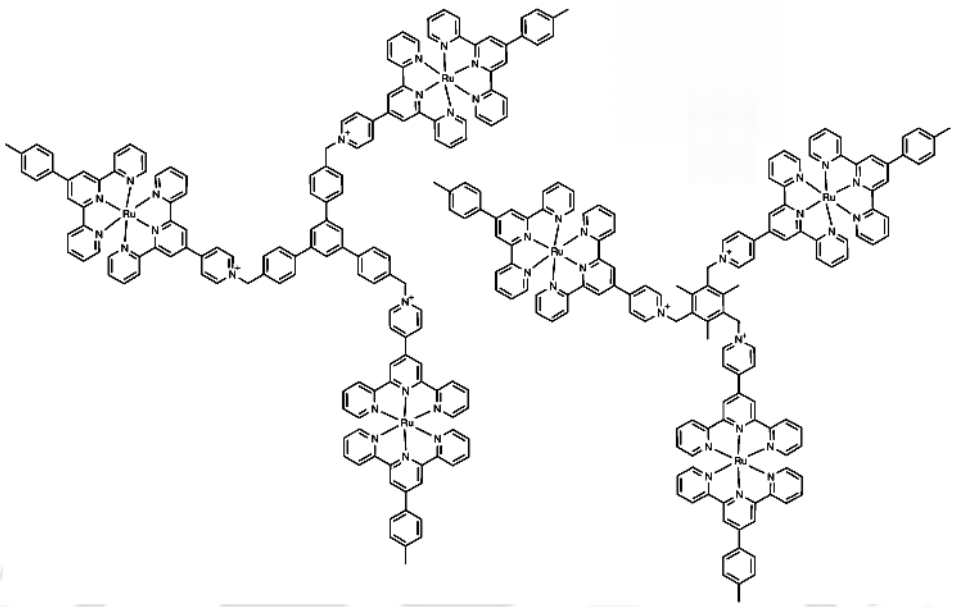

The one-dimensional coordination polymer $\{Ag(NO_3)(CH_3CN)Ru(\mathbf{L3''})_2\}^{2+}$ is assembled when the *N*-atom of the pendant (4-pyridyl) in $[Ru(\mathbf{L3''})_2]^{2+}$ linked through the $Ag(NO_3)(CH_3CN)$ moiety. In this case also, the (4-pyridyl) ring in the $[Ru(\mathbf{L3''})_2]^{2+}$ exemplify as an expanded 4,4′-bipyridine ligand.[206] Monolayers of $[Ru(bpy)_2(\mu\text{-bpytpy})M(\mathbf{L3''})][PF_6]_4$ salts (M = Os, Ru; bpy = 2,2'-bipyridine, bpytpy = 4'-(2,2'-bipyridin-4-yl)-2,2':6',2"-terpyridine were self-assembled on Pt surface and studied by fast-scan electrochemistry.[207] Self-assembled monolayers of $[Ru(tpy)(\mathbf{L3''})]^{2+}$ and $[Os(tpy)(\mathbf{L3''})]^{2+}$ salts on Pt surface were studied by STM and electrochemistry, in which the monolayer are found to be ordered in a hexagonal

array.[208] **L3″** usually behaves as a tridentate ligand towards a metal ion, but in $[Cp^*Ru(PPh_3)(\mathbf{L3''})]BF_4$ and $[(\eta^5\text{-indenyl})Ru(PPh_3)(\mathbf{L3''})]PF_6$, **L3″** is reported to bind to the Ru(II) ion in a bidentate fashion.[209] The mononuclear Ru(BSP)(CO) [BSP = N,N'-bis(3,5-di-tert-butylsalicylidene)-1,2-phenylenediamine] complex acts as a versatile supramolecular synthon, and it spontaneously forms linear and three dimensional assemblies through axial coordination with pyridyl Lewis bases. Using this motif, neutral and charged assemblies with **L3″** were prepared.[210]

A self-assembled octanuclear molecular squares of the type $[fac\text{-}Re(CO)_3Br\mathbf{L}]_4(PF_6)_8$ (**L** = $M(\mathbf{L3''})_2$, M = Fe, Ru, Os) were prepared by the reaction of $ReBr(CO)_5$ with $[ML_2](PF_6)_2$ and characterized by mass spectrometry.[211] Novel heterometallic square

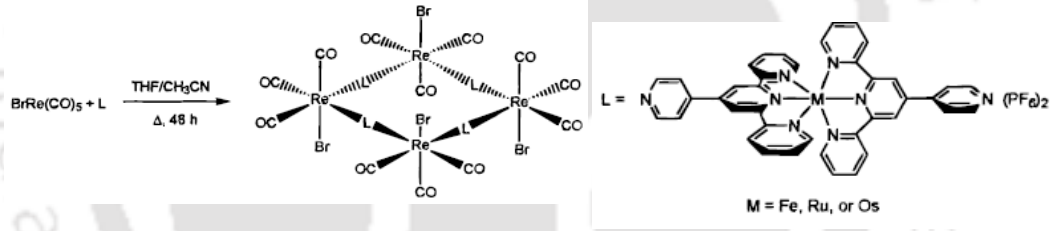

complexes $\{(dppf)Pd[\mu\text{-}(\mathbf{L3''})_2Ru]\}_4(PF_6)_8(OTf)_8$ (4), where M = Fe (1), Ru (2), or Os (3), dppf = 1,1'-bis(diphenylphosphino)ferrocene, were also prepared by self-assembly between $(dppf)Pd(H_2O)_2(OTf)_2$ and $(\mathbf{L3''})_2M(PF_6)_2$.[212]

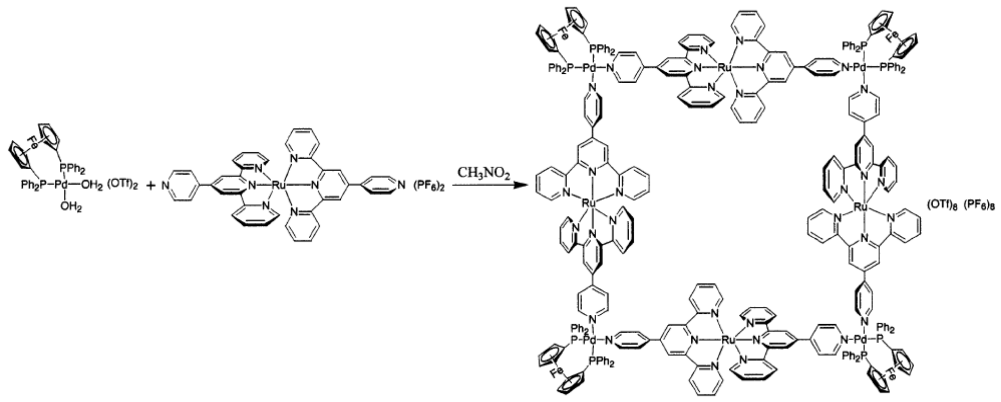

4'-(Ferrocenyl)-2,2':6',2"-terpyridine (Fctpy) and **L3″** were prepared from the respective carboxaldehydes and 2-acetylpyridine using the Kröhnke synthetic methodology.[213] Metal complexes, $[M(Fctpy)_2](PF_6)_2$ (M = Ru, Fe, Zn), $[Ru(tpy)(Fctpy)](PF_6)_2$ and $[Ru(\mathbf{L3''})_2](PF_6)_2$ were prepared and characterized by cyclic voltammetry, UV-visible, resonance Raman and emission studies.[214] The reaction of **L3″** and other extended triazine ligands with d^6-metal centers Ru^{II} and Re^{I} were performed and the products isolated were characterized. The emission properties of **L3″** complexes incorporating the $[Re(CO)_3(MeCN)]^+$, has the luminescence from intraligand state.[215] The synthesis and electronic, redox properties of Ru(II) complexes of a related ligand 4'-(4-pyridyl)-3,3';5',3"-bisdimethylene-2,2';6',2"-terpyridine are reported.[216]

Cobalt

The synthesis and characterization of the cobalt complexes, $[Co(\mathbf{L3''})_2](ClO_4)_2$ and $[Co(\mathbf{L3''})_2](ClO_4)_3$ and their interaction with calf thymus DNA has been studied by using absorption, emission spectral, electrochemical studies and viscosity

measurements.[217] One-dimensional cobalt(II) self-assemblies, [Co(**L3″**)$(NCS)_2$] and [Co(**L3″**)(SO_4)]·$(CH_3$ OH)$(C_2H_5OH)(H_2O)$ were reported to exist in a linear and zigzag chains respectively.[218]

Two N-atoms of the (4-pyridyl) ring of **L3″** moieties linked by a $–CH_2PhCH_2–$ arm and its metallo-supramolecular coordination polyelectrolyte was prepared by the reaction with Co(II). The active component was assembled in electrochromic films by sequential deposition using electrostatic layer-by-layer self-assembly, for its use as electochromic material.[219] The 1D polymeric compounds [Co(**L3″**)Cl_2]·MeOH and [Co(**L3″**)Cl_2]· $2H_2O$, in which the Co(II) is coordinated by three N-atoms of a tridentate **L3″**, two $Cl^–$ ions and are polymerized through the coordination of the N-atom of the pendent (4-pyridyl) ring of another molecule of coordinated **L3″**. The compound [Co(**L3″**)Cl_2]· MeOH formed the quasi 3D networks by making π-π stacking between the 1D chains and [Co(**L3″**)Cl_2]·$2H_2O$ exhibited an S = 3/2 (HS) S = 1/2 (LS) spin transition with a thermal hysteresis.[220] The rates and mechanisms of reactions of solvates of Co(II), Ni(II), Cu(II) and Zn(II) for substitution with 4'-(4-pyridyl)-2,2':6',2"-terpyridine that exhibit a single pseudo-first-order rate process has also been investigated by multi-wavelength stopped-flow spectrophotometry.[221]

Rhodium and Iridium

The synthesis of the mononuclear cationic complexes, [(η^5-Cp*)MCl(**L3″**)]$^+$, M = Rh, Ir; and characterization by IR and NMR spectroscopy were reported.[222] The preparation of the complexes of the formula, [Rh(tpy)(**L3″**)]$(PF_6)_3$, [Rh(**L3″**$)_2$]$(PF_6)_3$ and their structural characteristics has been described.[223] The homoleptic complex [Ir(**L3″**$)_2]^{3+}$, display structured emission with luminescence.[178] Reaction **L3″** with MeI in acetonitrile

results in the *N*-methylation of the 4′-(4-pyridyl) group and the Ir(III) mixed ligand complex is reported to display long-lived luminescence in solution and is quenched by the chloride ions.[187]

Rhenium

The electrochemical and spectroscopic properties of the complexes of the type $BrRe(CO)_3$(**L3″**) were reported.[224-225] The emission properties of the complex $[Re(\mathbf{L3''})(CO)_3(MeCN)]^+$ that arise from an intraligand state is also reported.[215]

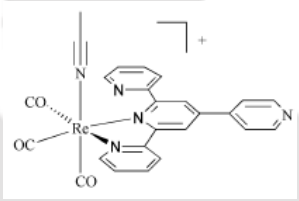

Nickel, Palladium and Lead

Kinetic and mechanistic studies of mono- and bis- nickel(II) complexes of **L3″** are reported.[226] The structural studies on $[Pd(\mathbf{L3''})Cl]Cl{\cdot}3H_2O{\cdot}DMF$ that contains rows of columns of [Pd(**L3″**)Cl]+ cations, which are supported by Pd···Pd interactions (3.367(1) and 3.440(1) Å are described.[227] Mononuclear $[Pb(\mathbf{L3''})(MeOH)I_2]{\cdot}MeOH$, acetate ion bridged dimeric $[Pb(\mathbf{L3''})(\mu\text{-}AcO)]_2(ClO_4)_2$, and polymeric $[Pb_3(\mathbf{L3''})_2(\mu^2\text{-}Cl)_3(\mu^3\text{-}Cl)_3]_n{\cdot}nMeOH$ have been synthesized and analyzed structurally.[228–229]

Copper, Zinc, Cadmium

Mixed-valent rectangular grid-type coordination polymers based on Cu(I)/Cu(II) and **L3″** are structurally characterized.[177] Structural studies on the supramolecular

complexes $[Cu(\mathbf{L3''})(O_2CCH_3)_2]\cdot H_2O$, $[Cu_2(\mathbf{L3''})_2(BDC)(NO_3)_2]\cdot 0.5H_2O$ BDC = 1,4-benzenedicar-boxylate, containing hydrogen-bonding and π···π interactions are reported.[179] The bis-copper(II) complex, $[Cu(\mathbf{L3''})_2](PF_6)_2$ has been structurally characterized and contain alternating 1-dimensional linear channels formed through π-π stacking interactions.[230]

The chiral heterometallic complex obtained by solvothermal reaction of $[Zn(\mathbf{L3''})_2](BF_4)_2$ and CuCN, are shown to exhibit a rare self-catenated network formed by two 3-dimensional cationic and one 3-dimensional anionic frameworks.[231] The Zn^{II} atom coordinated by **L3″** and two thiocyanate groups, with a distorted trigonal-bipyramidal coordination geometry is reported.[232] The luminescence studies on **L3″** and its Zn^{2+}, Fe^{2+}, Co^{2+}, Sm^{3+}, Eu^{3+} and Tb^{3+} were studied.[233] A molecular structure of the mononuclear complex $[Cd(\mathbf{L3''})(H_2O)(NO_3)_2]$ is found to have a Cd(II) center in a seven-coordinate environment and to behave as supramolar nodes.[234] Formation of stable monolayers of $[Fe(\mathbf{L3''})_2](BF_4)_2$ on the $CdCl_2$ surface has also been described.[235]

Osmium

In metal complexes, $[M(\mathbf{L3''})_2][PF_6]_2$, M = Ru(II) or Os(II), the absorption and luminescence spectra vary on changing the pH, because the protonation of the pendant pyridine unit makes it an electron acceptor by lowering the energy of its π* orbital and changes by the acid-base reactions for these complexes, and found that the two protonation stages exhibit different pK_a values both in the electronic ground state and in the lowest (emitting) excited state.[236]

1.5 Definition of the Problem

PART A: Metal Assisted Transformations of Imines Containing Pyridyl Groups

One domain of coordination chemistry which has flourished in recent years is the synthesis of complex architectures *via* suitably designed ligands and transition metal ions. Schiff bases have played an important role in the development of coordination chemistry as they readily form stable complexes with most of the transition metals. From the study of the available literature on the metal chemistry of the Schiff bases, "***A question arises that, can the pyridyl group containing Schiff bases be transformed/activated in presence of a metal?***" Based on this a systematic study was undertaken and the results are delineated in the Part A (Chapters 2, 3 and 4) of this thesis.

PART B: Transition Metal Chemistry of 4′-(2-Pyridyl)-2,2′:6′,2″-Terpyridine

One of the out come of the study described in Part A, is the ready formation of a 4′-(2-pyridyl)-2,2′:6′,2″-terpyridine (**L3**), from the one of the Schiff bases used in Chapter 2. The coordination chemistry of **L3**, was not sufficiently explored, as inferred from the literature. So a study of the coordination chemistry of **L3** was undertaken and the results are described in Part B (Chapters 5, 6 and 7) of this thesis.

1.6 Materials

$Fe(NO_3)_2{\cdot}9H_2O$, $Co(NO_3)_2{\cdot}6H_2O$, $Ni(NO_3)_2{\cdot}6H_2O$, $NiCl_2{\cdot}6H_2O$, $Cu(NO_3)_2{\cdot}3H_2O$, $[Cu(OAc)_2(H_2O)]_2$, $FeCl_3$, $K_2Cr_2O_7$, $MgSO_4$, Na_2SO_4, were purchased from Merck India. $RuCl_3{\cdot}xH_2O$ was purchased from Arora Matthey, Kolkata. $RuCl_2(DMSO)_4$ was prepared by the reported procedures.[237] Pyridine-2-carbaldehyde, 2-acetylpyridine, 2-picolylamine, 2-(2-aminoethyl)-pyridine, 2-aminopyridine, 2-amino-3-picoline, 2-amino-4-picoline, KPF_6, NH_4BF_4, KBr, and $CDCl_3$ were from M/S Aldrich, USA. All the chemicals and solvents were of reagent grade and were used as received without further purifications.

1.7 Instrumentation and Methods

Elemental analysis was performed by Elemental analyses were performed using a Carlo Erba 1108 elemental analyzer or Perkin-Elmer Series II CHNS/O Analyzer 2400. UV-Vis spectrum was recorded in Perkin-Elmer Lambda 25 spectrometer. A JASCO (J-810) was used for recording the CD spectra. FT-IR spectrum in the range 4000-250 cm^{-1} was recorded using Perkin-Elmer Spectrum One. Cary Eclipse EL05033882 was used for fluorescence spectra. ^{1}H and ^{13}C, NMR spectrum was recorded on a Varian Mercury plus 400 MHz NMR Spectrometer. A Lakshore VSM Setup for room temperature magnetic data, were used for performing the relevant measurements.

1.7.1 EPR Measurements

The X-band EPR spectrum (9.056 GHz frequency and 0.998 mW power) was recorded on a JEOL JES FA-200 X-band EPR spectrometer having a maximum field of 1.30 T with a spin sensitivity of 5 x 10^{9} spins / 10^{-4} T (at 100 kHz modulation) and homogeneity 1 x 10^{-5}. The measurement of g-tensors was achieved using the MnO lines marker which acts as a spin standard. The modulation frequency was 100 MHz, with a width of 0.35 mT kept constant for all the samples. The spectrometer fitted with a quartz dewar for measurements at liquid nitrogen temperature. The spectra were recorded for the polycrystalline sample or its solution at room as well 77K using suitable glass forming solvents within 0–800 mT.

1.7.2 AC Susceptibility

The AC susceptibility was measured as a function of temperature at AC field amplitude of 22 A/m by employing the mutual inductance bridge method and using Perkin Elmer (model 7265) dual phase lock-in-amplifier. The AC magnetic susceptibility of was recorded at an oscillator frequency of 333 Hz at 6 Oe; the magnetic field was generated using a Walker electromagnet. The temperature variation was achieved using a commercial closed cycle Helium refrigerator cryostat equipped with Lakshore

Temperature Controller (model-331). The temperature was measured using Lakshore calibrated GaAlAs sensor with an accuracy of better than ±50 mK.

1.7.3 X-Ray Crystallography

X-ray crystallographic data were collected using Bruker SMART APEX-CCD diffractometer with Mo Kα radiation (λ = 0.71073 Å). The intensity data were corrected for Lorentz and polarization effects and empirical absorption corrections was applied using SAINT program.[238-239] All the structures were solved by direct methods using SHELXS-97.[240] Non-hydrogen atoms located from the difference Fourier maps were refined anisotropically by full-matrix least-squares on F^2, using SHELXL-97.[240] The hydrogen atoms were included in the calculated positions and refined isotropically using a riding model and in some cases it has been added.

1.7.4 Thermal Measurements

Thermogravimetry were studied by a computer controlled METTLER TOLEDO STAR^e system of module TGA/SDTA851^e under static nitrogen atmosphere using platinum pan at a heating rate of 10 °C min^{-1} in the temperature range 25 °C to 700 °C. The instrument was calibrated using RTypSDTA sensor. Onset temperature obtained from DTG curve is used to evaluate the onset decomposition temperature of the samples.

Chapter 2

Reactivity of Schiff Bases Having a Methylene and Aldimine / Methylketimine Groups†

Abstract: The coordination chemistry of two Schiff bases, *N*-(2-pyridylmethyl)pyridine-2-carbaldimine (**L1**) and *N*-(2-pyridylmethyl)pyridine-2-methylketimine (**L2**) with Cu^{2+} are studied. **L1** reacted readily with $[Cu(OAc)_2(H_2O)]_2$ in methanol affording a compound of composition $[Cu(\mathbf{bpca})(OAc)(H_2O)]\cdot H_2O$ (**1**), (**bpca** = bis(2-pyridylcar-bonyl)amide ion), as confirmed by X-ray crystallographic study. During the course of the reaction, **L1** has been converted to a diimide, which remain bound to copper. The coordination of **L1** to a Cu^{2+} ion, followed by the oxidation of the active methylene group as well as the aldimine function by O_2/H_2O, are the important steps in the conversion of **L1** to **bpca** ion. In methanol, **L2** reacted with $Cu(NO_3)_2\cdot 3H_2O$ in air affording green colored solid. The X-ray crystallographic study of the green solid revealed the presence of complexes of formula $\{[Cu(\mathbf{L3})(OH)(NO_3)][Cu(\mathbf{L3})(NO_3)_2]\}\cdot 2H_2O$ (**2**), where **L3** is 4′-(2-pyridyl)-2,2′:6′,2″-terpyridine. Oxidation of the active-methylene group of **L2** to an imide, followed by its condensation with 2-acetylpyridine involving a C–C bond forming reaction, mediated by Cu^{2+} ion, are the essential steps involved in the conversion of **L2** to **L3**. **L3** is isolated by extrusion of Cu^{2+} with $EDTA^{2-}$. In frozen glass **2** exhibits an axial EPR spectrum with $g_{||} = 2.136$, $g_{\perp} = 2.086$ and $A_{||} = 188$ G.

† This work has been published in:

Padhi, S. K. and Manivannan, V. *Inorg. Chem.* **2006**, *45*, 7994-7996.

Chapter 2

Reactivity of Schiff Bases Having a Methylene and Aldimine / Methylketimine Groups

In this chapter, the coordination chemistry of *N*-(2-pyridylmethyl)pyridine-2-carbaldimine (**L1**) and *N*-(2-pyridylmethyl)pyridine-2-methylketimine (**L2**) towards the Cu^{2+} ion is described.

2.1 Experimental

2.1.1 Syntheses

***N*-(2-Pyridylmethyl)pyridine-2-carbaldimine (L1)**. To 2.5 g of anhydrous $MgSO_4$ suspended in 20 mL of CH_2Cl_2, 250 mg (2.31 mmol) of 2-picolylamine was added

followed by 250 mg (2.31 mmol) of pyridine-2-carbaldehyde. The reaction mixture was heated at reflux for 1.5 h and then stirred at ambient temperature for another 3 h. The solution was filtered, washed with 2 x 5 mL portions of CH_2Cl_2 and the volatile components in the combined solution were removed by evaporation in vacuum. The crude product was obtained as yellow oil, is pure enough as inferred from the ^1H NMR spectrum and was used without further purification. Yield: 430 mg (94%). IR, (neat, cm^{-1}): 1650 ($C=N_{im}$), 1590 ($C=N_{py}$).^1H NMR (δ (*J*, Hz), $CDCl_3$): 5.00 (2H, s), 7.14 (1H, t, 6.6), 7.28 (1H, t, 6.4), 7.16 (1H, d, 7.6), 7.39 (1H, d, 7.6), 7.63 (1H, t, 7.6), 7.70 (1H, t, 7.6), 8.05 (1H, d, 8.0), 8.54 (1H, s), 8.52 (1H, d, 4.4) and 8.62 (1H, d, 5.6).

***N*-(2-Pyridylmethyl)pyridine-2-methylketimine (L2).** Has been prepared, adopting the same method described for **L1**, using 10 mmol each of 2-picolylamine and 2-acetylpyridine. Yield: 2.90 g (94%); IR, (neat, cm^{-1}): 1637, 1590, 1463, 1434; ^1H NMR (δ (J, Hz), $CDCl_3$): 2.49 (3H, s), 4.89 (2H, s), 7.15 (1H, t, 6.0), 7.25 (1H, t, 5.4), 7.61 (1H, d, 7.6), 7.67 (2H, m), 8.20 (1H, d, 8.0), 8.54 (1H, d, 4.8), 8.57 (1H, d, 5.2).

[Cu(bpca)(OAc)H_2O]·H_2O (1). To **L1** (270 mg, 1.3 mmol) dissolved in 15 mL of ethanol, a clear ethanolic solution of $Cu(OAc)_2·H_2O$ (25 mg, 1.25 mmol) was added. Immediately the color of the solution changed to pink and the stirring was continued for 4 h, during this period the color changed to bluish green. The reaction mixture was kept for a week at ambient temperatures and the crystals obtained were washed with ice-cold water and characterized as [Cu(**bpca**)(OAc)H_2O]·H_2O (**bpca** = bis(2-pyridylcarbonyl) amide ion). Yield: 323 mg (63%). IR (KBr, cm^{-1}): 1715, 1630, 1605, 1570, 1420. Anal. Found: C, 43.96, H, 3.91; N, 10.45.Calcd. for $C_{14}H_{15}N_3O_5Cu$: C, 43.65, H, 3.92; N, 10.9%.

Bis(2-pyridylcarbonyl)amide (bpcaH): To [Cu(**bpca**)(OAc)H_2O]·H_2O (120 mg, 0.156 mmol) dissolved in H_2O (30 mL) was added, Na_2EDTA (230 mg, 0.68 mmol), 50 mL of $CHCl_3$ and stirred vigorously for 3.5 h. The $CHCl_3$ layer was separated, dried with anhydrous Na_2SO_4. A yellow colored **bpcaH** (32 mg, yield 90 %) was obtained after removal of $CHCl_3$. IR (KBr, cm^{-1}): 1753, 1595, 1470, 1435. ^{1}H NMR (δ (*J*, Hz), $CDCl_3$): 4.79 (1H, s), 7.56 (1H, t, 7.2), 7.93(1H, t, 7.2), 8.34 (1H, d, 7.2) and 8.74 (1H, d, 3.2).

{[Cu(L3)(OH)(NO_3)][Cu(L3)(NO_3)$_2$]}·2H_2O (**2**): To a methanolic solution (25 mL) of **L2** (180 mg, 0.85mmol), $Cu(NO_3)_2·3H_2O$ (164 mg, 0.68 mmol) dissolved in methanol (15 mL) was added with stirring. An initial violet color developed on mixing changed immediately to green; the solution was stirred for 24 h and left undisturbed. Green crystals deposited after a week were collected after washing with ice-cold methanol. Yield (Based on **L2**): 405 mg (48%). IR (KBr, cm^{-1}): 1657, 1600, 1473, 1384, 1289. Anal. Calcd. for: $C_{40}H_{33}N_{11}O_{12}Cu_2$: C, 48.66; H, 3.37; N, 15.61. Found: C, 48.45; H, 3.28; N, 16.02%.

4′-(2-Pyridyl)-2,2′:6′,2″-terpyridine (L3): To {[Cu(**L3**)(OH)(NO_3)][Cu(**L3**)(NO_3)$_2$]} ·2H_2O (150 mg, 0.15mmol) dissolved in H_2O (30 mL) was added, Na_2EDTA (230 mg, 0.68 mmol), 50 mL of $CHCl_3$ and stirred vigorously for 3.5 h. The $CHCl_3$ layer was separated, dried with anhydrous Na_2SO_4. A pale yellow colored **L3** (450 mg, yield 96%) was obtained after removal of $CHCl_3$. m.p. 230 ºC with sublimation. Yield: 450 mg (96%). IR (KBr, cm^{-1}): 1660, 1600, 1583, 1563, 1547, 1465, 1390. ^{1}H NMR (δ (*J*, Hz),

$CDCl_3$, Figure 1): 7.32(1H,t, 6.0), 7.33 (1H, t, 6.0), 7.81 (1H, t, 7.8), 7.85 (1H, d, 7.6), 8.05 (1H, d, 8.0), 8.64 (1H, t, 8.0), 8.72 (1H, t, 3.6), 8.77 (1H, d, 4.8), 9.07 (1H, s). 100 MHz ^{13}C NMR (δ, $CDCl_3$): 118.8 (Y3), 121.4 (X3, Z3), 123.8 (Z4), 123.9 (X5), 136.9 (X4, Z5), 148.7 (Y4), 149.2 (X6), 150.1 (Z6), 155.2 (X2), 156.3 (Y2, Z2).

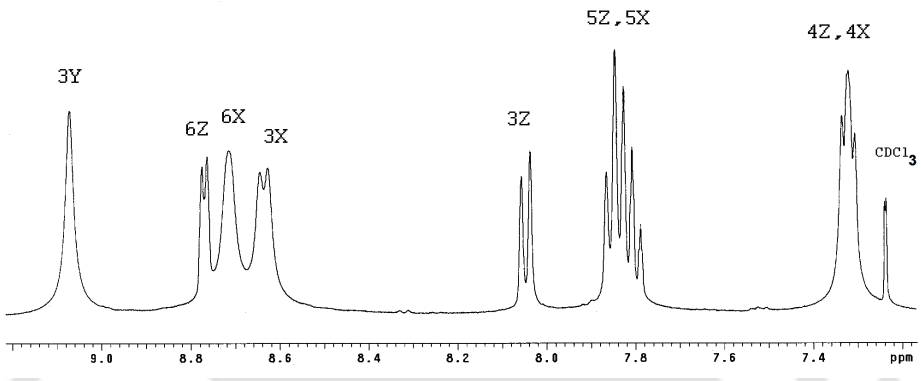

Figure 1. ^1H NMR spectrum of **L3** ($CDCl_3$, 400 MHz; Labels as per Scheme 1).

2.2 Results and Discussion

2.2.1 Syntheses

The ligands **L1** and **L2**, were synthesized (Scheme 1) in excellent yields, by refluxing equimolar quantities of pyridine-2-carbaldehyde/2-acetylpyridine and 2-picolylamine in dichloromethane using anhydrous $MgSO_4$ as Lewis acid as well as drying agent to absorb the water formed as product of condensation. The yellow-oily products obtained after removal of hydrated $MgSO_4$ and other volatile components, do not require further purifications and loses its identity on standing, as ascertained from ^1H NMR spectrum.

Therefore, freshly prepared ligands were used for the synthesis of complexes. This method of synthesis is advantageous over the reported procedure by shorter reaction time.[98]

Scheme 1

L1 reacted readily with $[Cu(OAc)_2(H_2O)]_2$ in methanol affording a compound of composition $[Cu(\mathbf{bpca})(OAc)(H_2O)]\cdot H_2O$ (**1**), (Scheme 2, other coligands were omitted for clarity). During the course of the reaction the Schiff's base has been converted to a diimide, which remain bound to the Cu^{2+} ion. Probable steps involved in the conversion are: initial coordination of **L1** to a Cu^{2+} ion, oxidation of the active methylene group ($-CH_2-$) as well as the imine function (=CH–) to carbonyl functions, which occur in the presence of O_2/H_2O. The crystalline yellow **bpcaH** is isolated as a solid by extrusion of Cu^{2+} using excess of Na_2EDTA.

Methanolic solution of **L2**, on reaction with $Cu(NO_3)_2\cdot 3H_2O$ in air afforded green colored solid of composition $\{[Cu(\mathbf{L3})(OH)(NO_3)][Cu(\mathbf{L3})(NO_3)_2]\}\cdot 2H_2O$ (**2**), where **L3** is 4′-(2-pyridyl)-2,2′:6′,2″-terpyridine. In this reaction Cu^{2+} ion mediates the

formation of the central pyridine (Y) ring of **L3** from Schiff base **L2**. Probable intermediates involved in the formation of **L3**,

Scheme 2

is shown in Scheme 3. Coordination of **L2** to Cu^{2+} ion (other coligands are omitted) occurs in generating **I**. Oxidation of active methylene group in **I** proceeds, in the presence of O_2 and H_2O to produce the meta-stable imide intermediate (step 1) **II**. In C–C bond forming step 2, **II** condenses with 2-acetylpyridine (**III**), which could have been released from **L2** in the presence of H^+ (generated in step 1) giving **IV** as the stable final product. **L3** is isolated by extracting into chloroform layer from the aqueous solution of the complex using excess of Na_2EDTA. ^1H NMR spectrum of **L3** is displayed in Figure 1.

Scheme 3

2.2.2 Optical Properties

The FT-IR spectrum of **L1** shows the presence of –C=N– stretching frequency for imine as well as pyridyl function at 1650 and 1590 cm^{-1} respectively. A new peak at 1720 cm^{-1} observed in **1** can be assigned to ν(C=O) of diimide group, shift to 1753 cm^{-1} in the free **bpcaH**.[241]

The X-ray crystal structure of **1** has been determined as a part of this thesis. The structure and spectroscopic properties of **1** has been reported by Folgado *et al.*, and the synthesis is by the hydrolysis of the triazine ring in 2,4,6-tris(pyridyl)triazine, in the presence of Cu^{2+} ion.[242] The spectroscopic properties are identical and hence the details of **1** are not discussed further.

In acetonitrile solution, **2** exhibits a broad d–d transition at λ_{max} = 675 nm along with a shoulder at 425 nm having ε values 30 and 20 $M^{-1}cm^{-1}$, respectively (Figure 2). The origins of these bands are respectively due to the transitions $d_{x^2-y^2} \rightarrow d_{z^2}$ and $d_{x^2-y^2} \rightarrow d_{xy}$. Sharp intra-ligand transitions occur at 350(9830), 335(11235), 290(32300), 280(25560), and 270(23875) nm($M^{-1}cm^{-1}$), along with shoulders at 304(15560) and 260(21505).[243]

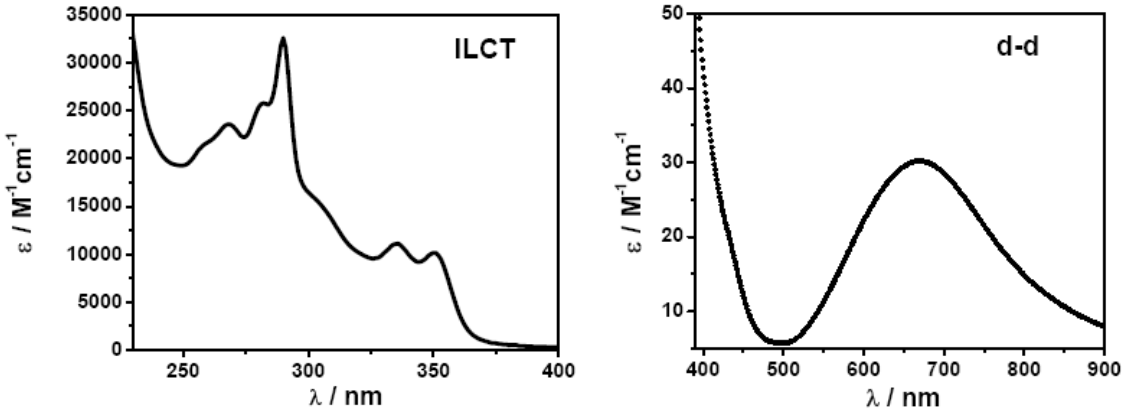

Figure 2. UV-Vis spectrum of **2** in acetonitrile.

2.2.3 EPR Spectra

The polycrystalline sample of complex **2** exhibits an isotropic spectrum at room temperature with g_{iso} = 2.013. But in frozen acetonitrile (Figure 3), an axial spectrum is observed having, $g_{||}$ = 2.136 ($A_{||}$ = 158 G); $g_{\perp}$ = 2.086. The $g_{||} > g_{\perp}$, is suggestive of the unpaired electron being in the $d_{x^2-y^2}$ orbital.[244-245]

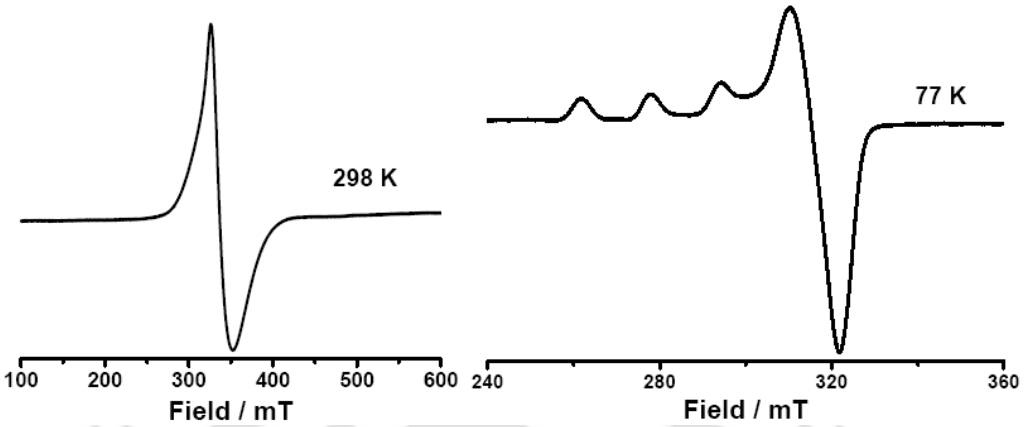

Figure 3. EPR spectrum of **2**, polycrystalline (298 K) and frozen acetonitrile (77 K).

2.2.4 Thermogravimetry (TG)

The thermogram of **2** reveals that the loss of two solvent water molecules occurs at the midpoint temperature of 110 °C (Figure 4). The loss of four moles of pyridine occurs at the midpoint temperature 320 °C and is very sharp within the temperature span of 275–325 °C. The nature of other volatile components was not analyzed.

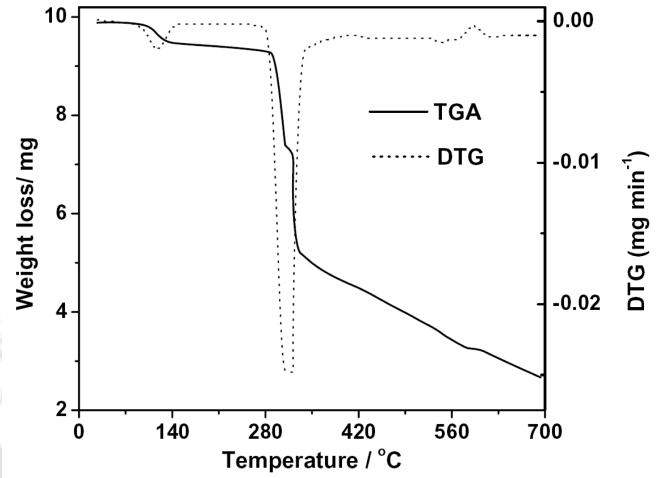

Figure 4. TG profile of **2**.

2.2.5 Molecular Structure

The molecular structures of **1** and **2** were determined and the crystal data and the refinement parameters are listed in Table 1. The selected bond distances and bond angles are provided respectively in Table 2 and Table 3.

Table 1. Crystal Data and Refinement Parameters for **1** and **2**

	1	**2**

Empirical formula	$C_{14}H_{15}N_3O_6Cu$	$C_{40}H_{33}N_{11}O_{12}Cu_2$
Formula weight	384.87	986.87
Temperature	296(2)	296(2)
Wavelength, Å	0.71073	0.71073
Crystal system	Triclinic	Triclinic
Space group	*P*	*P*
a, Å	7.3994(2)	8.5857(5)
b, Å	8.6119(3)	14.4378(10)
c, Å	13.0072(4)	17.1880(11)
α, deg	74.598(2)	91.504(4)
β, deg	84.827(2)	101.982(4)
γ, deg	80.993(2)	91.014(4)
V, Å^3	788.21(4)	2082.9(2)
Z	2	2
D_{calc} (g cm^{-3})	1.643	1.578
μ, (mm^{-1})	1.423	1.100
[a]GOF on F^2	1.065	1.001
R [I>2σ(I)]	[b]R_1 = 0.0150, [c]wR_2 = 0.0425	[b]R_1 = 0.0610, [c]wR_2 = 0.1940
R indices (all data)	[b]R_1 = 0.0150, [c]wR_2 = 0.0426	[b]R_1 =0.0904, [c]wR_2 = 0.2119

[a]GOF = $[\Sigma[w(F_0^2 - F_c^2)^2]/M - N]^{1/2}$ (M = number of reflections, N = number of parameters refined). [b]R_1 = Σ $||F_0| - |F_c||/\Sigma|F_0|$. [c]$wR_2$ =

$[\Sigma[w(F_0^2 - F_c^2)^2]/ \Sigma[w(F_0^2)^2]]$.

In **1**, the bivalent copper is penta-coordinated and has a distorted N_3O_2 square-pyramidal geometry ($\tau = 0.17$). The three nitrogen atoms of **bpca**, an oxygen atom of monodentate acetate ion occupy the equatorial positions and one molecule of water at the axial site. A perspective view of the [Cu(**bpca**)(OAc)(H_2O)] is shown in Figure 5. One water molecule is present in the crystal lattice and is hydrogen bonded to the oxygen atoms of the diimide function. This generates a centrosymmetric dimeric unit, in which the Cu···Cu non-bonded distance is 6.740 Å.

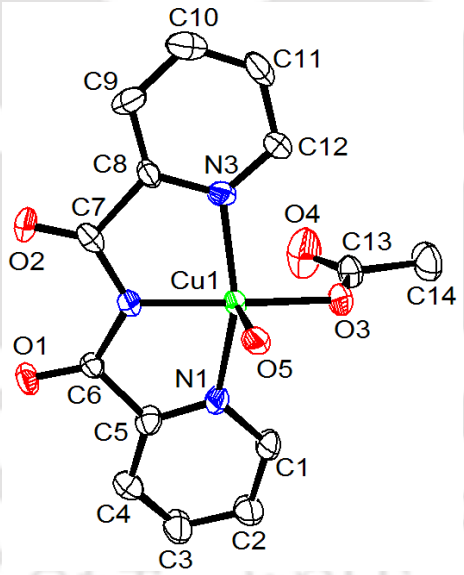

Figure 5. ORTEP (30% probability and H atoms are omitted) of [Cu(**bpca**)(OAc)H_2O].

The green solid of **2** crystallized in triclinic space group *P* *and the unit cell contained* an admixture of one molecule each of [Cu(**L3**)(OH)(NO_3)] (**2a**) and [Cu(**L3**)(NO_3)$_2$] (**2b**). A perspective view of molecular structure of the two complexes is shown in Figures 6 and 7. In **2a**, the copper center is hexa-coordinated having a *mer*-N_3O_3 environment and the Cu1–O4 distance is 2.2510(44) Å. The NO_3^- ion coordinate in the bidentate fashion with a short (Cu1–O1 1.9707(30) Å) and a long (Cu1–O2 2.5674(39) Å) bonds. While in **2b**, the copper center is penta-coordinated by the three-N atoms of the **L3**, two monodentate NO_3^- ions and has a distorted square pyramidal geometry as inferred from

Table 2. Selected Bond Distances (Å) in **1** and **2**

1		**2a**		**2b**	
Cu1–N1	1.9980(9)	Cu1–O1	1.9707(30)	Cu2–O5	2.1190(35)
Cu1–N2	1.9454(8)	Cu1–O2	2.5674(39)	Cu2–O8	2.0902(34)
Cu1–N3	1.9931(9)	Cu1–O4	2.2510(44)	Cu2–N6	2.0042(37)
Cu1–O3	1.9376(8)	Cu1–N1	2.0097(35)	Cu2–N7	1.9328(33)
Cu1–O5	2.3320(8)	Cu1–N2	1.9285(32)	Cu2–N8	2.0014(38)
		Cu1–N3	2.0216(37)	Cu2–O6	2.7942(48)
				Cu2–O9	2.6646(43)

Table 3. Selected Bond Angles (°) in **1** and **2**

1		**2a**		**2b**	
O3–Cu1–N2	172.36(4)	O1–Cu1–O2	55.33(13)	O5–Cu2–O8	82.61(13)
O3–Cu1–N3	97.12(4)	O1–Cu1–O4	98.88(15)	O5–Cu2–N6	96.94(15)
N2–Cu1–N3	81.86(4)	O1–Cu1–N1	98.28(14)	O5–Cu2–N7	135.20(14)

O3–Cu1–N1	97.46(4)	O1–Cu1–N2	159.56(13)	O5–Cu2–N8	96.91(15)
N2–Cu1–N1	82.35(4)	O1–Cu1–N3	99.77(14)	O8–Cu2–N6	96.62(15)
N3–Cu1–N1	162.28(4)	O2–Cu1–O4	153.80(14)	O8–Cu2–N7	142.18(13)
O3–Cu1–O5	91.20(3)	O2–Cu1–N1	97.02(14)	O8–Cu2–N8	98.31(14)
N2–Cu1–O5	96.44(3)	O2–Cu1–N2	104.37(13)	N6–Cu2–N7	80.16(15)
N3–Cu1–O5	97.61(4)	O2–Cu1–N3	87.81(14)	N6–Cu2–N8	160.79(15)
N1–Cu1–O5	92.12(3)	O4–Cu1–N1	90.87(16)	N7–Cu2–N8	80.64(14)
		O4–Cu1–N2	101.54(16)	O6–Cu2–O9	175.79(15)
		O4–Cu1–N3	92.91(16)		
		N1–Cu1–N2	80.64(14)		
		N1–Cu1–N3	160.75(15)		
		N2–Cu1–N3	80.11(14)		

the τ value of 0.02. The chelate bite angles are in the very narrow range 80.1–80.7° and intra-ligand *trans* angle, $N_{(X)}$–M–$N_{(X')}$ is 160.7–160.8° and deviates largely from linearity. In both **2a** and **2b**, the average Cu–N distance, in the Y ring (1.931(3) Å), is shorter than in X rings (2.010(4) Å). This trend, always observable in the transition metal complexes of terpyridines, has been ascribed to two factors: the efficient overlap of metal t_{2g} orbitals with the π* orbitals of the central pyridyl group and the geometrical constraints of the ligand, probably the former contributing more.[246, 267] Twisting of the Z-ring is –3.23(65)° and –3.42(67)°, respectively in **2a** and **2b**. X-rings twist in **2a** is 5.55(69)° and –4.53(69)°, while in **2b** is –0.88(72)° and 0.02(69)°.

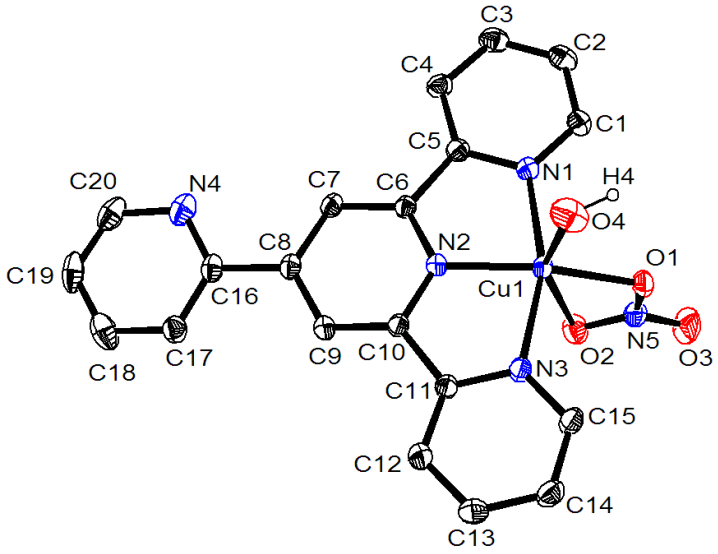

Figure 6. ORTEP (30% probability and H atoms except H4 are omitted for clarity) of **2a**.

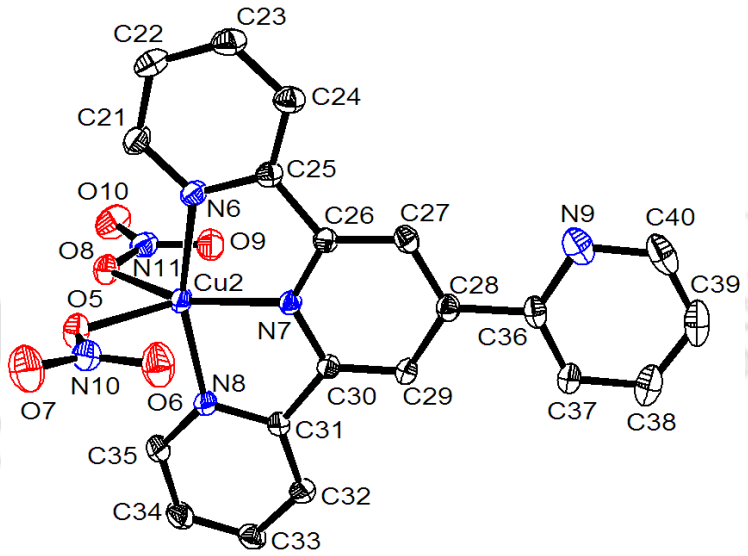

Figure 7. ORTEP (30% probability and H atoms are omitted for clarity) of **2b**.

The aromatic rings of **L3** in both the complexes are nearly-planar. The π–π interactions having the shortest intermolecular contact of C(6)···C(19), 3.3716(71) Å and C(19)···C(30), 3.3725(73) Å are present. Two disordered H_2O molecules present in the lattice were refined with variable site-occupancy factors and without added hydrogen atoms (O(11), 0.64204; O(14), 0.35796; O(12), 0.77456; O(13), 0.22544). These water

molecules held by C–H···O interactions, are present in the predominantly-hydrophobic channels of approximate cavity dimension 7.60 x 6.50 Å created by aromatic rings through π–π interactions (Figure 8). The channels are along the b-axis linked by O4···O7 (2.9111(62) Å) hydrogen-bond and O4···O10 (2.7584(71) Å) hydrogen-bond, interlinks these channels along *c*-axis. The O(4)–H(4)···O(7) and O(4)–H(4)···O(10) angles are respectively 73.48(15)° and 162.59(35)°.

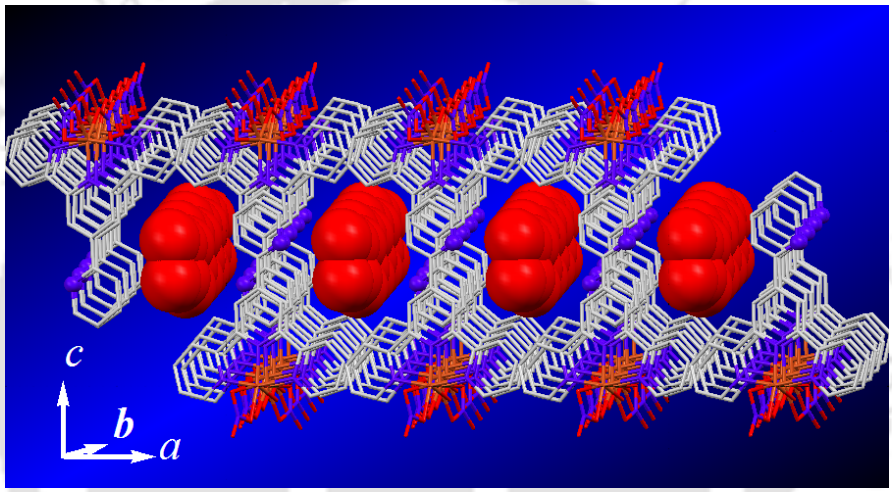

Figure 8. Packing diagram of **2**, showing the water channels.

2.3 Conclusion

The Schiff's base, **L1** reacted readily with $[Cu(OAc)_2(H_2O)]_2$ in methanol affording a compound of composition $[Cu(\mathbf{bpca})(OAc)(H_2O)]\cdot H_2O$ (**1**). During the course of the reaction, **L1** has been converted to a diimide, which remain bound to copper. The possible steps are the initial coordination of **L1** to a Cu^{2+} ion and oxidation of the active methylene group ($-CH_2-$) as well as the aldimine functions (=CH–) by O_2/H_2O.

In methanol, **L2** reacted with $Cu(NO_3)_2\cdot 3H_2O$ in air affording green colored solid. The X-ray crystallographic study of the green solid revealed the presence of complexes of formula $\{[Cu(\mathbf{L3})(OH)(NO_3)][Cu(\mathbf{L3})(NO_3)_2]\}\cdot 2H_2O$ (**2**), where **L3** is

4′-(2-pyridyl)-2,2′:6′,2″-terpyridine. That is, **L2** on reaction with $Cu(NO_3)_2 \cdot 3H_2O$ has been converted to **L3**. **L3** was isolated from **2** by extrusion of Cu^{2+} with $EDTA^{2-}$. The molecular structure of **2** consists an admixture of one molecule each of [Cu(**L3**)(OH)(NO_3)] (**2a**) and [Cu(**L3**)(NO_3)$_2$] (**2b**). In **2a**, Cu^{2+} has a distorted octahedral geometry, while in **2b**, has a square-pyramidal geometry. Two water molecules are held by C–H···O interactions and are present in the predominantly-hydrophobic channels of approximate cavity dimension 7.60 x 6.50 Å created by aromatic rings through π–π interactions. Thermogravimetric analysis shows that the loss the two water molecules occur at a mid point temperature of 110 °C. In frozen glass **2** exhibits an axial EPR spectrum with $g_{||} = 2.136$ and $g_{\perp} = 2.086$ having $A_{||} = 188$ G.

Chapter 3

Reactivity of Schiff Bases Having an Ethylene and Aldimine / Methylketimine Groups†

Abstract: The coordination chemistry of *N*-(2-pyridylethyl)pyridine-2-carbaldimine (**L4**) and *N*-(2-pyridylethyl)pyridine-2-methylketimine (**L5**) towards the Co^{2+}, Ni^{2+} and Cu^{2+} ions are described. The imines **L4** and **L5** having an intervening ethylene group when treated with methanolic solution of Co^{2+}, Ni^{2+} and Cu^{2+} nitrates coordinated readily to the bivalent metal center without any change in the ethylene and imine functions. The molecular structures of all the six complexes were determined. In each case the bivalent metal ion is coordinated by the three nitrogen atoms of tridentate **L4/L5** with two pyridine-N groups occupying the *trans* position. The optical and magnetic properties of the complexes are investigated.

† This work has been published in:

1. Padhi, S. K. and Manivannan, V. *Polyhedron* **2007**, *26*, 1619-1624.
2. Padhi, S. K. and Manivannan, V. *Polyhedron* **2007**, *26*, 3092-3096.

Chapter 3

Reactivity of Schiff Bases Having an Ethylene and Aldimine / Methylketimine Groups

In this chapter, the coordination chemistry of *N*-(2-pyridylethyl)pyridine-2-carbaldimine (**L4**) and *N*-(2-pyridylethyl)pyridine-2-methylketimine (**L5**) towards the Co^{2+}, Ni^{2+} and Cu^{2+} ions are described.

3.1 Experimental

3.1.1 Syntheses

N-(2-Pyridylethyl)pyridine-2-carbaldimine (L4). Has been prepared, adopting the procedure described for **L1** in Chapter 2, by using 4.62 mmol each of 2-(pyridyl)ethylamine and pyridine-2-carbaldehyde. Yield: 920 mg (95%). IR (neat, cm^{-1}): 1648 ($C=N_{im}$), 1590 ($C=N_{py}$). ^1H NMR (δ (*J*, Hz), $CDCl_3$): 3.22 (2H, t, 7.2), 4.08 (2H, t, 7.2), 7.08 (1H, t, 6), 7.16 (1H, d, 7.6), 7.26 (1H, t, 6), 7.54 (1H, t, 7.6), 7.69 (1H, t, 7.6), 7.93 (1H, d, 8), 8.31 (1H, s), 8.52 (1H, d, 4.4) and 8.59 (1H, d, 4.4).

N-(2-Pyridylethyl)pyridine-2-methylketimine (L5). Has been prepared, adopting the procedure described for **L1** in Chapter 2, by using 2.31 mmol each of 2-(pyridyl)ethylamine and 2-acetylpyridine. Yield: 385 mg (74%). IR (neat, cm^{-1}): 1639 ($C=N_{im}$), 1590 ($C=N_{py}$). ^1H NMR (δ (*J*, Hz), $CDCl_3$): 2.73 (3H, s), 2.92 (2H, t, 6.4), 3.11 (2H, t, 6.6), 7.10 (1H, t, 5.8), 7.15 (1H, d, 7.6), 7.45 (1H, t, 6.6), 7.58 (1H, t, 7.4), 7.81 (1H, t, 8.4), 8.02 (1H, d, 8.0), 8.51 (1H, d, 4.0) and 8.66 (1H, d, 4.8).

$[Co(L4)(NO_3)_2]$ (1). To 180 mg (0.85 mmol) of **L4** dissolved in 25 mL of methanol, was added 247 mg (0.85 mmol) of $Co(NO_3)_2 \cdot 6H_2O$ dissolved in 20 mL methanol with stirring. After stirring for 4 h, the reaction mixture was left to crystallize. Orange block like crystals of **1**, deposited after a week, were collected and washed with ice-cold methanol. Yield: 0.26 g (77%). IR (KBr, cm^{-1}): 1653 ($C=N_{im}$), 1610 ($C=N_{py}$). Anal. Calcd. for: $C_{13}H_{13}N_5O_6Co$: C, 39.57; H, 3.30; N, 17.76. Found: C, 39.25; H, 3.21; N, 16.50%.

$[Co(L5)(NO_3)_2]$ (2). Has been prepared, using the same method described for **1**, using 0.58 mmol each of $Co(NO_3)_2 \cdot 6H_2O$ and **L5**. Yield: 0.19 g (80%). IR (KBr, cm^{-1}): 1650 ($C=N_{im}$), 1602 ($C=N_{py}$). Anal. Calcd. for: $C_{14}H_{15}N_5O_6Co$: C, 41.15; H, 3.67; N, 17.15. Found: C, 41.26; H, 3.69; N, 17.34%.

$[Ni(L4)(NO_3)_2]$ (3). 180 mg (0.85 mmol) of **L4** dissolved in 25 mL of methanol, was added to 250 mg (0.85 mmol) of $Ni(NO_3)_2 \cdot 6H_2O$ dissolved in 20 mL of methanol with

stirring and stirring was continued overnight. The reaction mixture was kept undisturbed and pale green-colored block like crystals obtained after few days were collected after washing with ice-cold methanol. Yield: 0.25g (74%). IR (KBr, cm^{-1}): 1650($C=N_{im}$), 1600($C=N_{py}$). Anal. Calcd. for $C_{13}H_{13}N_5O_6Ni$: C, 39.59; H, 3.30; N, 17.77. Found: C, 39.35; H, 3.19; N, 17.14%.

[Ni(L5)$(NO_3)_2$] (4). Has been prepared, using the same method described for **3**, using 0.62 mmol each of $Ni(NO_3)_2 \cdot 6H_2O$ and **L5**. Yield: 180 mg (71%). IR (KBr, cm^{-1}): 1645 ($C=N_{im}$), 1600($C=N_{py}$). Anal. Calcd. for $C_{14}H_{15}N_5O_6Ni$: C, 41.17; H, 3.67; N, 17.16. Found: C, 41.39; H, 3.74; N, 17.44%.

[Cu(L4)$(NO_3)_2$] (5). To 180 mg (0.85 mmol) of **L4**, dissolved in 25 mL of methanol was added 205 mg (0.85 mmol) of $Cu(NO_3)_2 \cdot 3H_2O$. The reaction mixture was stirred at room temperature for overnight and blue precipitate deposited was filtered and washed thoroughly with methanol. Dark blue crystals were obtained by slow evaporation of acetonitrile solution. Yield: 0.33 g (97%). IR (KBr, cm^{-1}): 1653 ($C=N_{im}$), 1602 ($C=N_{py}$). Anal. Calcd. for: $C_{13}H_{13}N_5O_6Cu$: C, 39.11; H, 3.26; N, 17.55. Found: C, 39.18; H, 3.21; N, 17.50%.

[Cu(L5)$(NO_3)_2$] (6). To $Cu(NO_3)_2 \cdot 3H_2O$ (160 mg, 0.66 mmol) dissolved in 30 mL of methanol, **L5** (150 mg, 0.66 mmol) was added, stirred overnight and left undisturbed. Green crystals deposited after a week, were collected and washed with ice-cold methanol.

Yield: 150 mg (55%). IR (KBr, cm^{-1}): 1650 ($C=N_{im}$), 1602 ($C=N_{py}$). Anal. Calcd. for: $C_{14}H_{15}N_5O_6Cu$: C, 40.69; H, 3.63; N, 16.96. Found: C, 40.35; H, 3.71; N, 17.14%.

3.2 Results and Discussion

3.2.1 Syntheses

Six complexes (**1-6**) of molecular formula [M(**L4/L5**)$(NO_3)_2$], M = Co(II), Ni(II) and Cu(II) were synthesized in methanol using equimolar quantities each of **L4/L5** and the corresponding metal nitrate according to the Scheme 1.

Scheme 1

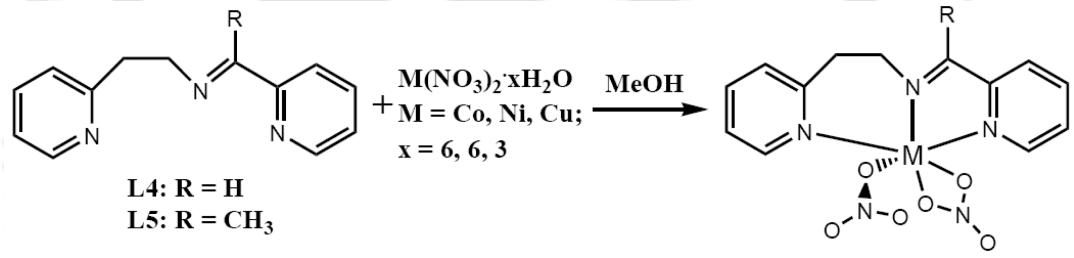

3.2.2 Optical Properties

UV-Vis spectra of **1-6** exhibit d-d transitions in acetonitrile solution (Figure 1). The curves were fitted for Gaussian to obtain the λ_{max} and the corresponding molar extinction coefficient values and the data are listed in Table 1.

For the complexes **1** and **2**, two transitions are observed in the visible region and both are of ligand field origin. The intra-ligand bands in both are observed in the ultraviolet region. Complex **3** and **4** exhibits the two typical $^3A_{2g} \rightarrow {}^3T_{2g}$ and $^3A_{2g} \rightarrow {}^3T_{1g}(P)$ transitions. A spin-forbidden at 745 is present in **3** and is obscured by the $^3A_{2g} \rightarrow {}^3T_{2g}$

transitions in **4**. But the transition $^3A_{2g} \rightarrow {}^3T_{1g}(F)$ was not observed in both **3** and **4**, which is usually appear in the UV-region, might have been obscured by the intra-ligand bands.

Both **5** and **6** have been established to have a pseudo octahedral geometry by structural studies (*vide infra*) and both show two d-d transitions in the visible region. Since, the axial distortion from the perfect octahedral symmetry removes the degeneracy of the ^2E_g state. Therefore these two transitions arise due to $d_{x^2-y^2} \rightarrow d_{z^2}$ and $d_{x^2-y^2} \rightarrow d_{xy}$ respectively. In all the six cases intra-ligand transitions occur in the 315-260 nm region. The molar extinction coefficient of these bands is higher than that observed for the free ligand.[243]

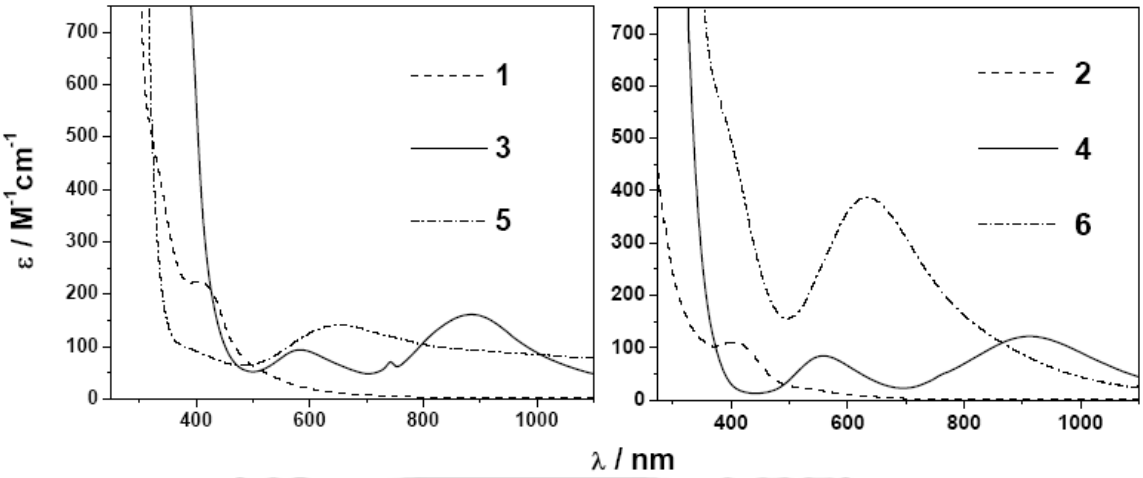

Figure 1. UV-Vis spectrum of **1–6** in acetonitrile.

Table 1. Spectroscopic and Magnetic data

	UV-Vis Spectra	μ_{eff}	EPR Spectra	
	λ_{max}, nm (ε, $M^{-1}cm^{-1}$)[a]	(B. M.)[f]	293 K	77 K
1	511(35), 417(120), 342(200), 326 (4500), 285 (18875), 265 (28200)	3.928	–	A = 91.7 G[e] g_0 = 2.01[a]
2	497(23), 407(110), 313(6,290), 285(16,470), 263(25,645)	3.967	–	g_{iso} = 1.931[c,d]
3	890(110), 745(20), 590(46), 295 (16860), 285 (25100), 270 (23580), 265 (22610)	3.897	–	–
4	920(112), 568(70), 290(18,200), 280(24,100), 270(26,575), 265(26,500)	3.886	–	–
5	675(55), 385(34), 300 (14100), 285 (18360), 270 (24680), 260 (27730)	1.952	g = 2.133[a], A = 73 G	g_1 = 2.310[c], A_1 = 198 G, g_2 = 2.102, g_3 = 2.036
6	640(385), 370(520)[b], 295(15,100), 285(21,260), 270(24,625), 265(26,820)	2.072	g = 2.136[a], A = 70 G	g_1 = 2.252[c], A_1 = 174 G, g_2 = 2.051, g_3 = 2.001

[a]In acetonitrile. [b]Shoulder. [c]Acetonitrile-Methanol (3:1) glass. [d]Very broad. [e]Powder Sample. [f]At 296 K.

3.2.3 Magnetism and EPR Spectra

The room temperature molar susceptibility (χ_M) data of the six complexes were collected and effective magnetic moment (μ_{eff}) values listed in Table 1. The μ_{eff} values are in accordance with: 3 (high-spin Co(II)) unpaired electrons (for **1** and **2**); 2 unpaired electrons (for **3** and **4**) and 1 unpaired electron (for **5** and **6**). In all the cases, the trend $\mu_{eff} > \mu_{so}$, is consistent with more than half-filled configuration for the metal ions. Since $\mu_{S+L} > \mu_{eff} > \mu_{so}$, there is an existence of spin–orbit coupling in the three complexes.[247-249]

At 77 K in the X-band (9.12 GHz), the powder EPR spectrum of **1** shows an eight lines hyperfine splitting of g_0 (^{59}Co, I = 7/2) with A = 91.7 G, whereas in acetonitrile solution an isotropic spectrum with g_0 = 2.01 is observed.[250-252] In the frozen glass **2** shows a broad single-line spectrum with g_{iso} = 1.931, but is not observable at room temperature. The acetonitrile solution as well as polycrystalline sample of **5** at 77 K, exhibit an axial spectrum having the $g_{||}$ and $g_{\perp}$ values 2.21 and 2.07 respectively and do not show hyperfine splitting. The trend $g_{||} > g_{\perp} > 2$, is in agreement with the unpaired electron being in the $d_{x^2-y^2}$ orbital. At room temperature, complex **6** in acetonitrile solution exhibits a four-line spectrum (Figure 2), which is due to the presence of hyperfine splitting of the single-line spectrum with g = 2.136, A = 70 G. However at 77 K, an axial spectrum with splitting due to a slight rhombic symmetry is present with g_1 = 2.252, g_2 = 2.051, g_3 = 2.001and the trend $g_1 > g_2 > g_3$ is observable. Hyperfine splitting of A_1 =

174 G is present. These features suggest that the unpaired electron is in the $d_{x^2-y^2}$ orbital.[244-245]

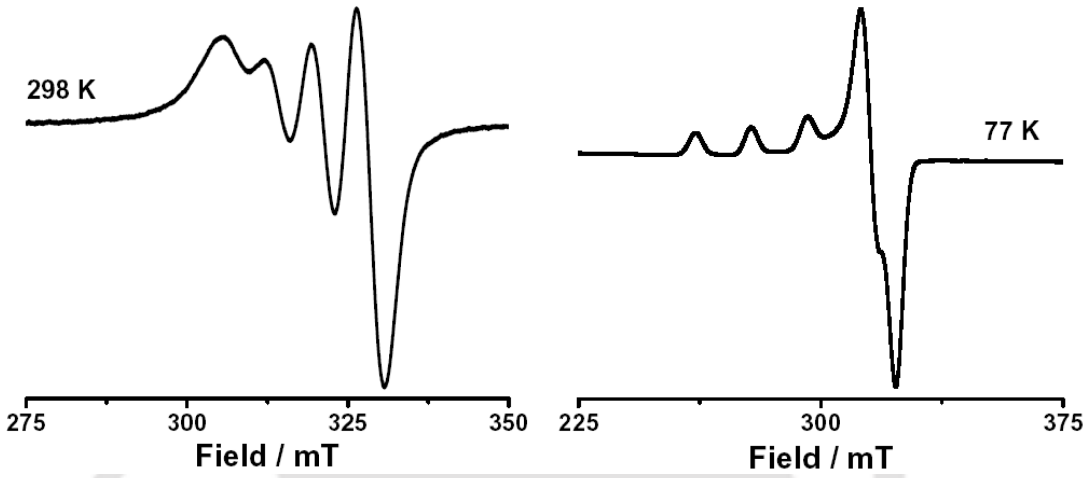

Figure 2. EPR spectrum of **6**, in acetonitrile (298 K) and frozen acetonitrile (77 K).

3.2.4 Molecular Structures

The molecular structure of all the six complexes was determined by X-ray crystallography. The crystallographic data and refinement parameters are summarized in Table 2. The selected bond distances and bond angles are listed in Table 3 and Table 4 respectively. The three complexes (**1**, **3**, **5**) containing **L4** are isomorphous and crystallized in the monoclinic *Cc*. In each case (**1-6**), the bivalent metal ion is coordinated by the three nitrogen atoms of the tridentate **L4**/**L5** ligand, with two pyridine-N occupying *trans* positions.

3.2.4.1 Structures of $[M(L4)(NO_3)_2]$

L4 binds to the metal ions by a near-planar five-membered and a puckered six-membered chelate rings. Of the two nitrate ions, one bind in bidentate and the other in monodentate fashions, giving an overall pseudo-octahedral geometry for the metal center. Therefore, the basal plane contains the three nitrogen (N1, N2 and N3) atoms of **L4** and oxygen (O1) of the bidentate nitrate. Apical positions being occupied by the oxygen atom (O2, O4) one from each of the two nitrate ions. While in **5**, the long axial Cu1···O4 contact is present 2.54(2) Å. A perspective view of **1** is shown in Figure 3. The N1–Co1–N2 angle of the five-membered chelate ring 73.9(2)º, while N2–Co1–N3 of the six-membered ring is 95.7(3)º. These angles are deviating significantly from the ideal value 90° due to the sizes of five-membered planar and the six-membered non-planar chelate rings. Average Co1–N lengths are shorter by 0.055(8) Å than that of the Co1–O distances of the bidentate NO_3^-. Bidentate NO_3^- has a shorter contact with Co1 than when it coordinates with one O-atom. The chelate bite angle of NO_3^- in **1** is 56.6(3)º. The O1–Co1–N2 angle 140.7(3)º deviates considerably from linearity by 39.3º due to smaller chelate bite and non-bonded O1···O5 interaction of 2.734(16) Å. A perspective view of **3** and **5** are shown in Figure 3. Oxygen atoms of the monodentate NO_3^- in **3** are disordered and reasonable disorder pattern could not be fixed. O3 oxygen atom of the bidentate NO_3^- in **5** is disordered and therefore refined with variable site occupancy factors (O3a, 0.37754; O3b, 0.62246). A non-bonded O1···O5 interaction is present at 2.984(14) Å in **3** and at 3.030(24) Å in **5**.

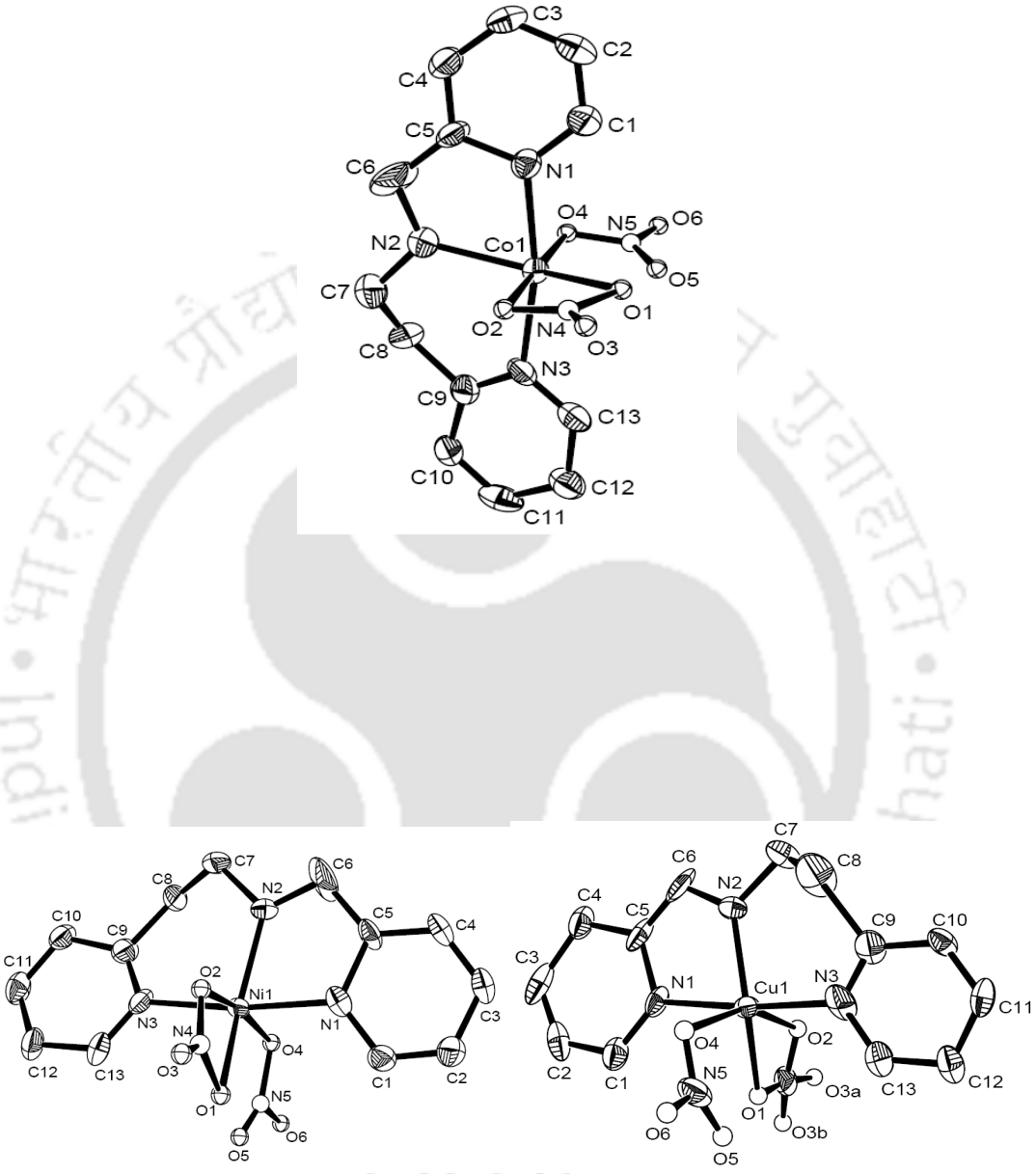

Figure 3. ORTEP diagram of **1, 3,** and **5** (30% probability, hydrogens are omitted).

On comparison, M–N_{im} and M–N_{py} bond lengths follow the order, Co > Ni > Cu consistent with the trend in the relative size of the bivalent ions. Six-membered chelate ring has a twisted conformation, N3–M–N2–C7, C9–N3–M–N2, M–N2–C7–C8 and N2–C7–C8–C9 torsional angles respectively lie in the range 0–2º, 10–14º, –(25–36º) and 61–70º. This clearly indicates that C8 and C9 atoms are deviating from the plane formed by N3–M–N2–C7 atoms. Twisting about C8 and C9 is more severe in **5** than in **1** and **3**. However, five-membered chelate ring is closer to planarity as shown the torsional angles Cu1–N2–C6–C5, N2–C6–C5–N1 and C6–C5–N1–Cu1 respectively being 11.6, –5.2º, and –2.5º. The values of these angles in order in **1** and **3** are 18.5º, –17.0º, 9.3º and 19.6º, –15.9º, 7.4º, respectively suggesting that deviation is marginal.

3.2.4.2 Structures of [M(L5)$(NO_3)_2$]

In **2** both the nitrates coordinate in a bidentate fashion and consequently the bivalent cobalt adopts distorted pentagonal bipyramidal geometry.

The atoms O1, O2, O4, O5, N2 form the pentagonal plane and N1, N3 occupy the apical positions. In **4** and **6**, of the two nitrate ions, one binds in bidentate fashion and the other in a monodentate fashion, resulting in an overall pseudo-octahedral geometry at the metal center. The basal plane contains the O1, O2, O4, N2 and the apical positions are occupied by N1, N3.

Structurally **L4** and **L5** are very similar in coordinating to a metal ion. The **L5** binds the metal ion by a five-membered and a six-membered chelate ring. Five-membered chelate ring is nearly planar in **2** and **4** but deviate from planarity to have an envelope conformation in **6**. Six-membered ring is puckered in all the three complexes. The N1–M–N2 angle of the five-membered chelate ring is 78.2(2)º, 79.8(2)º, and 82.8(8)º, while N2–M–N3 of the six-membered ring is 93.1(2)º, 94.5(2)º, and 93.0(8)º respectively

in **2**, **4**, and **6**. Average M–N lengths are shorter by 0.170(5) Å (**2**), 0.119(3) Å (**4**), 0.256(9) Å (**6**) than that of the M–O distances of the bidentate NO_3^-. Bidentate NO_3^- has a longer contact with Ni1 than when it coordinates with one oxygen atom but it is shorter in case of **6**. In **2** the NO_3^- chelate bite angles are 52.8(2)º and 55.3(2)º, while in **4** and **6** it is 58.9(2)º and 45.8(4)º respectively. A perspective view of **2** and **4** are shown in Figure 4, and **6** in Figure 5. In **6**, a long axial Cu1···O5 contact of 2.848(11) Å is present.

Table 2. Crystallographic data and refinement parameters refined). $b_{R_1} = \Sigma \|\|F_0\| - \|F_c\|\| / \Sigma \|F_0\|$. c_{wR_2} = $a_{GOF} = [\Sigma[w(F_0^2 - F_c^2)^2]/(M-N)]^{1/2}$ (M = number of reflections, N = number of	**6**	$C_{14}H_{15}N_5O_6Cu$	626664	412.85	296(2)	0.71073	Monoclinic	Cc	8.6226(2)	15.6562(4)	12.2668(2)	97.4760(10)	1641.91(6)	4	1.670	1.375	1.062	b_{R_1} = 0.06000, c_{wR_2} = 0.1521	b_{R_1} = 0.09919, c_{wR_2} = 0.1786
	5	$C_{13}H_{13}N_5O_6Cu$	295198	398.82	296(2)	0.71073	Monoclinic	Cc	8.5622(16)	14.7477(3)	12.3162(16)	96.622(3)	1544.8(5)	4	1.715	1.458	1.062	b_{R_1} = 0.06003, c_{wR_2} = 0.1576	b_{R_1} = 0.06993, c_{wR_2} = 0.1703
	4	$C_{14}H_{15}N_5O_6Ni$	626663	408.02	296(2)	0.71073	Monoclinic	P21/c	8.4604(4)	19.9967(8)	9.9209(4)	95.610(3)	1670.38(12)	4	1.622	1.205	1.045	b_{R_1} = 0.05023, c_{wR_2} = 0.1296	b_{R_1} = 0.10026, c_{wR_2} = 0.1603

rameters	**3**	$C_{13}H_{13}N_5O_6Ni$	295200	393.99	296(2)	0.71073	Monoclinic	Cc	8.5688(5)	14.6361(8)	12.5218(7)	97.317(3)	1557.62(15)	4	1.680	1.289	1.057	b_{R_1} = 0.0527, cwR 2 = 0.1418	b_{R_1} = 0.0568, cwR 2 = 0.1467	$[\Sigma[w(F_0{}^2 - F_c{}^2)^2]/\Sigma[w(F_0{}^2)^2]]$.
	2	$C_{14}H_{15}N_5O_6Co$	630610	408.24	296(2)	0.71073	Monoclinic	P2 1/c	8.6923(3)	15.5099(6)	14.2193(6)	119.579(3)	1667.17(11)	4	1.628	1.076	1.077	b_{R_1} = 0.0692, cwR 2 = 0.2100	b_{R_1} = 0.0769, cwR 2 = 0.2166	
	1	$C_{13}H_{13}N_5O_6Co$	295199	394.21	296(2)	0.71073	Monoclinic	Cc	8.6093(6)	14.4532(6)	12.8749(10)	98.314(6)	1585.21(18)	4	1.652	1.126	1.032	b_{R_1} = 0.0438, cwR 2 = 0.1139	b_{R_1} = 0.0540, cwR 2 = 0.1234	

Empirical formula	
CCDC number	
Formula weight	
Temperature	
Wavelength, Å	
Crystal system	
Space group	
a, Å	
b, Å	
c, Å	
β, deg	
V, Å3	
Z	
Dcalc (gcm–3)	
μ, (mm–1)	
aGOFonF2	
R[I > 2σ(I)]	
R indices (all data)	

Table 3. Selected Bond Distances (Å)

Bond	1	3	5	Bond	2	4	6
M–N1	2.096(8)	2.039(9)	1.997(9)	M–N1	2.089(4)	2.056(3)	2.037(9)
M–N2	2.094(4)	2.040(4)	1.978(5)	M–N2	2.094(7)	2.023(3)	1.958(6)
M–N3	2.150(8)	2.085(8)	1.988(14)	M–N3	2.115(4)	2.051(3)	1.928(13)
M–O1	2.178(6)	2.167(5)	2.061(6)	M–O1	2.293(7)	2.198(4)	2.143(6)
M–O2	2.159(7)	2.036(7)	2.320(18)	M–O2	2.272(5)	2.127(3)	2.317(15)
M–O4	2.244(9)	2.158(9)	2.538(15)	M–O4	2.298(4)	2.062(3)	2.334(16)
N2–C6	1.403(10)	1.380(14)	1.392(16)	M–O5	2.214(5)		
N2–C7	1.457(6)	1.456(7)	1.468(10)	N2–C6	1.400(8)	1.291(5)	1.644(31)
C5–C6	1.388(16)	1.454(18)	1.322(23)	N2–C7	1.301(12)	1.445(5)	1.329(18)
C7–C8	1.281(12)	1.318(13)	1.376(23)	C6–C14	1.360(12)	1.483(6)	1.190(23)
C8–C9	1.545(14)	1.497 (15)	1.691(27)	C5–C6	1.439(7)	1.502(6)	1.522(24)
N1–C5	1.412(10)	1.453(11)	1.462(17)	C7–C8	1.335(12)	1.526(6)	1.334(14)
N3–C9	1.274(12)	1.246(12)	1.232(21)	C8–C9	1.489(9)	1.509(6)	1.490(17)
O2–N4	1.190(11)	1.213(10)	1.143(15)	N1–C5	1.344(6)	1.342(5)	1.374(15)
				N3–C9	1.314(6)	1.363(5)	1.318(15)

Table 4. Selected Bond Angles (°)

Angle	1	3	5	Angle	2	4	6
O1–M–O2	56.6(3)	58.2(2)	49.6(4)	O1–M–O2	52.8(2)	58.9(2)	45.8(4)
O1–M–O4	122.0(3)	111.8(3)	109.9(3)	O1–M–O4	128.4(2)	112.3(2)	72.2(3)
O1–M–N1	90.2(2)	89.1(2)	86.1(3)	O2–M–O4	178.7(2)	171.2(2)	117.3(5)
O1–M–N2	140.7(3)	146.1(2)	143.4(2)	O4–M–O5	55.3 (2)		
O1–M–N3	97.4(3)	96.2(3)	98.6(5)	O1–M–N1	95.7(2)	93.4(2)	86.6(3)
O2–M–O4	178.5(2)	169.9(2)	159.2(2)	O1–M–N2	142.6(2)	152.4(2)	142.3(5)
O2–M–N1	91.2(3)	90.9(3)	92.1(5)	O1–M–N3	91.4(2)	91.5(2)	95.6(4)
O2–M–N2	87.5(2)	91.7(2)	98.6(4)	O2–M–N1	89.2(2)	90.7(2)	91.3(4)
O2–M–N3	86.9(3)	88.0(3)	88.5(5)	O2–M–N2	90.1(2)	94.2(2)	98.3(5)
O4–M–N1	89.0(3)	90.0(3)	89.4(3)	O2–M–N3	96.6(2)	89.4(2)	87.4(4)
O4–M–N2	94.0(2)	98.2(2)	101.9(2)	O4–M–N1	91.2(2)	90.1(2)	93.6(5)
O4–M–N3	93.1(3)	92.2(3)	92.1(3)	O4–M–N2	88.8(2)	94.6(2)	144.4(5)
N1–M–N2	73.9(2)	75.1(2)	76.6(3)	O4–M–N3	88.4(2)	90.6(2)	90.9(5)
N2–M–N3	95.7(3)	98.0(2)	97.7(4)	N1–M–N2	78.2(2)	79.8(2)	82.8(8)
N1–M–N3	169.4(3)	172.9(4)	174.3(3)	N2–M–N3	93.1(2)	94.5(2)	93.0(8)
				N1–M–N3	171.2(2)	174.3(2)	175.4(3)

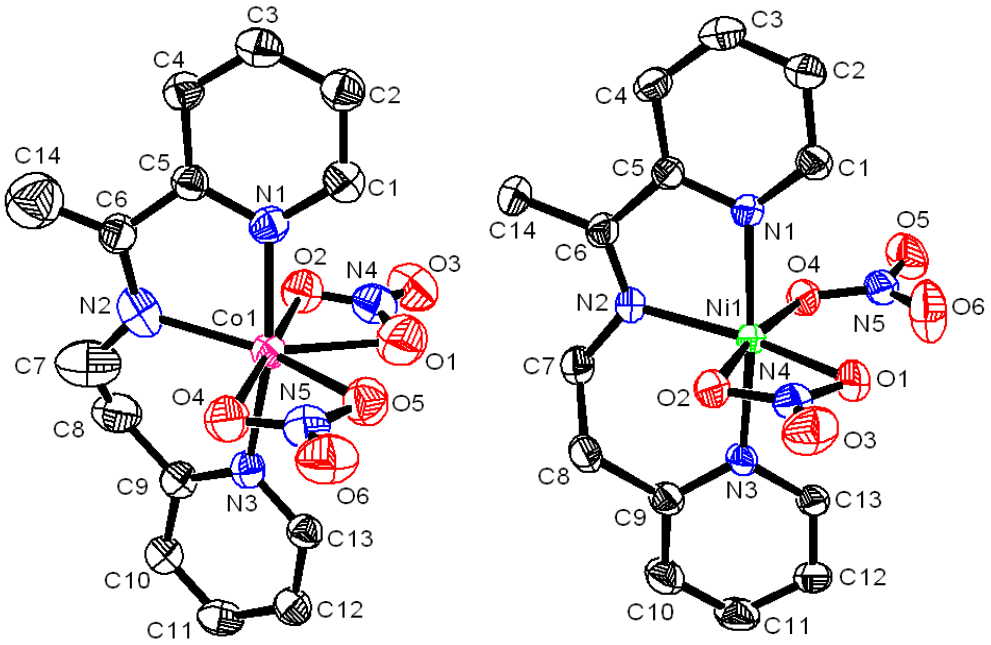

Figure 4. ORTEP diagram of **2** and **4** (30% probability, hydrogens are omitted).

The $M–N_{im}$ and $M–N_{py}$ bond lengths follow the order Co > Ni > Cu and is consistent with the trend in the relative size of the bivalent ions. Notable is the parameters of the methylketimine function in complex **6**: N2–C6 and C6–C14 bonds in **6** are respectively longer and shorter than those observed in **2** and **4**. In **6**, the sum of the three angles subtended at N2 and C6 are respectively 355.7(16)º and 354.3(19)º and these values are very much closer to 360º in **2** and **4**. A perspective view of molecular packing diagram of **2** shown in Figure 6, indicates the presence of C3···O2, C3···O4, C11···O2, C11···O4, C13···O6, and C14···O5 donor-acceptor interactions. The molecular packing of **4** shows a transverse wave like pattern along the *b*-axis with a distance of around 18.91 Å between two crests (Figure 7). The intermolecular interactions C3···O4, C4···O4, C4···O5, and C12···O6, are present in this packing. In case of **6**, a layered sheet observed on viewing down the *b*-axis. Non-bonded intermolecular contacts C11···O5, C12···O6, C14···O4, C3···O5, C2···O3, C1···O3, and π–π interaction of 3.365(13) Å between C4···C10, are important factors responsible for layered stacking.

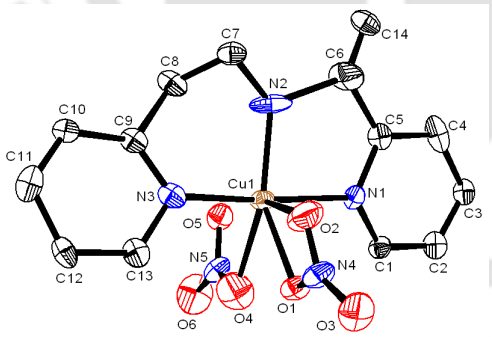

Figure 5. ORTEP diagram of **6** (30% probability, hydrogens are omitted).

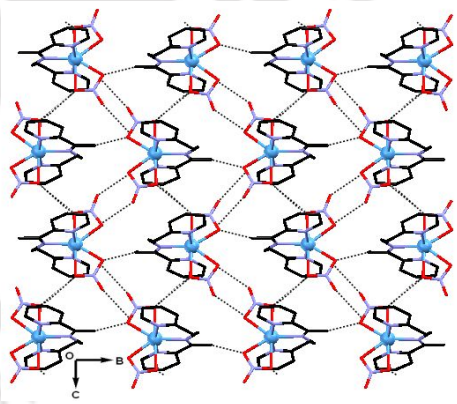

Figure 6. Molecular packing of **2** viewing down the *a*-axis.

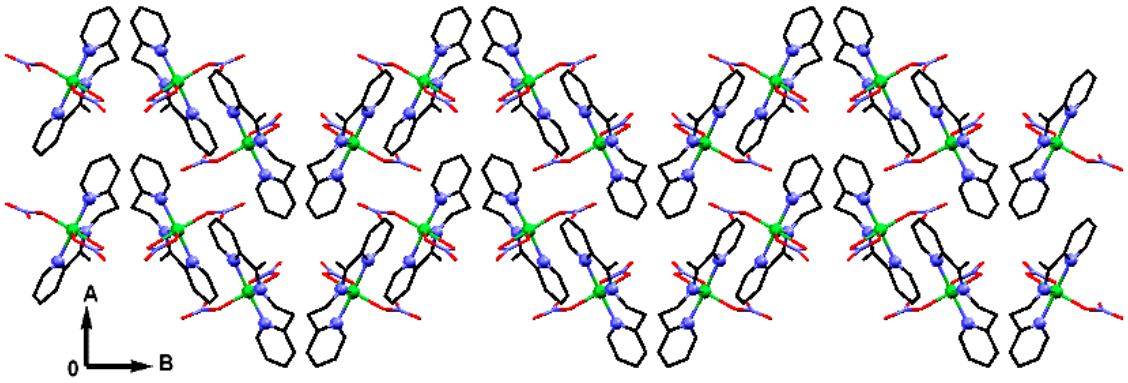

Figure 7. Molecular packing of **4,** viewing down the *c*-axis.

2.1.5 Thermogravimetric (TG) Analysis

TG and DTG curves, shown in Figure 8, (all the temperatures noted in this section are onset mid-point temperatures) of **1** and **3** shows weight loss in two distinct steps: in the first step, loss of the ligand **L4** (found 52.9, 52.7%; *ca*. 53.6, 53.5%;) occurs at 276 °C and 273 °C respectively and in the second step, loss of two moles of NO_2 and half mole of O_2 gas are at 570 °C and 482 °C. Whereas, in **5** the loss (84.3%) of ligand **L4**, two moles of NO_2 and one mole of O_2 (*ca.* 84.2%) all occurring in a single step at 266 °C. This indicates that the thermal stability order Co(II) > Ni(II) > Cu(II).

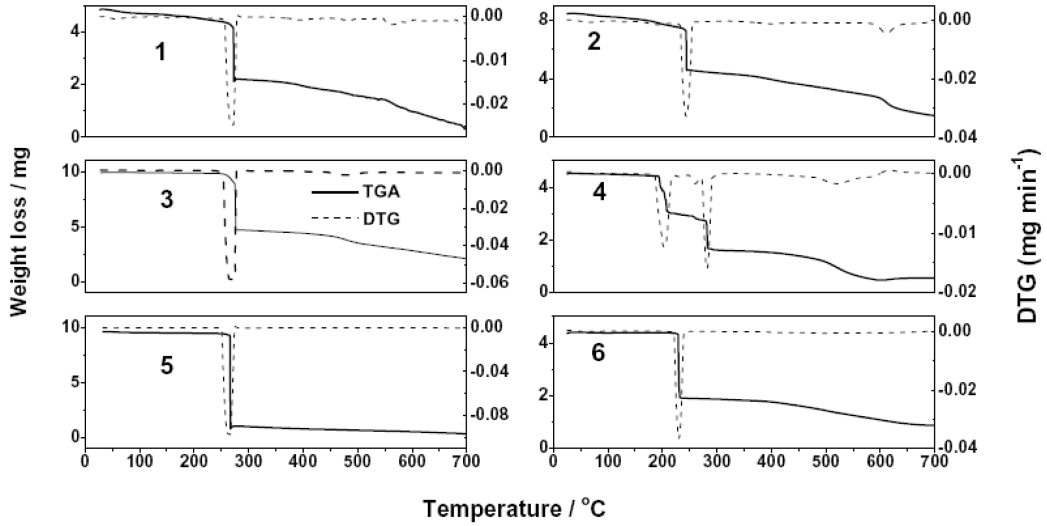

Figure 8. TG profiles of **1–6**.

Complex **2** show three steps of pyrolysis. At 189 °C release of one mole of O_2 (found 7.91%; *ca.* 7.84%) occurs, followed by two moles of pyridine (found 38.81%; *ca.* 38.75%) at 252 °C. The third step is at 609 °C wherein two moles of NO along with half mole of O_2 (found 18.58%; *ca.* 18.62%) are released. Complex **4** also shows weight loss in three distinct steps: first step is the loss of the two moles of pyridine (found 38.72%; *ca*. 38.84%) occurs at 225 °C; loss of two moles of NO_2 and half mole of O_2 (found 26.46%; *ca*. 26.54%) at 280 °C; and finally release of half mole of O_2 at 540 °C (found 4.51%; *ca.* 4.41%). In **6**, the loss (found 57.01%; *ca.* 56.67%) of two moles of pyridine, two moles of NO and half mole of O_2, all occur in a single step at 230 °C. In all the cases, the identities of the final residuals were not analyzed.

3.3 Conclusion

The complexes of the type [M(**L4**/**L5**)$(NO_3)_2$] (M = Co(II), Ni(II), Cu(II)) based on a tridentate N_3–donor ligand, were isolated and characterized using spectral, thermal and

single crystal X-ray studies. The imines **L4** and **L5** having an intervening ethylene group when treated with methanolic solution of Co^{2+}, Ni^{2+} and Cu^{2+} nitrates coordinated readily to the bivalent metal centre without any change in the ethylene and imine functions. In **1**, cobalt(II) has overall distorted pentagonal bipyramidal geometry with N_3O_4 chromophore whereas in **2**, has pseudo-octahedral geometry with N_3O_3 chromophore including all other complexes. The $M–N_{im}$ and $M–N_{py}$ bond lengths follow the order Co > Ni > Cu. All the complexes exhibit d-d transitions in the visible region and intraligand charge transfer in the visible region. The X-band EPR spectra of **4** and **5** shows an isotropic spectrum split by hyperfine coupling at room temperature and an axial spectrum with splitting due to a slight rhombic symmetry at 77 K. The trend, $g_1 > g_2 > g_3$ and hyperfine splitting of the g_1 signal are observed. Thermal stability order is **1** > **3** > **5**, showing a reverse Irving-Williams trend.

Chapter 4

Reactivity of Schiff Bases Having an Imine Function Only

Abstract: The Schiff base ligands **L6–L10** reacted readily with $Co(NO_3)_2 \cdot 6H_2O$ and form complexes having the molecular formulae $[Co(\mathbf{L6O})_2]NO_3$ (**1**), $[Co(\mathbf{L7O})_2]NO_3 \cdot xH_2O$ (**2a**, x = 2; **2b**, x = 3), $[Co(\mathbf{L8O})_2]NO_3$ (**3**), $[Co(\mathbf{L9O})_2]NO_3 \cdot 2H_2O$ (**4**), $[Co(\mathbf{L10O})_2]NO_3$ (**5**) and $[Co(\mathbf{L7O})_2]PF_6$ (**6**). In these reactions one molecule of water has added across the imine function and the resulting alcoholate ion remain bound in a facial tridentate N_2O fashion to the low-spin cobalt(III). X-ray crystal structure determination revealed the presence of *trans-trans-trans*-N_AN_PO (A = aminopyridyl and P = pyridyl) disposition in **2a** and *cis-cis-trans*-N_AN_PO in **2b**, **4** and **6**. A water dimer in **2a**, **2b** and **4** and water–nitrate ion network in **2a** are notable features in the crystal packing. The UV-Visible spectra of the complexes exhibit the two spin-allowed transitions $^1A_{1g} \rightarrow {}^1T_{1g}$ and $^1A_{1g} \rightarrow {}^1T_{2g}$.

Chapter 4

Reactivity of Schiff Bases Having an Imine Function Only

In this chapter, the reactivity of the Schiff base containing the imine function only, with bivalent cobalt is described.

	R	R_1	R_2
L6	CH_3	H	H
L7	H	CH_3	H
L8	CH_3	CH_3	H
L9	H	H	CH_3
L10	CH_3	H	CH_3

4.1 Experimental

4.1.1 Syntheses

The ligands used in this study *viz.,* **L6**, **L7**, **L8**, **L9** and **L10**, were prepared by adopting the procedure described for **L1** (Chapter 2) using 4.57 mmol each of appropriate amine and aldehyde or ketone.

N-[1-Pyridine-2-ylethylidene]pyridine-2-amine (L6). Yield: 775 mg, 86%. ^{1}H NMR (δ (*J*, Hz), $CDCl_3$): 2.73 (3H,s), 6.47 (1H, d, 8.4), 6.59 (1H, m), 7.39 (1H, m), 7.44 (1H, m), 7.80 (1H, m), 8.01 (1H, d, 10), 8.02 (1H, d, 3.2), 8.66 (1H, d, 6.4). IR (neat, cm^{-1}): 1695 ($C=N_{im}$), 1620 ($C=N_{py}$).

3-Methyl-N-[1-pyridine-2-ylmethylidene]pyridine-2-amine (L7). Yield: 740 mg, 82%. ^{1}H NMR (δ (*J*, Hz), $CDCl_3$): 2.10 (3H, s), 6.57 (1H, t, 6.0), 7.22 (1H, d, 8.8), 7.49 (1H, t, 6.8), 7.82 (1H, t, 7.2), 7.91 (1H, d, 6.8), 7.93 (1H, d,7.6), 8.76 (1H, d, 6.0), 10.5 (1H, s). IR (neat, cm^{-1}): 1695 ($C=N_{im}$), 1620 ($C=N_{py}$).

3-Methyl-N-[1-pyridine-2-ylethylidene]pyridine-2-amine (L8). Yield: 820 mg, 87%. ^{1}H NMR (δ (*J*, Hz), $CDCl_3$, Figure 1): 2.10 (3H, s), 2.72 (3H, s), 6.57 (1H, t, 6.0), 7.22 (1H, d, 9.6), 7.45 (1H, t, 6.2), 7.79 (1H, t, 8.6), 7.90 (1H, d, 4.8), 8.01 (1H, d, 10), 8.65 (1H, d, 6.4). IR (neat, cm^{-1}): 1715 ($C=N_{im}$), 1590 ($C=N_{py}$).

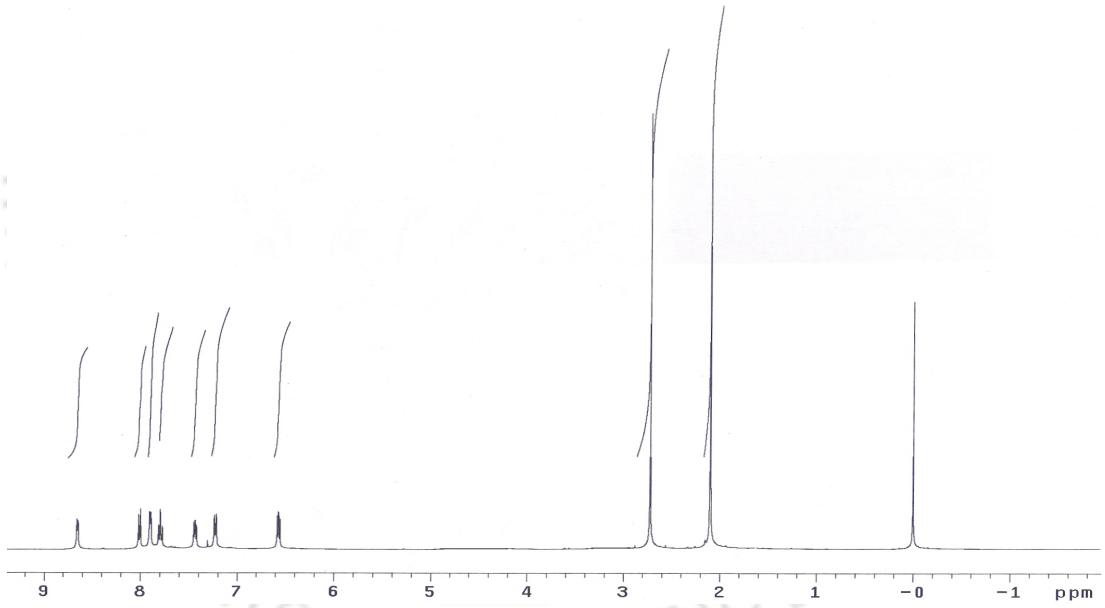

Figure 1. ^{1}H NMR Spectrum of **L8** (400 MHz, $CDCl_3$).

4-Methyl-N-[1-pyridine-2-ylmethylidene]pyridine-2-amine (L9). Yield: 740 mg, 82%. ^{1}H NMR (δ (*J*, Hz), $CDCl_3$): 2.15 (3H, s), 6.36 (1H, s), 6.44 (1H, d, 8.4), 7.49 (1H, t, 6.2), 7.61 (1H, t, 7.6), 7.86 (1H, d, 5.6), 7.94 (1H, d, 8.8), 8.76 (1H, d, 4.4), 10.05(1H, s). IR (neat, cm^{-1}): 1695 ($C=N_{im}$), 1620 ($C=N_{py}$).

4-Methyl-N-[1-pyridine-2-ylethylidene]pyridine-2-amine (L10). Yield: 790 mg, 82%. ^{1}H NMR (δ (*J*, Hz), $CDCl_3$): 2.22 (3H, s), 2.73 (3H, s), 6.31 (1H, s), 6.45 (1H, d, 5.6), 7.45 (1H, t, 6.8), 7.81 (1H, t, 8.4), 7.90 (1H, d, 5.2), 8.01 (1H, d,8.8), 8.66 (1H, d, 6.4). IR (neat, cm^{-1}): 1715 ($C=N_{im}$), 1595 ($C=N_{py}$).

$[Co(L6O)_2]NO_3$ (1): To 167 mg (0.85 mmol) of **L6** dissolved in 25 mL of methanol, was added 123 mg (0.42 mmol) of $Co(NO_3)_2{\cdot}6H_2O$ dissolved in 20 mL methanol with stirring. After stirring for 4 h, the pink colored solid precipitated was separated by filtration, washed thoroughly with ice-cold methanol and dried over P_4O_{10} under vacuum. Yield: 130 mg 56%. $C_{24}H_{24}N_7O_5Co$ (549.4): calcd. C 52.44, H 4.41, N 17.85; found C 52.20, H 4.33, N 17.57%. IR (KBr, cm^{-1}): 1635 ($C=N_{py}$), 1512, 1385 (NO_3).

Complexes **2**, **3**, **4**, **5**, were prepared following the same procedure described for **1** using 0.85 mmol of respective **L** and 0.42 mmol of $Co(NO_3)_2{\cdot}6H_2O$.

$[Co(L7O)_2]NO_3{\cdot}xH_2O$ (2): Yield: 170 mg, 75%. $C_{24}H_{24}N_7O_5Co$ (549.1): calcd. C 52.44, H 4.41, N 17.85; found C 52.25, H 4.29, N 17.62%. IR (KBr, cm^{-1}): 1640 ($C=N_{py}$), 1510, 1385 (NO_3). Crystals of X-ray quality were grown by slow evaporation of methanol (**2a**, $x = 2$) solution and acetonitrile (**2b**, $x = 3$).

$[Co(L8O)_2]NO_3$ (3): Yield: 153 mg, 63%. $C_{26}H_{28}N_7O_5Co$ (577.2): calcd. C 54.06, H 4.89, N 16.98; found C 54.25, H 4.91, N 16.79%. IR (KBr, cm^{-1}): 1634 ($C=N_{py}$), 1514, 1383 (NO_3).

$[Co(L9O)_2]NO_3 \cdot 2H_2O$ (4): Yield: 108 mg, 47%. $C_{24}H_{28}N_7O_7Co$ (549.1): calcd. C 52.44, H 4.41, N 17.85; found C 52.59, H 4.35, N 17.73%. IR (KBr, cm^{-1}): 1637 ($C=N_{py}$), 1513, 1384 (NO_3). Crystals of X-ray quality were grown by slow evaporation of acetonitrile solution.

$[Co(L10O)_2]NO_3$ (5): Yield: 119 mg, 49%. calcd. $C_{26}H_{28}N_7O_5Co$ (577.2): C 54.06, H 4.89, N 16.98; found C 53.93, H 4.78, N 16.79%. IR (KBr, cm^{-1}): 1636 ($C=N_{py}$), 1515, 1384 (NO_3).

$[Co(L7O)_2]PF_6$ (6): To 180 mg (0.33 mmol) of **2** dissolved in 25 mL of acetonitrile, was added an aqueous solution of 184 mg (1 mmol) of KPF_6 and stirred vigorously for 1h. The solution was evaporated to dryness in vacuum, the solid was dissolved in acetonitrile, filtered and to the filtrate another 184 mg (1 mmol) of KPF_6 and repeated as above. The X-ray quality crystals were obtained by slow-evaporation of acetonitrile solution. Yield: 170 mg, 82%. $C_{24}H_{24}N_6O_2PF_6Co$ (632.4): calcd. C 45.54, H 3.83, N 13.28; found C 45.41, H 3.76, N 13.16%. IR (KBr, cm^{-1}): 1619($C=N_{py}$), 1514, 838 (P–F).

4.2 Results and Discussion

4.2.1 Synthesis

The coordination chemistry of **L1** and **L2** with Cu^{2+} ion presented in Chapter 2 and that of **L4** and **L5** towards the bivalent ions presented in Chapter 3, prompted to explore

the chemistry of **L6–L10** with the bivalent metal ions. A crystalline solid product could be isolated in the reactions of **L6–L10** with $Co(NO_3)_2 \cdot 6H_2O$ (Scheme 1). In these reactions Co^{2+} is oxidized to Co^{3+} and the –(R)C=N– (R = H or CH_3) group are converted to –(R)(OH)C–NH– group. That is, one molecule of water has been added across the imine function. The Schiff bases are known to undergo complete hydrolysis in presence protic/Lewis acids, to the respective amine and aldehyde/ketone. This hydrolysis involves nucleophilic addition of a molecule of water to the imine function, forming the unstable alcoholate intermediate which readily dissociates. In the reaction of **L6–L10** with Co^{2+} ion, the coordination of two molecules of the Schiff base to one Co^{2+} ion could occur in which **L6–L10** bind in a bidentate fashion and having a seven-membered chelate ring (but a tridentate coordination will have a four- and five-membered rings). At this point one molecule of water (may be from the bulk or that coordinated to the metal center) attack the imine function that is accompanied by the oxidation of the Co^{2+} to Co^{3+} and since the low-spin Co^{3+} is substitutionally inert ion, the further dissociation of the alcoholate intermediate is stopped and remain coordinated to the Co^{3+} ion. Or if the *trans*–$[Co(\mathbf{L})_2(H_2O)_2]^{2+}$ ion (structural studies revealed that the disposition of the two O atoms is always *trans, vide infra*) is pre-formed then the sequence of nucleophilic addition of water or oxidation of Co^{2+}, should be studied with suitable methods. The molecular structure of the related compound, bis[(2-pyridyl)(2-pyridylamino)methanolato]cobalt(III) perchlorate complex, synthesized by the oxidative deamination of tris(pyridyl)aminal, *viz.,* (2-pyridyl)bis(2-pyridylamino) methanol ligand has been reported earlier.[253–254] With Cu^{2+} and Ni^{2+} salts complete hydrolysis of **L6–L10** has been observed.

Scheme 1

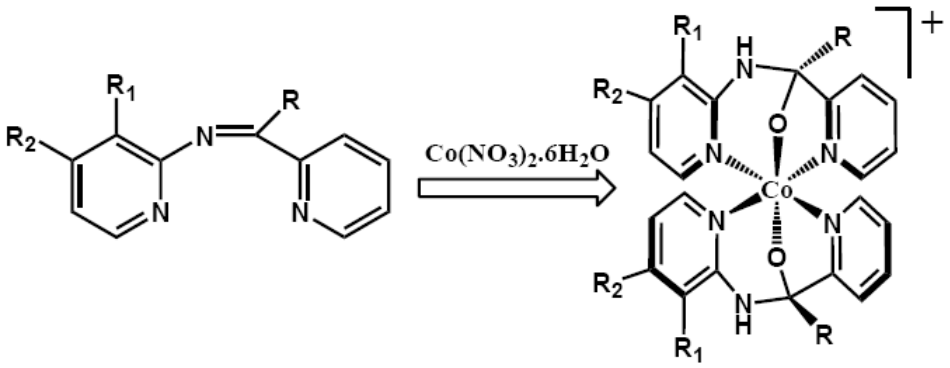

4.2.2 Optical Properties

The UV-Visible spectra of the complexes were recorded in the region of 200–1100 nm in methanol. Low-spin cobalt(III) complexes has a $^1A_{1g}$ ground state and therefore the spin-allowed transitions $^1A_{1g} \rightarrow {}^1T_{1g}$ and $^1A_{1g} \rightarrow {}^1T_{2g}$ are usually observed. In **1**–**6**, the former occur in the range 510 – 520 nm and the later at around 395 nm as a shoulder of the intense intra-ligand transitions.[243] The λ_{max} and their molar extinction coefficient values are listed in Table 1.

Table 1. Electronic Excitation Data in the Complexes **1**–**6** in methanol

Complex	λ_{max}, nm (ε, M^{-1} cm^{-1})
1	515(90), 395(250)[a], 267(915), 227(1320)
2	516(75), 395(220)[a], 304(1070), 266(1125), 230(2630)
3	518(75), 395(165)[a], 268(1445), 224(3390)
4	516(60), 395(200)[a], 317(600), 267(2290), 222(5370)
5	507(150), 395(280)[a], 310(600), 268(2140), 224(5010)
6	513(125), 395(380)[a], 305(1150), 267(1860), 234(3630)

[a] Shoulder

4.2.3 Molecular Structures

The molecular structures of **2a**, **2b**, **6**, and **4** were determined by X-ray crystallography. The crystallographic data and refinement parameters are summarized in Table 2.

In each case, the low-spin cobalt(III) is hexa-coordinated and has a pseudo-octahedral geometry. Two mono-anionic, facially coordinating, tridentate-N_2O ligands are bound to the metal center. The four pyridyl nitrogen atoms occupy the basal plane and the two oxygen atoms are at the apical positions leading to an overall *trans*-N_4O_2 chromophoric environment. The ligand forms a five and six membered chelate ring, both having the envelope conformation with the oxygen atom being at the apex of the flap. The Co–N bond distance in the six membered chelate rings is longer than that of the five membered one and the Co–N bond distances are longer than the Co–O distances. These feature are also observed in bis[(2-pyridyl)(2-pyridylamino)methanolato]cobalt(III) perchlorate.[254] The selected bond distances listed in Table 3 and the bond angles are provided Tables 4 and 5.

The complex $[Co(\mathbf{L7O})_2]NO_3 \cdot 2H_2O$ (**2a**), crystallized in the orthorhombic *Pbca*. The asymmetric unit contains a centro-symmetric half molecule along with two waters of crystallization and a nitrate ion that refined poorly. The two amine nitrogen atoms are *trans* to each other and the overall stereochemistry is *trans-trans-trans*-N_ANpO (A = aminopyridyl and P = pyridyl). A perspective view of $[Co(\mathbf{L7O})_2]^+$ ion in **2a** is shown in Figure 2. The Co–N bond distance in the six membered chelate rings is longer by 0.087 (3) Å than that of the five membered one and the Co–N bond distances are longer than the Co–O distance. The atoms Co1–N1–C5–C6, Co1–N3–C7–N2–C6, respectively form the base of the envelope, in five membered, six membered chelate rings and lie in a plane.

The molecular packing diagram reveals the presence of water–nitrate ion network as shown in Figure 2. Layers of this network is present along the *ab* plane and incorporates

a water dimer (O2···O3, 2.68 (3) Å) linked by the nitrate ion. The link contains the following non-bonded contacts: O4···O5 (2.85 (3) Å); O5···O3 (2. 80 (3) Å); O6···O3 (2.74 (1) Å) and O2···O6 (2.85 (1) Å). These layers are in turn linked to the $[Co(\mathbf{L7O})_2]^+$ units by N2···O5 (2.86 (1) Å) and O1···O2 (2.70 (1) Å) hydrogen bonds.

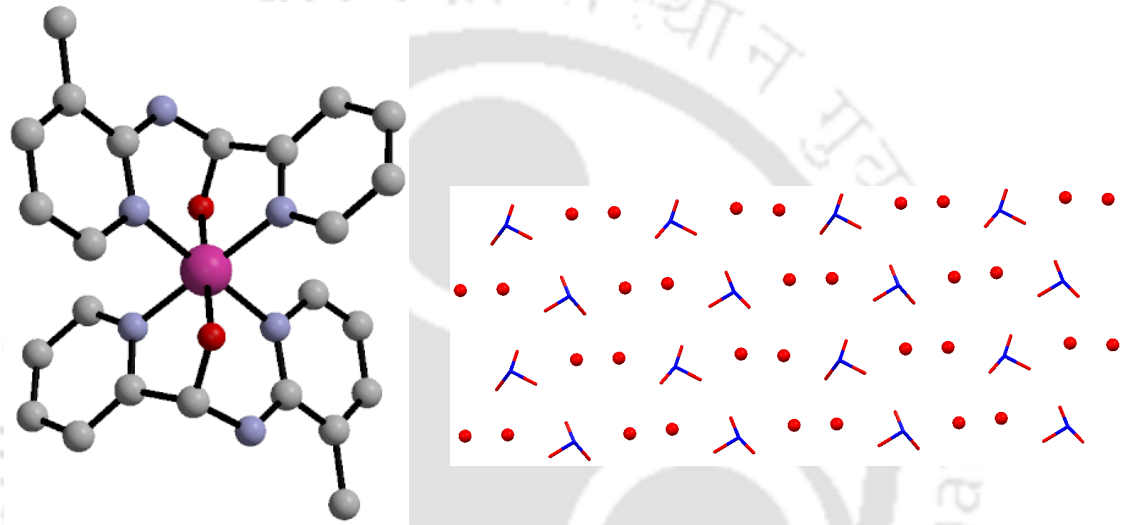

Figure 2. Ball and Stick diagram of **$[Co(L7O)_2]^+$** and water–nitrate ion network in **2a**.

Crystals of $[Co(\mathbf{L7O})_2]NO_3 \cdot 3H_2O$ (**2b**) were obtained from slow evaporation of the acetonitrile solutions. One water molecule is disordered and refined with variable site occupancy factors (O8 = 0.6 and O9 = 0.4). In this case, the two amine nitrogen atoms are *cis* to each other in the $[Co(\mathbf{L7O})_2]^+$ unit and the overall stereochemistry is *cis-cis-trans*-N_ANPO (A = aminopyridyl and P = pyridyl). A perspective view of

[Co(L7O)$_2$]NO$_3$ is shown in Figure 3. The *trans* spanning angles O1–Co1–O2, 174.17(9)°; N1–Co1–N6, 179.05(12)° and N3–Co1–N4, 177.82(1)° deviate from linearity. The packing diagram (Figure 3) shows the presence of a water dimer O6···O7, 2.87 (1) Å, and is hydrogen bonded to the [Co(**L7O**)$_2$]$^+$ unit through O6···O2, 2.70 (1) Å and O7···N2, 3.04 (1) Å. The notable D···A interactions present are: N5···O4, 2.84(1) Å; N1···O1, 2.71(1) Å: N2···O1, 2.32(1) Å; N3···O1, 2.55(1) Å; N4···O1, 2.80(1) Å and N6···O1, 2.71(1) Å. C24···N5, 2.834(5) Å. The C–H···O interactions C1–H1···O2, 2.911(4) Å; C11–H11···O2, 2.968(4) Å and C23–H23···O1 2.910(4) Å along with the C–H···N interaction C24···N5, 2.834(5) Å are also present.

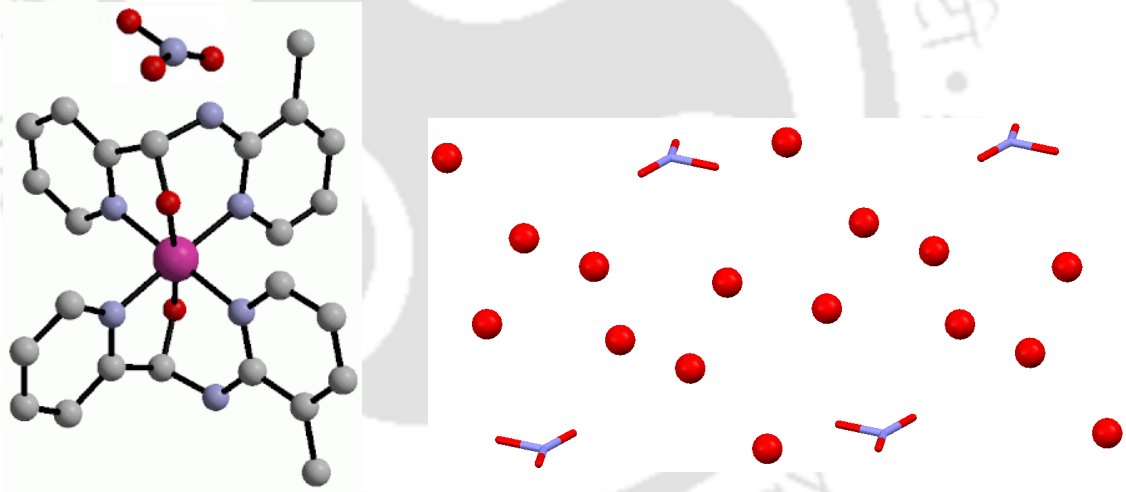

Figure 3. Ball and Stick diagram of **[Co(L7O)$_2$]NO$_3$** and water–nitrate ion links in **2b**.

Complex **6** crystallized in the triclinic *P1*, the asymmetric unit contain the *cis*-$[Co(\mathbf{L7O})_2]^+$ and $[PF_6]^-$ ions and have no solvent of crystallization. The two amine nitrogen atoms are *cis* to each other in the $[Co(\mathbf{L7O})_2]^+$ units, as observed in **2b** and the overall stereochemistry is *cis-cis-trans*-N_ANpO (A = aminopyridyl and P = pyridyl). A perspective view of **6** is shown in Figure 4. The *trans* angles N1–Co1–N5, 179.6(3)°; N2–Co1–N4, 178.8(3)° and O1–Co1–O2, 177.1(4)° deviates from linearity. The molecular packing show the existence of C–H···O, C–H···F, C–H···N and N–H···F hydrogen bonding, is displayed in Figure 4.

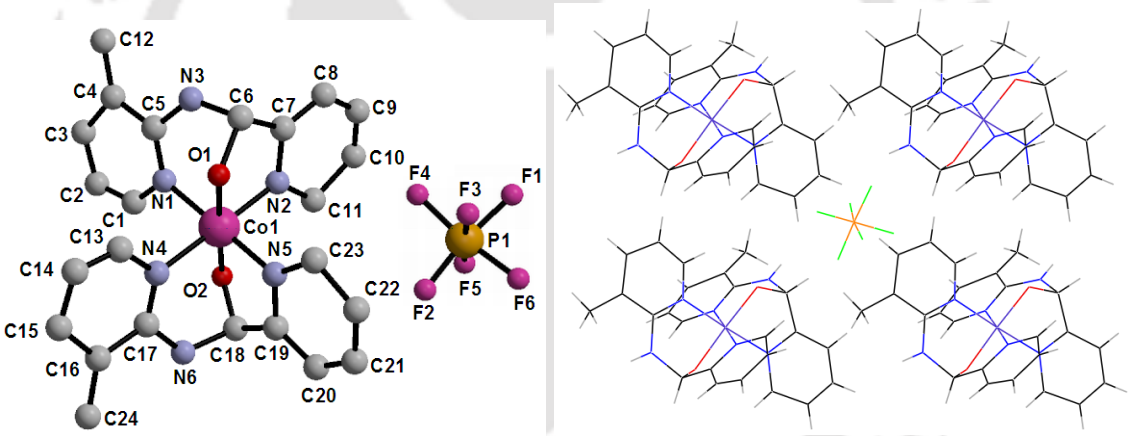

Figure 4. Ball and Stick representation of **$[Co(\mathbf{L7O})_2](PF_6)$** and Molecular packing of **6**.

Complex **4** crystallized in the orthorhombic *Pccn* and the asymmetric unit contains a half molecule of $[Co(\mathbf{L9O})_2]^+$ and a nitrate ion along with two water molecules of crystallization. The two amine nitrogen atoms are *cis* to each other in the $[Co(\mathbf{L9O})_2]^+$

units as observed in **2b** and **6**, the overall stereochemistry is *cis-cis-trans*-N_ANPO (A = aminopyridyl and P = pyridyl). A perspective view of **4** is shown in Figure 5. The *trans* angles N1–Co1–N3A, 177.3(1)° and O1–Co1–O1A, 173.6(1)° deviates from linearity. The packing diagram (Figure 5) shows the presence of a water dimer O5···O6, 2.73 (1) Å and the following significant hydrogen bonding interactions, O1···O5, 2.74 (1) Å; O3···O5, 2.84 (1) Å; O2···O6, 2.90 (1) Å and N2···O6, 2.82 (1) Å.

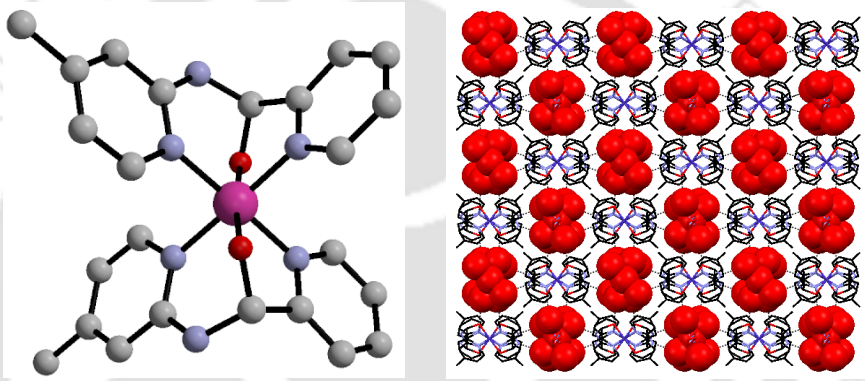

Figure 5. Ball and Stick representation of **$[Co(L9O)_2]^+$** and Molecular packing of **4**.

Table 2. Crystal data and Refinement Parameters

	2a	**2b**	**6**	**4**
Empirical formula	$C_{24}H_{28}N_7O_7Co$	$C_{24}H_{30}N_7O_8Co$	$C_{24}H_{24}F_6N_6O_2PCo$	$C_{24}H_{28}N_7O_7Co$
Formula weight	585.43	603.43	632.39	603.43
Temperature	296(2)	296(2)	296(2)	296(2)
Wavelength, Å	0.71073	0.71073	0.71073	0.71073
Crystal system	Orthorhombic	Triclinic	Triclinic	Orthorhombic

Space group	*Pbca*	*P*	*P1*	*Pccn*
a, Å	19.009(1)	8.463(1)	7.860(1)	12.307(1)
b, Å	8.412(1)	10.289(1)	8.556(1)	14.068(1)
c, Å	19.009(1)	15.954(1)	9.892(1)	16.6978(1)
α, deg		89.521(2)	88.110(2)	
β, deg		87.510(2)	85.931(2)	
γ, deg		84.385(2)	73.999(2)	
V, Å3	3040.0(1)	1381.3(18)	637.8(1)	2890.9(2)
Z	4	2	1	4
D_{calc}, (g cm^{-3})	1.484	1.436	1.646	1.534
μ, (mm^{-1})	0.614	0.681	0.816	0.673
[a]GOF on F^2	1.015	1.024	1.031	1.022
R [I>2σ(I)]	[b]R_1 = 0.0645	[b]R_1 = 0.0563	[b]R_1 = 0.0619	[b]R_1 = 0.0478
	[c]wR_2 = 0.1292	[c]wR_2 = 0.1674	[c]wR_2 = 0.1577	[c]wR_2 = 0.1313
R indices (all data)	[b]R_1 = 0.1743	[b]R_1 = 0.0817	[b]R_1 = 0.0751	[b]R_1 = 0.0824
	[c]wR_2 = 0.2104	[c]wR_2 = 0.1932	[c]wR_2 = 0.1693	[c]wR_2 = 0.1580

[a]GOF = $[\Sigma[w(F_0^2 - F_c^2)^2]/M - N]^{1/2}$ (M = number of reflections, N = number of parameters refined). [b]$R_1 = \Sigma ||F_0| - |F_c||/\Sigma|F_0|$. [c]$wR_2 = [\Sigma[w(F_0^2 - F_c^2)^2]/ \Sigma[w(F_0^2)^2]]$.

Table 3. Selected Bond Distances (Å)

2a		**2b**		**4**		**6**	
Co1–N1	1.906(3)	Co1–N1	1.970(3)	Co1–N1	1.967(2)	Co1–N1	1.950(6)
Co1–N3	1.993(3)	Co1–N3	1.927(3)	Co1–N3	1.926(2)	Co1–N3	1.928(6)
Co1–N4		Co1–N4	1.972(2)	Co1–N4		Co1–N4	1.970(6)

Co1–N6		Co1–N6	1.917(3)	Co1–N6		Co1–N6	1.907(7)
Co1–O1	1.862(3)	Co1–O1	1.865(2)	Co1–O1	1.884(2)	Co1–O1	1.883(6)
Co1–O2		Co1–O2	1.893(2)	Co1–O2		Co1–O2	1.891(5)

Table 4. Selected Bond Angles (º)

2a		**4**	
O1–Co1–O1A	180.00(3)	O1–Co1–O1A	173.62(10)
O1–Co1–N1	85.33(12)	O1–Co1–N1	90.89(8)
O1–Co1–N1A	94.67(12)	O1–Co1–N1A	93.65(8)
O1–Co1–N3	91.92(12)	O1–Co1–N3	91.79(8)
O1–Co1–N3A	88.08(12)	O1–Co1–N3A	83.70(8)
N1–Co1–N3	90.38(13)	N1–Co1–N3	90.11(8)
N1–Co1–N3A	89.61(13)	N1–Co1–N3A	177.32(8)
N1–Co1–N1A	180.00(3)	N1–Co1–N1A	89.49(11)
N3–Co1–N3A	179.99 (1)	N3–Co1–N3A	90.41(11)

Table 5. Selected Bond Angles (º)

6		**2b**	
O1–Co1–O2	177.1(4)	O1–Co1–O2	174.17(9)
O1–Co1–N1	89.1(3)	O1–Co1–N1	89.74(11)
O1–Co1–N3	85.4(3)	O1–Co1–N3	84.44(10)
O1–Co1–N4	92.6(3)	O1–Co1–N4	93.53(10)
O1–Co1–N6	92.0(3)	O1–Co1–N6	91.19(11)
O2–Co1–N1	93.3(3)	O2–Co1–N1	95.17(11)
O2–Co1–N3	92.9(3)	O2–Co1–N3	92.43(11)
O2–Co1–N4	89.2(3)	O2–Co1–N4	89.67(10)
O2–Co1–N6	85.7(3)	O2–Co1–N6	83.89(11)
N1–Co1–N3	89.7(2)	N1–Co1–N3	89.75(11)
N1–Co1–N4	89.2(3)	N1–Co1–N4	89.46(10)
N1–Co1–N6	179.0(4)	N1–Co1–N6	179.05(11)
N3–Co1–N4	177.7(3)	N3–Co1–N4	177.82(10)
N3–Co1–N6	90.5(3)	N3–Co1–N6	90.18(11)
N4–Co1–N6	90.7(3)	N4–Co1–N6	90.65(11)

4.3 Conclusion

The Schiff base ligands **L6–L10** reacted readily with $Co(NO_3)_2 \cdot 6H_2O$ and form complexes having the molecular formulae $[Co(\mathbf{L6O})_2]NO_3$ (**1**), $[Co(\mathbf{L7O})_2]NO_3 \cdot xH_2O$ (**2a**, $x = 2$; **2b**, $x = 3$), $[Co(\mathbf{L8O})_2]NO_3$ (**3**), $[Co(\mathbf{L9O})_2]NO_3 \cdot 2H_2O$ (**4**), $[Co(\mathbf{L10O})_2]NO_3$ (**5**) and $[Co(\mathbf{L7O})_2]PF_6$ (**6**). In this reaction one molecule of water has added across the imine function and the resulting alcoholate ion remain bound in a facial tridentate N_2O fashion to the low-spin cobalt(III). X-ray crystal structure determination revealed the presence of *trans-trans-trans*-N_ANPO disposition in **2a** and *cis-cis-trans*-N_ANPO in **2b**, **4** and **6**.

SUMMARY of PART A

Following Scheme represents the summary (with the exclusion of the metal salt utilized in the reaction) of Part A, "Metal assisted Transformations in Schiff Bases Containing Pyridyl Groups".

- **L1** reacted readily with $[Cu(OAc)_2(H_2O)]_2$ in methanol affording a compound of composition $[Cu(\mathbf{bpca})(OAc)(H_2O)]\cdot H_2O$, (**bpca** = bis(2-pyridylcarbonyl)amide ion). The active methylene group as well as the imine =CH– undergo oxidation.
- In methanol, **L2** reacted with $Cu(NO_3)_2\cdot 3H_2O$ in air affording green colored solid of formula $\{[Cu(\mathbf{L3})(OH)(NO_3)][Cu(\mathbf{L3})(NO_3)_2]\}\cdot 2H_2O$, where **L3** is 4′-(2-pyridyl)-2,2′:6′,2″-terpyridine. Oxidation of the active-methylene group of **L2** to an imide, followed by its double condensation with 2-acetylpyridine involving a C–C bond forming reaction, mediated by Cu^{2+} ion, are the essential steps involved in the conversion of **L2** to **L3**.

- Imines **L4** and **L5** having an intervening ethylene group remains coordinated to the bivalent metal ion (Co^{2+}, Ni^{2+} and Cu^{2+}) as it is.
- Imines **L6**–**L10** having no intervening group add water across the imine in function on reaction with $Co(NO_3)_2 \cdot 6H_2O$ and convert into the corresponding alcoholate which remain bound to low-spin Co(III).
- The ligands, **bpcaH** and **L3** were isolated in the free form, but **L6OH-L10OH** could not be isolated.

Chapter 5

Binding of 4′-(2-Pyridyl)-2,2′:6′,2″-Terpyridine with Nickel(II)†

Abstract: The mono- and bis- Ni(II) chelates of 4′-(2-pyridyl)-2,2′:6′,2″-terpyridine (**L3**) having the molecular formula $[[Ni(\mathbf{L3})(H_2O)_3](NO_3)_2]_3[Ni(\mathbf{L3})(NO_3)(H_2O)_2](NO_3)\cdot 5H_2O$ (**1**) and $[Ni(\mathbf{L3})_2](PF_6)_2\cdot 2H_2O$ (**2**) respectively are synthesized. The structural, optical and magnetic characteristics are described. The asymmetric unit of (**1**) contains three $[Ni(\mathbf{L3})(H_2O)_3]^{2+}$ (**1a**) and one $[Ni(\mathbf{L3})(NO_3)(H_2O)_2]^{+}$ (**1b**) species along with five water molecules and seven nitrate ions. In both **1a** and **1b**, the bivalent nickel has pseudo-octahedral *mer*-N_3O_3 and in **2**, *mer*-N_3N_3 environments. The molecular packing reveals the presence of water–nitrate ion network, $(NO_3^-)\cdots\pi$ interaction in **1** and $F\cdots\pi$ interaction in **2** and water dimer in both. Both **1** and **2** exhibits d-d transitions in visible and intra-ligand charge transfer (ILCT) in UV regions. The emission spectra are of $\pi \rightarrow \pi^*$ character for λ_{ex} = 345 nm.

† This work has been published in:

Padhi, S. K.; Sahu, R. and Manivannan, V. *Polyhedron* **2008**, *27*, 2221-2225.

Chapter 5

Binding of 4′-(2-Pyridyl)-2,2′:6′,2″-Terpyridine with Nickel(II)

In this chapter the binding of **L3** with bivalent nickel is discussed. The synthesis, spectral properties and the structures of mono- and bis- Ni(II) chelates containing water-nitrate ion network and anion···π interaction are described.

5.1 Experimental

5.1.1 Syntheses

4′-(2-Pyridyl)-2,2′:6′,2″-terpyridine (L3): Has been synthesized using the procedure described in Chapter 2.

[[Ni(L3)(H_2O)$_3$](NO_3)$_2$]$_3$[Ni(L3)(NO_3)(H_2O)$_2$](NO_3)·5H_2O (1): To 41 mg (0.13 mmol) of 4′-(2-pyridyl)-2,2′:6′,2″-terpyridine (**L3**) dissolved in 20 mL of methanol, a methanolic solution (10 mL) of 115 mg (0.395 mmol) $Ni(NO_3)_2·6H_2O$ was added and

stirred for 1 h. After a week, pale green crystals deposited were collected after washing with ice-cold methanol. Yield: 37 mg (50 % based on **L3**). IR, (KBr), cm^{-1}: 1614 ($C{=}N_{py}$), 1558, 1384 (NO_3). Anal. Calcd. for: $C_{80}H_{88}N_{24}O_{40}Ni_4$: C, 42.46; H, 3.89; N, 14.86. Found: C, 42.62; H, 3.96; N, 14.71%. During the crystallization small amounts of reddish-brown crystals of composition $[Ni(\mathbf{L3})_2](NO_3)_2$ were also isolated.

$[Ni(L3)_2](PF_6)_2 \cdot 2H_2O$ (2) To 30 mg (0.10 mmol) of $Ni(NO_3)_2 \cdot 6H_2O$ dissolved in 50 mL of methanol, 63 mg (0.21 mmol) of 4′-(2-pyridyl)-2,2′:6′,2′′-terpyridine and then an aqueous solution of 50 mg (0.27 mmol) of KPF_6 were added with stirring. The reaction mixture was stirred for another 4h and left undisturbed. Block like reddish brown crystals of **2** were obtained after a week. Yield: 62 mg (60%). IR, (KBr), cm^{-1}: 1614 ($C{=}N_{py}$), 1603 ($C{=}N_{py}$), 1573, 1557, 842 (P–F). Anal. Calcd. for: $C_{40}H_{32}F_{12}N_8O_2P_2Ni$: C, 47.74; H, 3.18; N, 11.14. Found: C, 47.81; H, 3.23; N, 11.05%.

5.2 Results and Discussion

5.2.1 Optical Spectra and Magnetism

The UV-Vis spectrum of **1** and **2** in methanol (Figure 1), exhibits d-d transitions in visible and intra-ligand charge transfer (ILCT) in UV regions. The λ_{max} and their molar extinction coefficient values obtained after fitting to Gaussian are listed in Table 1. Both the complexes display the typical transitions, $^3A_{2g} \rightarrow {}^3T_{2g}$ at a lower and $^3A_{2g} \rightarrow {}^3T_{1g}(P)$ at the higher energies. The energy of the $^3A_{2g} \rightarrow {}^3T_{2g}$ transition, follow the trend **2** > **1** in accordance with strong field nature of **L3** compared to H_2O/NO_3^-, while that of the $^3A_{2g} \rightarrow {}^3T_{1g}(P)$ remain invariant. But the transition $^3A_{2g} \rightarrow {}^3T_{1g}(F)$ was not observed which may be obscured by the intra-ligand bands. In case of **1**, and **2** a sharp

spin forbidden transition observed having their maxima at 770 and 750 nm respectively. The intra-ligand charge transfer transitions are of $\pi \rightarrow \pi^*$ and $n \rightarrow \pi^*$(from 4′-(2-pyridyl)) in origin.[243]

Table 1. UV-Visible Data[a]

Complex	λ_{max}, nm (ε, M^{-1} cm^{-1})	
	d–d transition	**ILCT**
1	890(14), 770(1.5), 570(15)	344(8770), 330(10065), 296(15665), 288(28665), 265(37045)
2	800(18), 750(1), 570(13)	347(12010), 330(14630), 358(15250), 300(19170), 288(36880)

[a] In methanol

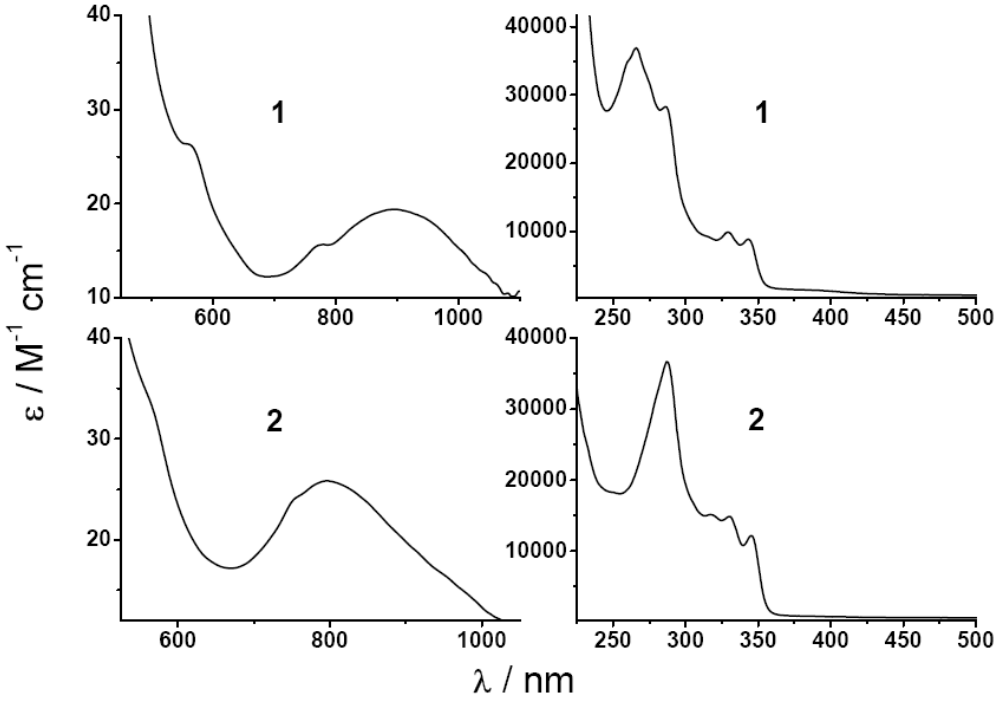

Figure 1. UV-Vis Spectra of **1** and **2**.

The emission spectra of **1** and **2** in acetonitrile, exhibit $\pi \rightarrow \pi^*$ character and indicates that the emission is from a significantly intra-ligand $\pi \rightarrow \pi^*$ state. The envelope of the vibronic structure has a 'domed' shape and the energy spacing within the transition is of the order 8.5 x 10^4 cm^{-1}. This is a typical signature of Frank–Condon envelope type $\pi \rightarrow \pi^*$ emission in polypyridine complexes.[255-259] The structured bands with vibronic

components at 384, 397, 423 and 454 nm (for **1**) and at 385, 403, 423 and 455 nm (for **2**) are observed for λ_{ex} = 345 nm.

The μ_{eff} values calculated from the least square fitting of the initial magnetization curve (χ = M/H) for **1** and **2** are respectively 2.97 and 3.66 B. M. The value is slightly higher than the $\mu_{s.o.}$ value for **1**, and is largely higher for **2**. The complex **2** exhibits a distinct hysteresis loop having the coercivity loss is 186 G.[247-249]

5.2.2 Molecular Structures

The molecular structures of $[[Ni(\mathbf{L3})(H_2O)_3](NO_3)_2]_3[Ni(\mathbf{L3})(NO_3)(H_2O)_2]NO_3\cdot 5H_2O$ (**1**), and $[Ni(\mathbf{L3})_2](PF_6)_2\cdot 2H_2O$ (**2**) were determined by X-ray crystallography. The crystallographic data and refinement parameters are summarized in Table 2. The selected bond distances and bond angles are listed respectively in Table 3 and Table 4.

Table 2. Crystallographic Data and Refinement Parameters

	1	**2**
Empirical formula	$C_{80}H_{88}N_{24}O_{40}Ni_4$	$C_{80}H_{64}F_{24}N_{16}O_4P_4Ni_2$
CCDC number	648157	648158
Formula weight	2260.49	2010.72
Temperature, K	296(2)	296(2)
Wavelength, Å	0.71073	0.71073
Crystal system	Triclinic	Triclinic
Space group	*P*	*P*
a, Å	15.965(1)	16.405(1)
b, Å	17.020(1)	16.461(1)

c, Å	19.960(1)	17.587(1)
α, deg	97.940(2)	94.215(2)
β, deg	110.611(2)	99.433(2)
γ, deg	106.047(2)	113.753(2)
V, Å^3	4708.6(4)	4236.6(3)
Z	2	2
D_{calc}, (g cm^{-3})	1.594	1.578
μ, (mm^{-1})	0.893	0.634
[a]GOF on F^2	1.050	1.044
R [I>2σ(I)]	[b]R_1 = 0.0293	[b]R_1 = 0.0762
	[c]wR_2 = 0.0712	[c]wR_2 = 0.2053
R indices (all data)	[b]R_1 = 0.0293	[b]R_1 = 0.0762
	[c]wR_2 = 0.0713	[c]wR_2 = 0.2053

[a] GOF = $[\Sigma[w(F_0^2 - F_c^2)^2]/M - N]^{1/2}$ (M = number of reflections, N = number of parameters refined) [b]R_1 = $\Sigma \; ||F_0| - |F_c||/\Sigma|F_0|$, [c] wR_2 = $[\Sigma[w(F_0^2 - F_c^2)^2]/ \Sigma[w(F_0^2)^2]]$

The asymmetric unit of **1** contains three dicationic $[Ni(\mathbf{L3})(H_2O)_3]^{2+}$ (**1a**) species and a mono-cationic $[Ni(\mathbf{L3})(NO_3)(H_2O)_2]^{+}$ (**1b**) unit along with five water molecules. Overall, seven nitrate ions are present in the outer sphere to balance the cationic charge. The bond parameters in the three identical **1a** are comparable with each other. A perspective view of one of the **1a** and the **1b** are shown in Figure 2.

Table 3. Selected Bond Distances (Å)

1a		**1b**		**2**	
Ni1–N1	2.115(1)	Ni4–N13	2.144(1)	Ni1–N1	2.118(3)
Ni1–N2	1.988(1)	Ni4–N14	1.993(1)	Ni1–N2	2.005(3)
Ni1–N3	2.093(1)	Ni4–N15	2.114(1)	Ni1–N3	2.117(3)
Ni1–O1	2.097(1)	Ni4–O10	2.068(1)	Ni1–N5	2.123(3)
Ni1–O2	2.067(1)	Ni4–O11	2.107(1)	Ni1–N6	1.989(3)

Ni1–O3	2.024(1)	Ni4–O12	2.069(1)	Ni1–N7	2.121(3)

Table 4. Selected Bond Angles (º)

1a		**1b**		**2**	
N1–Ni1–N2	78.53(5)	N13–Ni4–N14	77.87(5)	N1–Ni1–N2	77.35(12)
N2–Ni1–N3	78.69(5)	N14–Ni4–N15	77.82(5)	N2–Ni1–N3	77.97(11)
N1–Ni1–N3	157.20(5)	N13–Ni4–N15	155.27(5)	N5–Ni1–N6	77.89(12)
N1–Ni1–O1	90.84(5)	N13–Ni4–O10	88.69(5)	N6–Ni1–N7	77.79(12)
N1–Ni1–O2	92.14(6)	N13–Ni4–O11	98.46(5)	N1–Ni1–N3	155.29(12)
N1–Ni1–O3	100.72(6)	N13–Ni4–O12	108.62(6)	N5–Ni1–N7	155.47(12)
N2–Ni1–O1	89.47(5)	N14–Ni4–O10	95.72(5)	N1–Ni1–N5	90.14(13)
N2–Ni1–O2	93.65(5)	N14–Ni4–O11	89.27(5)	N1–Ni1–N6	107.75(12)
N2–Ni1–O3	179.11(6)	N14–Ni4–O12	173.03(6)	N1–Ni1–N7	94.18(12)
N3–Ni1–O1	88.13(5)	N15–Ni4–O10	89.29(5)	N2–Ni1–N5	102.77(12)
N3–Ni1–O2	90.13(6)	N15–Ni4–O11	85.68(5)	N2–Ni1–N6	174.89(12)
N3–Ni1–O3	102.05(6)	N15–Ni4–O12	95.89(6)	N2–Ni1–N7	101.74(12)
O1–Ni1–O2	176.07(6)	O10–Ni4–O11	172.02(5)	N3–Ni1–N5	94.17(12)
O1–Ni1–O3	90.06(5)	O10–Ni4–O12	87.12(6)	N3–Ni1–N6	96.94(11)
O2–Ni1–O3	86.85(6)	O11–Ni4–O12	87.25(5)	N3–Ni1–N7	91.93(12)

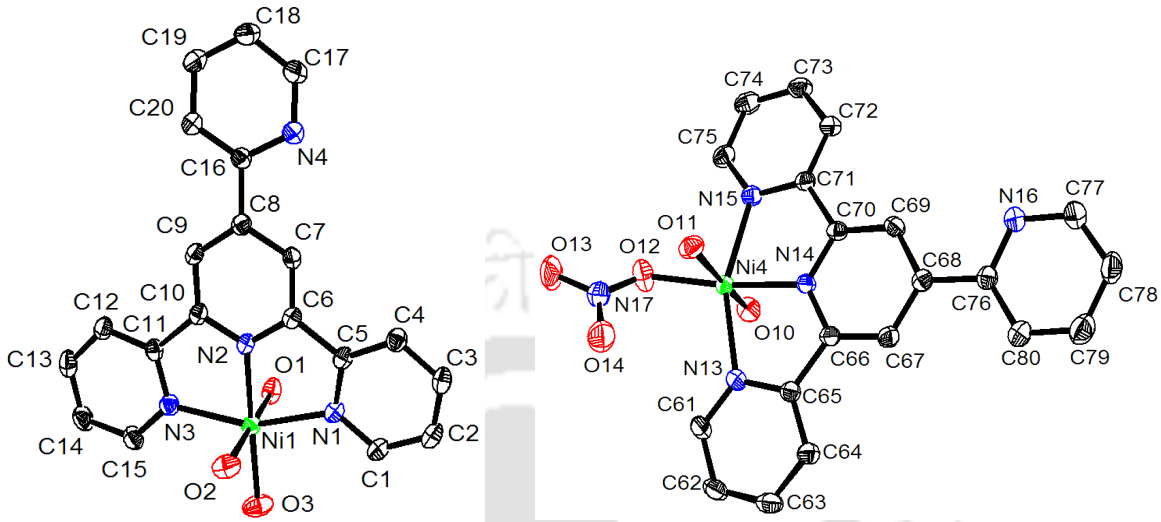

Figure 2. ORTEP (30% probability and hydrogen atoms are omitted) of **1a** and **1b**.

In both **1a** and **1b**, the bivalent nickel is hexa-coordinated and has a distorted octahedral geometry having a *mer*-N_3O_3 environment. The three nitrogen atoms of **L3** occupy sites in the equatorial plane and the fourth equatorial site is occupied by the oxygen atom of a water molecule in **1a** and a monodentate nitrate ion in **1b**. The two axial sites are occupied by two water molecules in both the species. In general, the $Ni–N_{(Y)}$ distances are shorter by 0.124(1) Å than $Ni–N_{(X)}$ and a similar trend is reported in the mono-chelates of terpyridine and its 4′-(phenyl) derivatives.[260-265] This is observed in transition metal complexes of terpyridine and substituted terpyridines is due to a more efficient overlap of metal t_{2g} orbitals with the π* orbitals of the central pyridyl ring. Within the **1b** units, the $Ni–O_{(ax)}$ distances are longer by 0.049(1) Å than that of the $Ni–O_{(eq)}$ distances. In **1a** and **1b**, the intersection of the planes of NiN_3 and NiO_3

deviate from a right angle by 0–4°. The bond angles subtended at the metal center is suggestive of a distorted octahedral geometry. The distortion around the chelating ligand **L3** is more severe as is evident from the *cis*-angles lying in the range 77–79°, while the *trans*-angles are in the range 155–158°. The **Z** rings of **L3** deviate from planarity with respect to **Y** ring by about 5–12(1)°.

The molecular packing of **1** on viewing down the *a*-axis is shown in Figure 3 and contains bands of **1a** and **1b**, juxtaposed with each other exposing the coordinated water and the nitrate for interlinking. The bands also incorporate four of nitrate ions and among them two are held by π–π stacking (with aromatic rings)[266] as well as hydrogen bonding interactions and the other two are by hydrogen bonding interactions only (Figure 3A). These bands are interlinked by layers of five water molecules and the three nitrate ions through hydrogen bonds, leading the network structure. The network consists of centrosymmetric half-units containing crown–shaped $H_2O\cdots H_2O\cdots NO_3\cdots H_2O$–Ni1–$H_2O\cdots NO_3\cdots H_2O$ and chair form of $H_2O\cdots NO_3\cdots H_2O\cdots H_2O\cdots NO_3\cdots H_2O\cdots NO_3\cdots H_2O$ links (Figure 3B). Other notable feature is the presence of a water dimer O36···O40 (2.795(1) Å). The relevant non-bonded interactions are listed in Table 5.

A **B**

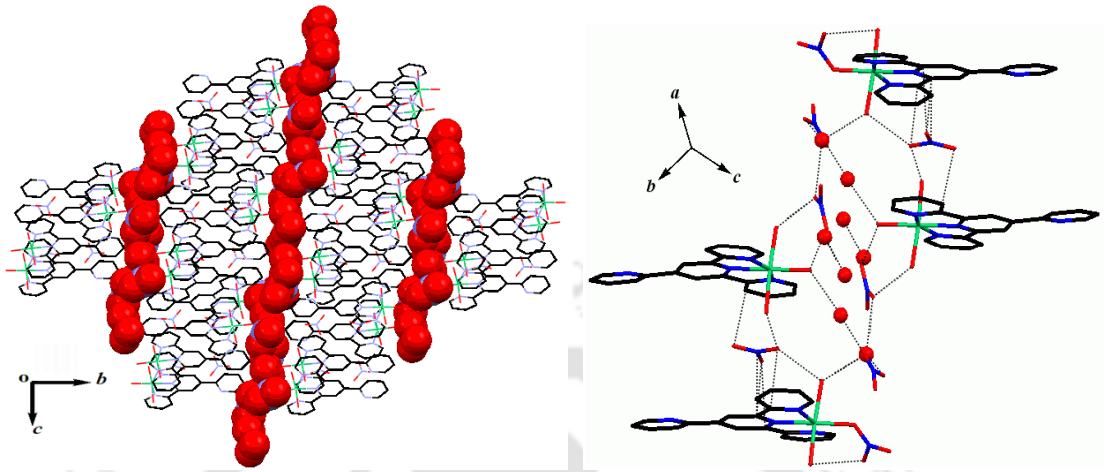

Figure 3. Molecular packing (**A**) and Nitrate ion in π–π interaction and Water-nitrate ions network (**B**).

Complex **2** crystallized in a triclinic space group *P* *and the asymmetric unit contains* two $[Ni(\mathbf{L3})_2]^{2+}$ species and four PF_6^- anions along with four water molecules. The bond parameters in both of the $[Ni(\mathbf{L3})_2]^{2+}$ units are within comparable limits. A perspective view of one of the $[Ni(\mathbf{L3})_2]^{2+}$ ion is shown in Figure 4. The bivalent nickel atom is coordinated by six nitrogen atoms of two **L3** ligands in a distorted octahedral fashion. The distortion around the nickel atom is evident from the *cis*- and *trans*-angles ranges of 77–78° and about 155° respectively, within the **L3**. The two NiN_3 planes intersect by 88°. As noted in **1**, the $Ni–N_{(Y)}$ distances in **2** are shorter than those of $Ni–N_{(X)}$ by about 0.121(1) Å and a similar trend is observed in the Ni(II) bis-chelates of

terpyridine and its 4′-(phenyl) analog.[267-272] The **Z** rings of **L3** deviate widely from planarity with respect to **Y** ring as inferred from the torsional angle range 2–31°.

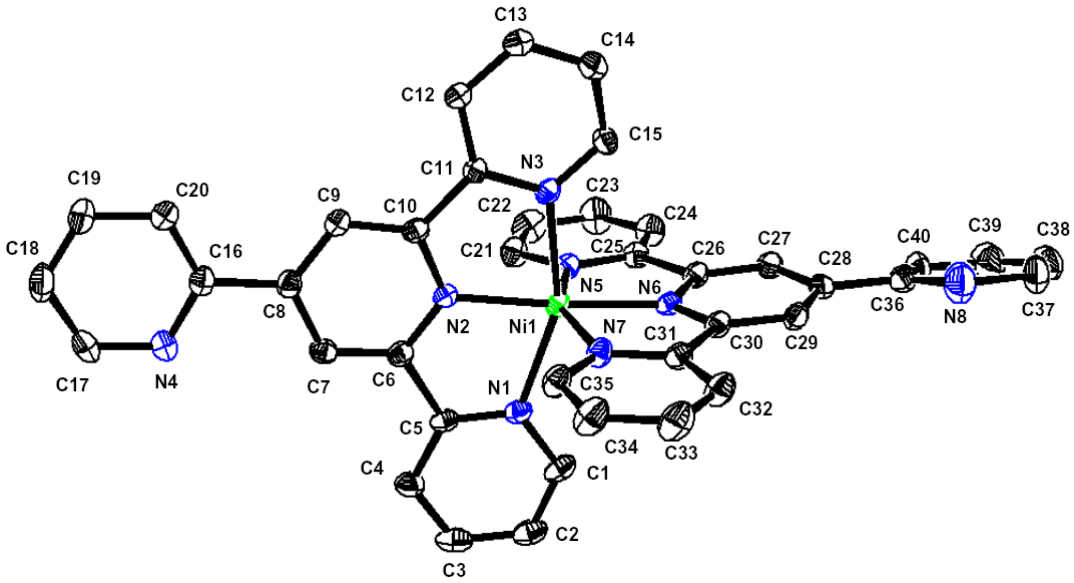

Figure 4. ORTEP (30% probability and hydrogen atoms are omitted) of $[Ni(\mathbf{L3})_2]^{2+}$ ion.

The packing diagram of **2** depicting the presence of F···π interactions[273] with the aromatic ring is shown in Figure 5. These non-bonded contacts lie in the narrow range 3.08(1)–3.12(1) Å. The PF_6^- anions also form C–H···F hydrogen bonds and the H···F non-bonded distances are included in Table 5. In addition, C–H···O and C–H···N interactions and the presence of a water dimer, O1···O2 having a distance of 2.622(1) Å are significant to note.

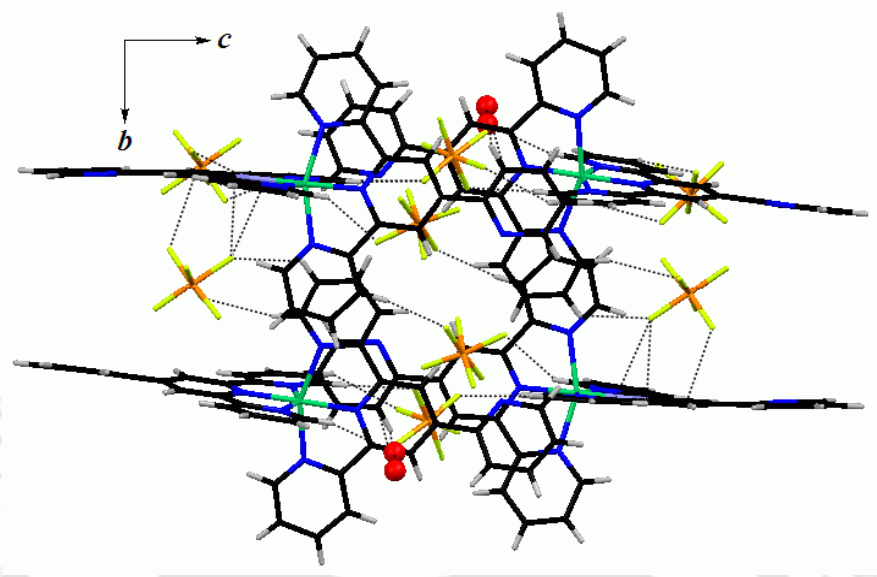

Figure 5. Packing diagram of **2**.

Table 5. Non-bonded Interactions (Å) in complex **1** and **2**

1				**2**	
O9···O39	2.7239(1)	O36···O40	2.7950(1)	O1···O2	2.622(1)
O6···O13	2.7298(1)	O22···O36	3.0300(1)	F2···C9	3.121(1)
O8···O35	2.7570(1)	O2···O19	2.7568(1)	F3···C10	3.082(1)
O5···O22	2.7721(1)	O8···O35	2.7570(1)	F3···C11	3.118(1)
O8···O21	2.7725(1)	O10···O17	2.8947(1)	F16···C15	3.116(1)
O11···O33	2.7944(1)	O11···O14	2.9859(1)	F11···C27	3.093(1)
O7···O32	2.7983(1)	O1···O17	2.8160(1)	H13···F2	2.635(1)
O4···O20	2.8258(1)	O37···O38	3.0530(1)	H3···F5	2.418(1)
O1···N16	2.8544(1)	O39···O26	3.0100(1)	H15···F16	2.350(1)
O4···N12	2.8625(1)	O21···O36	2.9960(1)	H43···F10	2.477(1)

O14···O40	2.8705(1)	O40···O27	2.9930(1)	H63···F23	2.646(1)
O29···O37	2.8812(1)	O37···O10	2.7900(1)	H12···F6	2.408(1)
N4···O11	2.8893(1)	O2···O29	2.7230(1)	H75···F17	2.402(1)
O7···N8	2.9109(1)	O3···O27	2.7760(1)	H74···F13	2.609(1)
O6···O24	2.9128(1)	O24···O37	2.9558(1)	C7···N4	2.777(1)
O23···O39	2.9234(1)	O25···O38	2.7971(1)	C27···N8	2.960(1)

5.3 Conclusion

The **L3** prepared as described in Chapter 2, has been utilized to synthesize mono- and bis-chelates of nickel(II). Their electronic spectra reveal that the energy of the $^3A_{2g} \rightarrow {}^3T_{2g}$ transition, follow the trend **2** > **1** and that of the $^3A_{2g} \rightarrow {}^3T_{1g}(P)$ remain invariant. The complexes exhibit $\pi \rightarrow \pi^*$ type emission and behave as two-electron paramagnets.

Structural studies shows the presence of a water dimer (in both) as well as $(NO_3^-)\cdots\pi$ and F$\cdots\pi$ interactions, in **1** and **2** respectively. In **1**, water-nitrate ion network having crown and chair forms are present.

Chapter 6

Binding of 4′-(2-Pyridyl)-2,2′:6′,2″-Terpyridine with Iron(II)

Abstract: Compounds of the molecular formula, [**L3H**$_3$](NO$_3$)$_3$, [Fe(**L3H**)$_2$](PF$_6$)$_4$·5H$_2$O (**1**), [Fe(**L3**)$_2$][Fe(**L3**)(**L3H**)](PF$_6$)$_5$·H$_2$O (**2**), [Fe(**L3**)$_2$][Fe(**L3**)(**L3H**)](BF$_4$)$_5$·2H$_2$O (**3**) and [Fe(**L3**)$_2$](Cr$_2$O$_7$)·6H$_2$O (**4**) were synthesized, characterized by structural and spectroscopic methods. Complexes **1-4** exhibit MLCT and ILCT transitions respectively in the visible and UV regions and the d-d transitions were not observed. The emission spectra are of π→π* in origin. All the Fe(II) complexes are high spin at room temperature and upon cooling a gradual spin-transition is observed. Among the compounds, hydrogen-bonding, π···π, and anion···π interactions as well as water tetramer and pentamer are present in the molecular packing.

Chapter 6

Binding of 4′-(2-Pyridyl)-2,2′:6′,2″-Terpyridine with Iron(II)

In this chapter the protonation behaviors of **L3**, and its bis-chelated Fe(II) complexes are studied.

6.1 Experimental

6.1.1 Syntheses

4′-(2-Pyridyl)-2,2′:6′,2″-terpyridine (L3): Has been synthesized using the procedure described in Chapter 2. The syntheses of **1-3**, were carried out in plastic wares.

$[L3H_3](NO_3)_3$: To 40 mg (0.129 mmol) of **L3**, dissolved in 10 mL of methanol was added 1 mL of 16 N HNO_3, drop wise with stirring. The mixture was left undisturbed and the pale yellow crystals obtained after a week were collected. IR, (KBr, cm^{-1}): 1614 ($C{=}N_{py}$), 1384 (NO_3^-). Anal. Calcd. for: $C_{20}H_{17}N_7O_9$: C, 48.10; H, 3.41; N, 19.64. Found: C, 48.33; H, 3.49; N, 19.38%.

$[Fe(L3H)_2](PF_6)_4{\cdot}5H_2O$ (1): To $Fe(NO_3)_2{\cdot}9H_2O$ (23 mg, 0.056 mmol) dissolved in methanol (15 mL), was added a methanolic solution (25 mL) of **L3 (**35 mg, 0.113 mmol). After stirring for 1 h, an aqueous saturated solution of KPF_6 (5 mL) and 2 drops of HPF_6 were added, stirred for 1 h and left undisturbed. Blocks of dark crystals of **1**, were obtained after two weeks. Yield: 71 mg (94%). IR, (KBr, cm^{-1}): 1614 ($C{=}N_{py}$), 1600

($C{=}N_{py}$), 1573, 1557, 843 (P–F). Anal. Found: C, 36.02; H, 3.03; N, 8.14. Calcd. For $C_{40}H_{40}N_8O_5P_4F_{24}Fe$: C, 35.59; H, 2.96; N, 8.31%.

$[Fe(L3)_2][Fe(L3)(L3H)](PF_6)_5 \cdot H_2O$ (2): To $Fe(NO_3)_2 \cdot 9H_2O$ (30 mg, 0.074 mmol) dissolved in methanol (25 mL), was added a methanolic solution (25 mL) of **L3** (46 mg, 0.148 mmol), followed by an aqueous solution of KPF_6 (27 mg, 0.148 mmol). Blocks of dark crystals were isolated after a week, on standing. Yield: 73 mg (85%, per metal). IR, (KBr, cm^{-1}): 1615 ($C{=}N_{py}$), 1600 ($C{=}N_{py}$), 1573, 1557, 842 (P–F). Anal. Found: C, 41.48; H, 2.57; N, 19.10. Calcd. For $C_{80}H_{59}N_{32}OP_5F_{30}Fe_2$: C, 41.36; H, 2.54; N, 19.30%.

$[Fe(L3)_2][Fe(L3)(L3H)](BF_4)_5 \cdot 2H_2O$ (3): To $Fe(NO_3)_2 \cdot 9H_2O$ (30 mg, 0.074 mmol) dissolved in methanol (25 mL), was added a methanolic solution (25 mL) of **L3** (46 mg, 0.148 mmol), followed by an aqueous solution of NH_4BF_4 (16 mg, 0.15 mmol). Dark colored crystals were obtained after five days of standing. Yield: 75 mg (98%, per metal). IR, (KBr, cm^{-1}): 1613 ($C{=}N_{py}$), 1603 ($C{=}N_{py}$), 1573, 1557, 1029 (B–F). Anal. Found: C, 46.96; H, 3.08; N, 21.15. Calcd. For $C_{80}H_{61}N_{32}O_2B_5F_{20}Fe_2$: C, 46.87; H, 2.97; N, 21.87%.

$[Fe(L3)_2](Cr_2O_7) \cdot 6H_2O$ (4): To $Fe(NO_3)_2 \cdot 9H_2O$ (30 mg, 0.074 mmol) dissolved in methanol (25 mL), was added a methanolic solution (25 mL) of **L3** (46 mg, 0.148 mmol), followed by an aqueous solution of $K_2Cr_2O_7$ (22 mg, 0.074 mmol). Reddish brown colored crystals obtained after a week, on standing, were collected. Yield: 70 mg (95%). IR, (KBr), cm^{-1}: 1614 ($C{=}N_{py}$), 1603 ($C{=}N_{py}$), 1573, 1557, 934 (Cr–O). Anal. Found:

C, 48.11; H, 3.92; N, 11.06. Calcd. For $C_{40}H_{40}N_8O_{13}Cr_2Fe$: C, 48.01; H, 4.03; N, 11.20%.

6.2 Results and Discussion

6.2.1 Syntheses

The nitrogen atoms in pyridyl groups can undergo protonation due to the presence of lone pair of electrons. Accordingly the tri-protonated salt, **[L3H$_3$](NO$_3$)$_3$**, could be crystallized from the methanol solution of **L3** containing few drops of concentrated HNO_3. This process prompted to work out the similar protonation behavior in the Fe(II) complexes of **L3**. Compound **1** could be obtained by the addition of HPF_6. While **2** and **3**, are formed from the acid impurity present in the respective salts, as the commercially available KPF_6 and NH_4BF_4 contain small quantities of free acids as impurity. Attempts to isolate crystalline compounds of non-protonated species having PF_6^-/BF_4^- counter ions using bases like KOH, pyridine, picolines or Et_3N could not be succeeded so far. However, the non-protonated compound **4**, was isolated by adding aqueous $K_2Cr_2O_7$ solution. Therefore, the protonation of the pendent pyridyl-N in **1-3**, was the effect of the concentration of the free acid present in the solution. Using the related ligand, 4′-(4-pyridyl)-2,2′:6′,2″-terpyridine (**L3″**), the structures of the trication [Fe(**L3″**)(**HL3″**)]$^{3+}$ were reported with $[Fe(NCS)_6]^{3-}$ and $[ClO_4]^-$ as counter anions.[196]

6.2.2 Optical Spectra

The $[Fe(tpy)_2]^{2+}$ complexes usually exhibit three types electronic transitions: (i) intraligand $\pi \rightarrow \pi^*$ between 250–400 nm; (ii) MLCT absorptions in the visible region and

(iii) weak d–d transitions at around 835 nm.[274-276] The UV-Visible spectral and magnetism data (for **1–4**) are listed in Table 1.

Table 1. UV-Visible spectra and Magnetism Data

Complex	λ_{max}, nm (ε, M^{-1} cm^{-1})[a]	μ_{eff} [b]
1	570(8550), 365(2030), 335(12620), 325(15200), 285(22620), 280(18180)	5.41
2	570(6130), 365(2255), 335(10545), 325(12140), 285(22235), 280(20700)	*
3	570(5685), 365(4880), 335(12760), 325(14500), 285(23055), 280(22125)	5.11
4	570(8450), 365(2480), 335(12635), 325(14710), 285(21920), 280(17845)	5.13

[a] In acetonitrile. [b] in B. M. at 296 K. * Not determined.

In complexes **1–4**, the n→π* transitions appear at 280 nm (from 4′-(2-pyridyl)). The intraligand π→π* transitions occur in the 285–365 nm region. All the four complexes exhibit a MLCT band at 570 nm, with shoulders at 490 and 630 nm, may be of vibrational structures. The visuals of **1**, **2**, **4** are shown in Figure 1 and the spectra of **1-4** are shown in Figure 2.

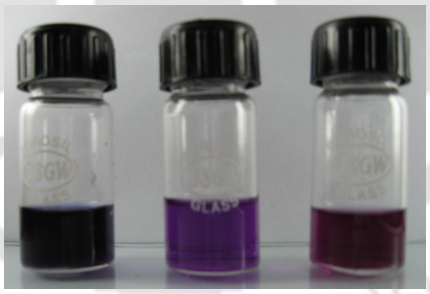

Figure 1. Visuals of **1**, **2** and **4**.

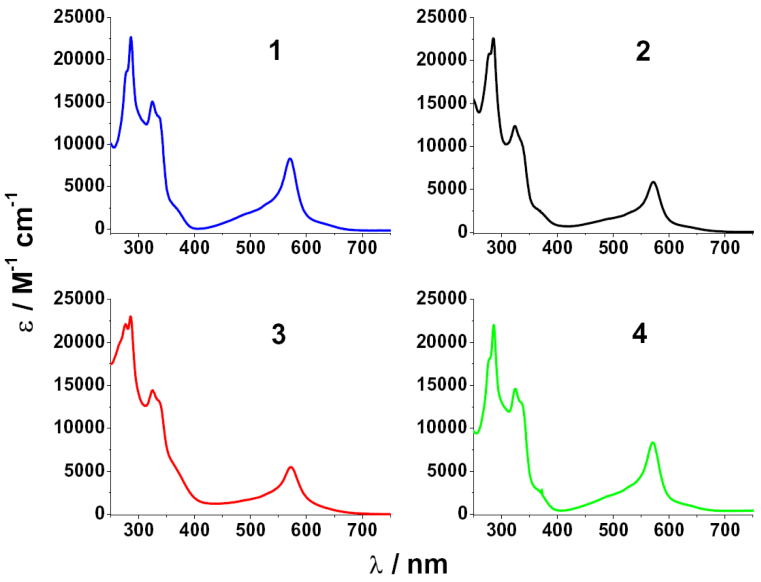

Figure 2. UV-Vis spectra of complexes **1**-**4**.

A ~10^{-5} M acetonitrile solution of **1** (1.4 mL) was titrated in the cuvette with methanolic KOH (~10^{-5} M) and the UV-Visible spectrum was recorded after addition of each aliquots (2 μL) of KOH solution. The presence of isosbestic points at 315, 350, 510 and 600 nm, is evident from Figure 3. The optical density of MLCT band decreases while that of the n→π* increases with the addition of KOH. This may be suggestive that upon protonation of the N-atom of the 4′-(2-pyridyl) ring, the MLCT is more facilitated while that the n→π* is less facilitated.

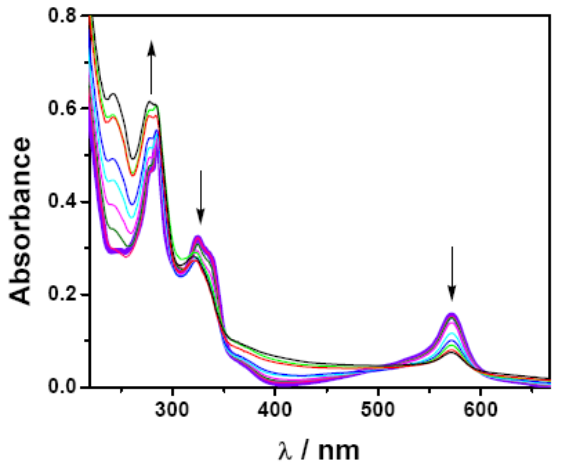

Figure 3. The UV-Visible spectra of **1** after addition of each aliquots of KOH.

The emission spectra (Figure 4) of **1-4** were recorded in acetonitrile at λ_{ex} = 315 nm; and complex **1** exhibits an emission from the significant intraligand π→π* state. Here the envelope of the vibronic structure has a 'domed' shape i.e. a longer wavelength vibronic component becomes the most intense transition, where the energy spacing within the transition is of the order 2610 cm^{-1} for a typical C–C and C–N stretching motion of the terpyridyl framework. This sort of signature is attributed to a Frank–Condon type envelope for the polypyridine-centered π→π* emission. In complexes **2**–**4**, the emission occurs without vibronic components and the π→π* emission appears in the range 365–395 nm.[255–259]

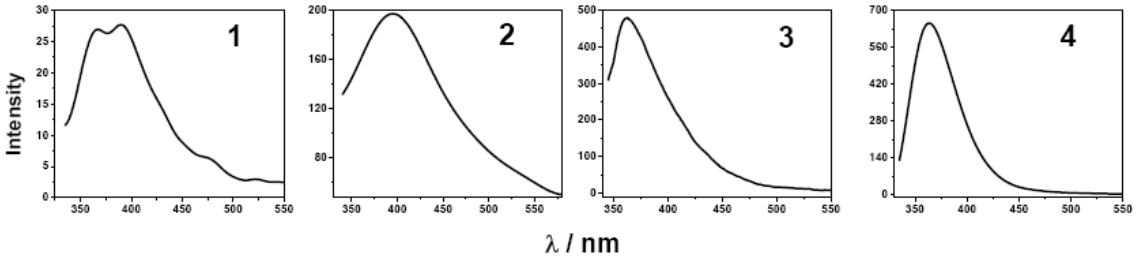

Figure 4. Emission spectra of complexes **1**-**4**.

6.2.3 Magnetism

The μ_{eff} values in the temperature range 50-300 K, of **1**, **3** and **4** were calculated from the real component of AC susceptibility obtained by mutual inductance method. The bivalent iron has a d^6 electronic configuration for the free ion and its octahedral complexes can exist in high-spin $t_{2g}^4e_g^2$ or low-spin $t_{2g}^6e_g^0$ configurations. The high-spin and low-spin states respectively show 4-electron paramagnetism and diamagnetism. However, polypyridyl complexes of iron(II) generally show temperature dependent spin cross-over phenomenon, that is conversion from paramagnetism to diamagnetism with the decrease of temperature.[247–249] Complex **1** has a higher μ_{eff} value of 5.41 B.M. compared to **3** and **4**, (~5.10 B.M.) at room temperature and is slightly higher than the $\mu_{s.o.}$ value of 4.90 B.M. consistent with the high-spin state. A plot of temperature (300-50 K) *vs.* μ_{eff}, *vs.* χ_M and *vs.* $1/\chi_M$ for **1**, **3** and **4**, is displayed in Figure 5. As the temperature is decreased, the μ_{eff} values decrease gradually. From the χ_M plot it is evident that the value increases and then decrease with a maximum in the temperature range 110–125 K. The nature of the plots reveals that in all cases there is no sharp transition but a gradual spin transition towards the low-spin complex observed.[277-280]

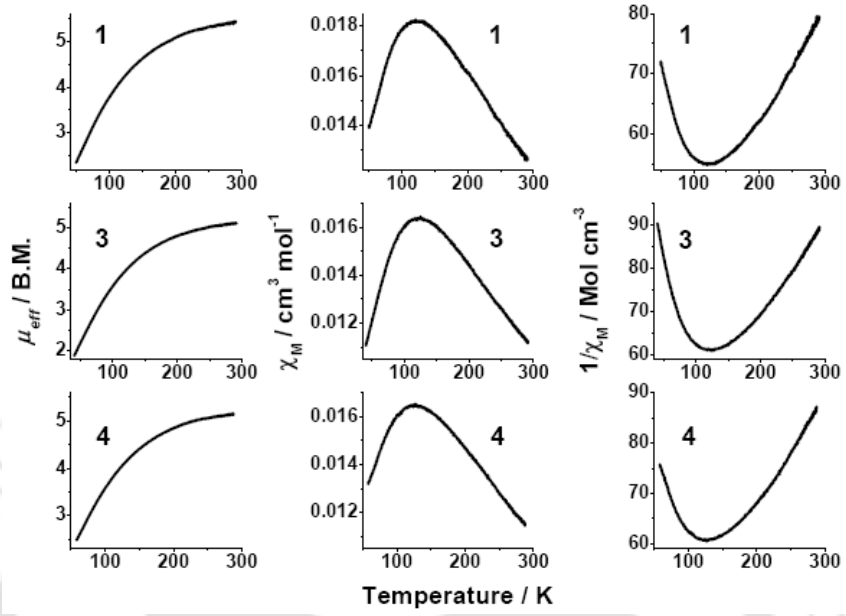

Figure 5. Temperature dependent magnetism in **1**, **3** and **4**.

6.2.4 Molecular Structures

The molecular structures of [**L3H$_3$**](**NO$_3$**)$_3$ and **1-4** have been determined. The crystallographic data and refinement parameters are summarized in Table 2. The selected bond distances and bond angles are listed respectively in Table 3 and Table 4. In all the cases, the iron(II) is hexa-coordinated by two meridionally coordinating **L3**/**L3H** and has a distorted octahedral geometry.

The asymmetric unit of [**L3H$_3$**](**NO$_3$**)$_3$ consists of one tri-cation [**L3H$_3$**]$^{3+}$ and three nitrate ions. Of the four pyridine-N atoms in **L3** that can be protonated, the X- and Z-rings are protonated, while the sterically crowded Y-ring is not, under these conditions.

The N-atom in a ring was identified by the relative weightages of the Q-peaks generated from the FMAP. All the hydrogen atoms could be located from the FMAP and refined isotropically. The twisting with respect to Y-ring, of the two X-rings are 5.8(1)° and 11.3(1)° and that of the Z-ring is 33.0(1)°. The large twist in the Z-ring is due to the steric repulsion between the H9···H4A and H7···H20.

One oxygen atom (O5) of the nitrate ion is involved in hydrogen bond (O5···N1, 2.719(1) Å; O5···N2, 2.972(1) Å) with the protonated N1, N3 atoms of the X-ring as well as a non-bonded interaction with the N2 atom of Y-ring (O5···N3, 2.740(1) Å), which in turn involve in a anion···π interaction (N6···C9, 3.200(1) Å; C8···O6, 3.174(1) Å) with another $[\mathbf{L3H_3}]^{3+}$ (Figure 6).[281-282] The protonated N4 of the Z-ring is hydrogen bonded to another nitrate ion having the contact, N4···O8, 2.738(1) Å.

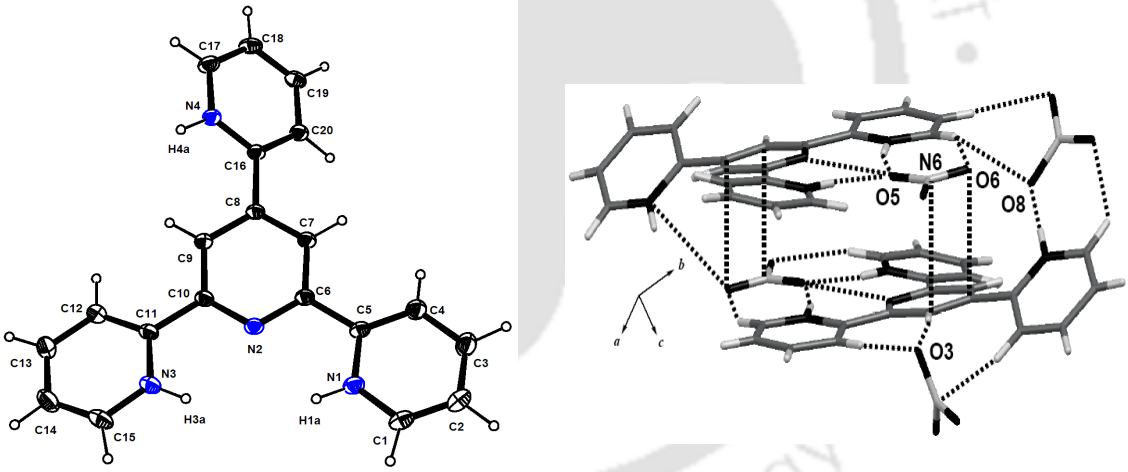

Figure 6. ORTEP of $\mathbf{[L3H_3]}^{3+}$ and non-bonded interactions in $\mathbf{[L3H_3](NO_3)_3}$.

Complex **1** crystallized in a triclinic space group $P\bar{1}$. *The asymmetric unit contain one* tetra-cationic species $[Fe(\mathbf{L3H})_2]^{4+}$ (Figure 7), four PF_6^- counter anions along with four

water molecules. The bivalent iron is coordinated by two **L3H** ligands, in which the nitrogen atom of the Z-ring is protonated and has a distorted octahedral geometry having a *mer*-N_3N_3 chromophore. Overall, the chelate bite angles are in the range 80.1–80.6(2)° while the other *cis* angles span a wider range, 89.6–100.2(2)°. The intra-ligand *trans* angle, $N_{(X)}$–M–$N_{(X')}$ is 160.7(2)6° and deviates largely from linearity. While the inter-ligand *trans* angle made by the two Y-rings, N2–M–N6 is 179.4(2)°. The Fe–N bond lengths follow the trend Fe–N_X>Fe–N_Y by ~0.101(1) Å. This trend is always observed in the metal complexes of terpyridines, has been ascribed to two factors: the efficient overlap of metal t_{2g} orbitals with the π* orbitals of the central pyridyl group and the geometrical constraints of the ligand, probably the former contributing more. [246, 268] The two planes, $FeN_XN_YN_X$' from each of the **L3H** intersects by 88.09(2)°.

Table 2. Crystallographic data and refinement parameters

[L3H3](NO3)34																		
$C_{20}H_{17}N_7O_9$	499.41	296(2)	0.71073	Orthorhombic	P21/c	8.2913(5)	21.7014(14)	12.167(8)			2180.2(2)	4	1.521	0.123	1.000	b_{R_1} = 0.06096, cwR2 = 0.15103	b_{R_1} = 0.10445, cwR2 = 0.16883
$C_{40}H_{40}N_8O_{13}Cr_2Fe$	100000.63	296(2)	0.71073	Triclinic	$P\bar{1}$	8.9242(3)	12.6090(5)	20.1907(9)	75.466(10)	83.104(10)	69.360(10)	2056.92(14)	2	1.496	0.931	1.043	b_{R_1} = 0.05000, cwR2 = 0.14777	b_{R_1} = 0.05782, cwR2 = 0.15882

a GOF = $[\Sigma[w(F_0^2 - F_c^2)^2]/(M-N)]^{1/2}$ (M = number of reflections, N = number of parameters refined

3	$C_{80}H_{61}N_{32}O_2B_5F_{20}Fe_2F_{24}Fe$	2048.36	296(2)	0.71073	Triclinic	*P*$\bar{1}$	11.1853(2)	17.7749(2)	20.8931(3)	79.6250(10)	86.5860(10)	74.7250(10)	39.4133(10)	2	1.726	0.492	1.057	b_{R_1} = 0.0633, cwR_2 = 0.1873	b_{R_1} = 0.0633, cwR_2 = 0.1874	). $b_{R_1} = \Sigma \|\|F_0\| - \|F_c\|\| / \Sigma \|F_0\|$. $cwR_2 = [\Sigma [w(F_0^2 - F_c^2)^2] / \Sigma [w(F_0^2)^2]]$.
2	$C_{80}H_{59}N_{32}OP_5F_{30}Fe_2$	2321.14	296(2)	0.71073	Triclinic	*P*$\bar{1}$	13.6846(5)	17.0121(7)	17.9763(7)	101.096(2)	91.854(3)	94.473(3)	40.89.4(3)	2	1.885	0.596	1.011	b_{R_1} = 0.0979, cwR_2 = 0.1970	b_{R_1} = 0.0979, cwR_2 = 0.1970	

1	$C_{40}H_{40}N_8O_5P_4F_{24}Fe$	1348.51	296(2)	0.71073	Triclinic	$P\bar{1}$	8.7234(8)	16.8847(16)	18.6780(17)	77.303(3)	87.990(3)	77.679(3)	2621.8(4)	2	1.706	0.547	1.007	b_{R1} = 0.0878, cwR2 = 0.2473	b_{R1} = 0.1706, cwR2 = 0.3120
	Empirical formula	Formula weight	Temperature	Wavelength, Å	Crystal system	Space group	*a*, Å	*b*, Å	*c*, Å	*α*, deg	*β*, deg	*γ*, deg	*V*, Å3	*Z*	*D* calc (g cm−3)	*μ*, (mm−1)	aGOF on F2	R [I > 2σ(I)]	R indices (all data)

Table 3. Selected Bond Distances (Å)

	1	**2a**	**3a**	**4**		**2b**	**3b**
Fe1–N1	2.004(4)	1.991(2)	1.991(2)	1.986(2)	Fe2–N9	1.978(2)	1.978(2)
Fe1–N3	2.008(5)	1.981(2)	1.981(2)	1.982(2)	Fe2–N11	1.973(2)	1.973(2)
Fe1–N5	2.007(4)	1.996(2)	1.996(2)	1.985(2)	Fe2–N13	1.978(3)	1.978(3)
Fe1–N7	1.998(4)	1.976(2)	1.976(2)	1.978(2)	Fe2–N15	1.976(3)	1.976(3)
Fe1–N2	1.891(4)	1.887(2)	1.887(2)	1.887(2)	Fe2–N10	1.881(2)	1.881(2)
Fe1–N6	1.907(4)	1.871(2)	1.871(2)	1.884(2)	Fe2–N14	1.864(2)	1.864(2)

Table 4. Selected Bond Angles (º)

	1	**2a**	**3a**	**4**		**2b**	**3b**
N2–Fe1–N6	179.4(2)	178.7(1)	178.7(1)	178.4(1)	N14–Fe2–N10	178.9(1)	178.9(1)
N1–Fe1–N3	160.7(2)	161.1(1)	161.1(1)	161.7(1)	N11–Fe2–N9	162.0(1)	162.0(1)
N7–Fe1–N5	160.7(2)	160.9(1)	160.9(1)	161.3(1)	N15–Fe2–N13	162.0(1)	162.0(1)
N2–Fe1–N1	80.1(2)	80.7(1)	80.7(1)	80.8(1)	N10–Fe2–N9	81.2(1)	81.2(1)
N2–Fe1–N3	80.6(2)	80.5(1)	80.5(1)	81.0(1)	N10–Fe2–N11	80.8(1)	80.8(1)
N6–Fe1–N5	80.4(2)	80.4(1)	80.4(1)	80.6(1)	N14–Fe2–N13	81.0(1)	81.0(1)
N6–Fe1–N7	80.4(2)	80.5(1)	80.5(1)	80.8(1)	N14–Fe2–N15	81.0(1)	81.0(1)
N1–Fe1–N5	89.6(2)	92.4(1)	92.4(1)	92.1(1)	N15–Fe2–N9	90.9(1)	90.9(1)
N7–Fe1–N3	89.9(2)	90.9(1)	90.9(1)	91.7(1)	N11–Fe2–N13	91.1(1)	91.1(1)
N5–Fe1–N3	93.1(2)	92.4(1)	92.4(1)	92.3(1)	N13–Fe2–N9	91.8(1)	91.8(1)
N7–Fe1–N1	93.9(2)	90.5(1)	90.5(1)	89.8(1)	N11–Fe2–N15	91.9(1)	91.9(1)
N2–Fe1–N5	99.1(2)	100.0(1)	100.0(1)	98.5(1)	N10–Fe2–N15	98.0(1)	98.0(1)
N6–Fe1–N3	99.5(2)	98.2(1)	98.2(1)	97.7(1)	N14–Fe2–N9	98.2(1)	98.2(1)
N6–Fe1–N1	99.8(2)	100.6(1)	100.6(1)	100.5(1)	N14–Fe2–N11	99.8(1)	99.8(1)
N2–Fe1–N7	100.2(2)	99.1(1)	99.1(1)	100.2(1)	N10–Fe2–N13	100.0(1)	100.0(1)

The **Z** rings deviate largely from planarity with respect to **Y** ring as inferred from the dihedral angles 27.0(2)° and 47.3(2)°. This deviation is more severe in one of the ligands as compared to that observed in $[\mathbf{L3H_3}]^{3+}$ (*vide supra*) and this is attributable to the steric repulsion between the H atoms.

The C–H···π *viz.,* C3–H3···C21 2.770(1) Å, C33–H33···C14 2.892 Å, as well as anion···π interactions *viz.,* F10···C7 3.001(1) Å, F12···C16 3.107(1), F12···C17 3.162(1) Å, and F12···N4 2.840(1) Å are significant, shown in Figure 8. A water tetramer exists between O3···O2···O5···O1 where in O1···O5, 2.783 Å; O2···O5, 2.902(1) Å; O2···O3 2.829(1) Å. The water tetramer is hydrogen bonded to $[Fe(\mathbf{L3H})_2]^{4+}$ through O3···N8, 2.765(1) Å; O1···N4, 2.737(1) Å and to $[PF_6]^-$ through O2···F20 2.897(1) Å. The O4 remain isolated.

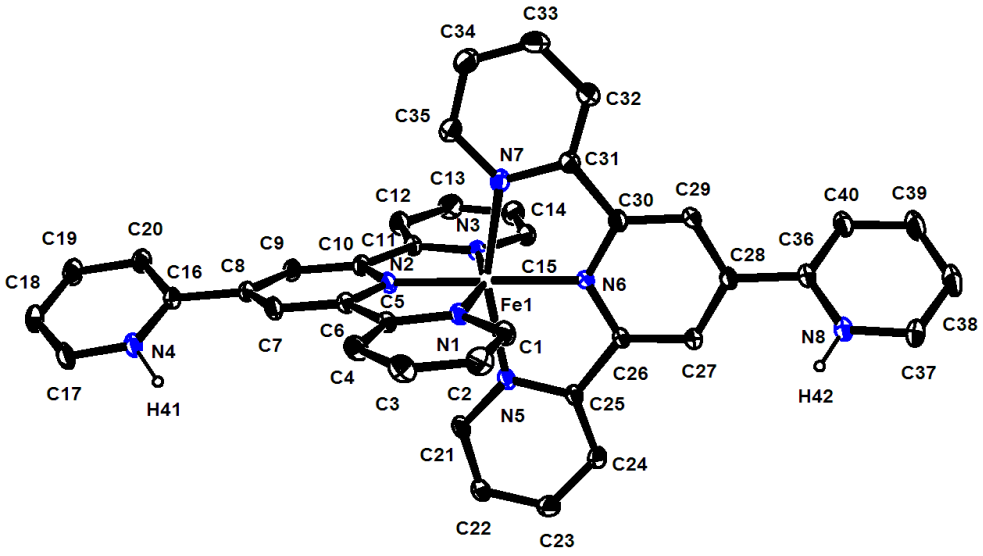

Figure 7. ORTEP of $[Fe(L3H)_2]^{4+}$.

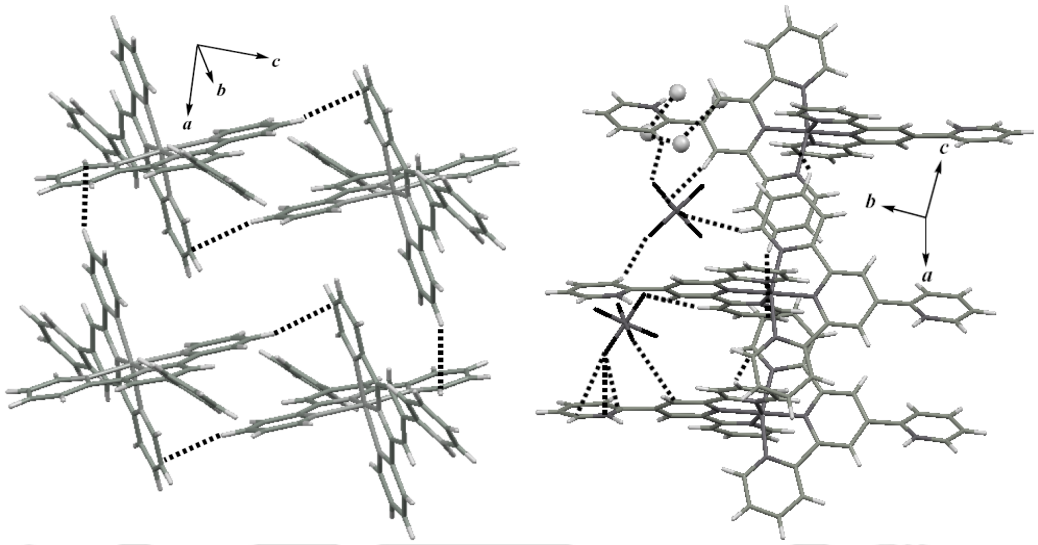

Figure 8. C–H···π and anion···π interactions in **1**.

Complex **2** also crystallized in a triclinic space group $P\bar{1}$. *The asymmetric unit contain* one each of tri-cationic $[Fe(\mathbf{L3})(\mathbf{L3H})]^{3+}$ (**2a**), di-cationic $[Fe(\mathbf{L3})_2]^{2+}$ (**2b**), species and five PF_6^- along with one water molecule. In **2a**, the bivalent iron is coordinated by one **L3** and one **L3H** (in which the nitrogen atom of the Z-ring is protonated) while in **2b**, by two **L3** ligands. In both **2a** and **2b**, the bivalent iron is hexa-coordinated and has a distorted octahedral geometry having a *mer*-N_3N_3 chromophore. An ORTEP of **2a** is displayed in Figure 9. There are no gross deviations in the structural parameters within **2a** and **2b**, and are comparable with that observed in **1**.

In the packing of **2** (Figure 10), the significant non-bonded interactions present are: C–H···π *viz.,* C33–H33···C17, 2.843(1) Å; C37–H37···C19, 2.846(1) Å; C39–H39···C2,

2.878(1) Å; anion···π *viz.,* F20···C76, 3.089(1) Å; F2···C4, 3.089(1) Å; F12···C35, 2.922(1) Å; F12···C34, 3.100(1) Å; π···π *viz.,*. C33···C37, 3.367(1) Å. The water O1 is involved in two C–H···O interactions.

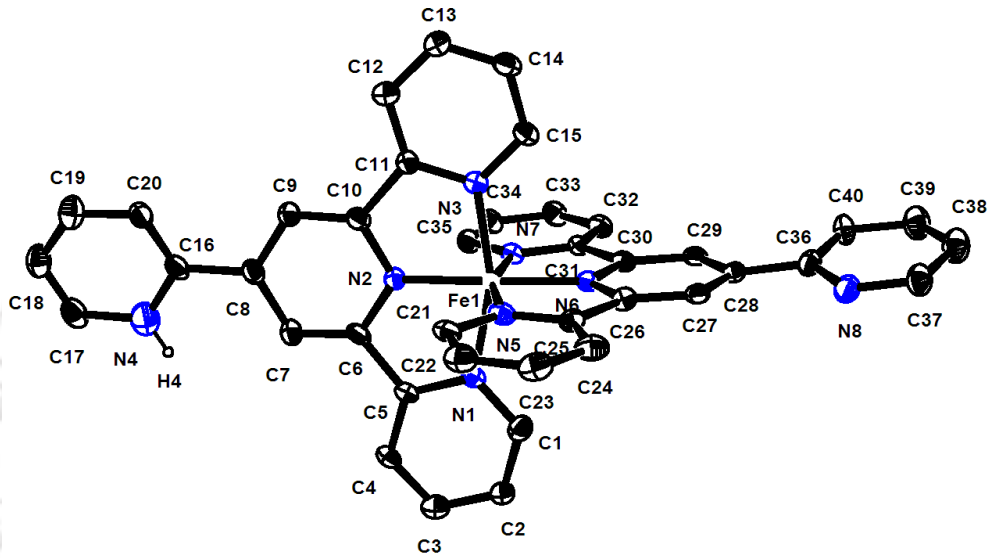

Figure 9. ORTEP of **2a**.

Complex **3** also crystallized in a triclinic space group $P\bar{1}$. *The asymmetric unit contain* one each of tri-cationic $[Fe(\mathbf{L3})(\mathbf{L3H})]^{3+}$ (**3a**), di-cationic $[Fe(\mathbf{L3})_2]^{2+}$ (**3b**), species and five BF_4^- along with two water molecules. The structural features and parameters within **3a**, **3b** are identical to those of **2a**, **2b** respectively and the details are not elaborated further.

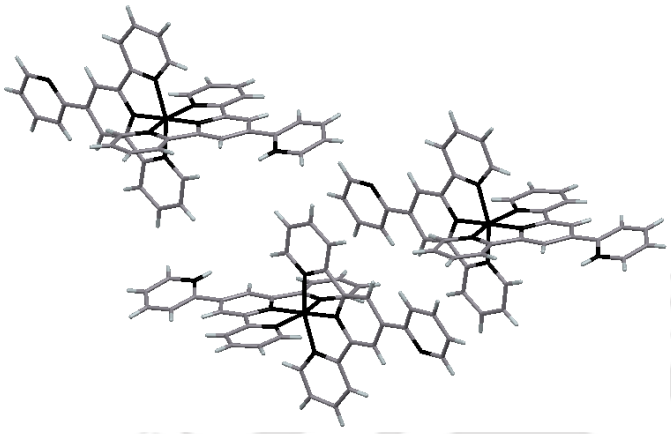

Figure 10. C–H···π, π···π and anion···π interactions in **2**.

An approximately linear π···π stacking C73···C77···C77···C73 (Figure 11) having a distance C77···C77, 3.378(1) Å; C77···C73, 3.253(1) Å is present and the angle at C77 being 174.6(1)°. Apart from the C–H···F, the significant anion···π interactions *viz.,* F13···C35, 3.055(1) Å; F13···C4, 3.159(1) Å; F38···C21, 3.103(1) Å; F38···C11 3.034(1) Å are also present. There is an existence of hydrogen bonds involving the solvent water with the Z-ring nitrogen atom of **L3**, O2···N4, 2.855(1) Å and O1···N16, 2.955(1) Å.

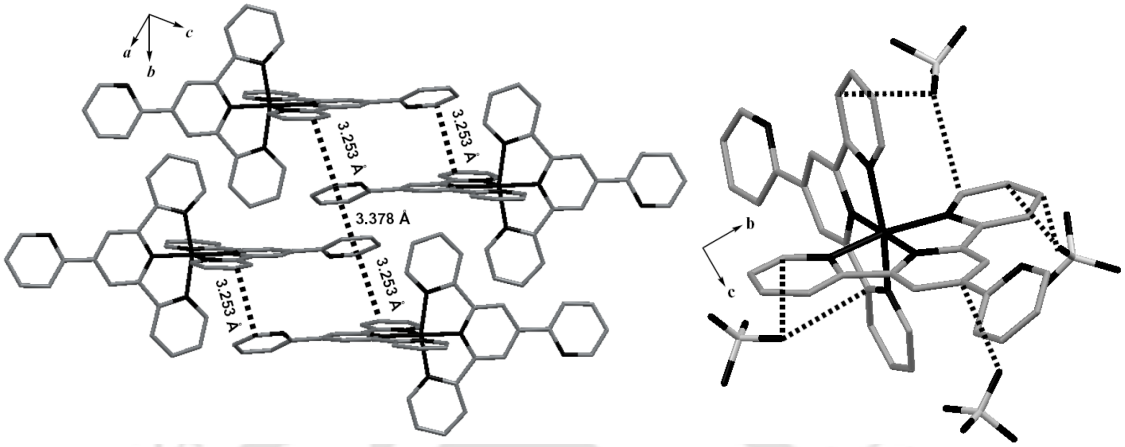

Figure 11. π···π and anion···π interactions in **3**.

Complex **4** belongs to a triclinic *P* *space group and consists of the di-cationic* $[Fe(\mathbf{L3})_2]^{2+}$ as shown in Figure 12, a di-anionic $Cr_2O_7^{2-}$ and six water molecules as the solvate. The bivalent iron is coordinated by two **L3** ligands and has a distorted octahedral geometry having a *mer*-N_3N_3 chromophore. The structural features and parameters are comparable to those of **2b** and 3**b**, and the details are not elaborated further. It is relevant to note that the average Fe–N bond length is shorter in $[Fe(\mathbf{L3})_2]^{2+}$ and $[Fe(\mathbf{L3})(\mathbf{L3H})]^{3+}$ compared to $[Fe(\mathbf{L3H})_2]^{4+}$ by about 0.020(4) Å. The twisting the Z-ring in one **L3** is 0.5(1)° and on the other is more severe by 40.2(1)°.

An approximately linear π···π stacking between C37···C38···C22 is present (Figure 13) and the distance is respectively 3.331(1) Å and 3.376(1) Å. The angle subtended at C38 is 165.3(1)°. The D–H···A interaction of O12···C35, 3.168(1) Å; O4···C1, 3.112(1) Å are

also present. A zig-zag shaped water pentamer, O8···O10···O9···O11···O12 with the respective distances, 2.791(1) Å, 2.791(1) Å, 2.769(1) Å, 2.648(1) Å is present and hydrogen bonded by the contacts *viz.,* O8···N8, 2.885(1) Å; O11···N4, 2.841(1) Å; O8···O2, 2.980(1) Å; O9···O2, 2.801(1) Å.

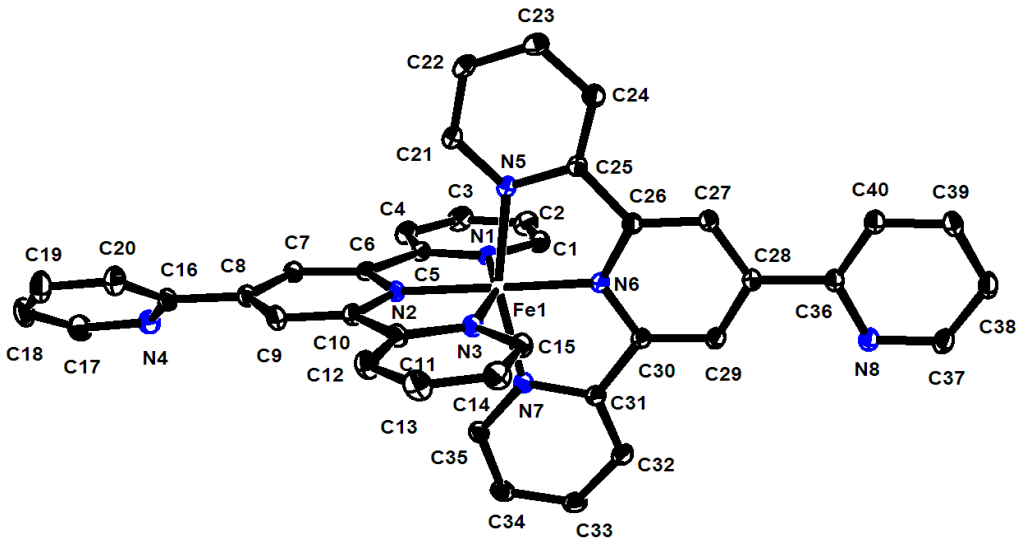

Figure 12. ORTEP of $[Fe(\mathbf{L3})_2]^{2+}$.

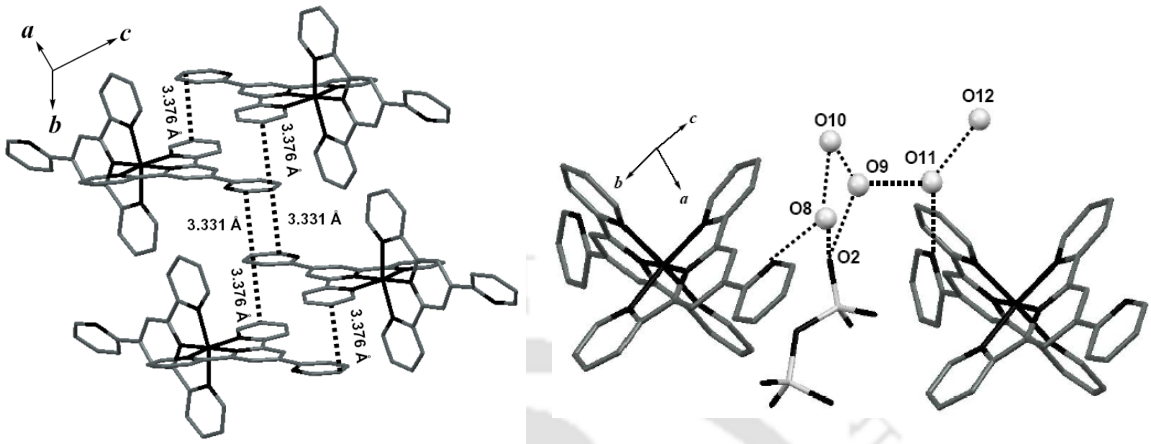

Figure 13. The water pentamer and π···π interactions in **4**.

6.3 Conclusion

The tri-protonated salt, **[L3H$_3$](NO$_3$)$_3$**, Fe(II) bis-chelates of **L3** with the pendant 4′-(2-pyridyl) groups having: both N-atoms protonated; one protonated and both non-protonated were synthesized and structurally characterized. All the Fe(II) complexes exhibit MLCT and ILCT transitions respectively in the visible and UV regions; but the d-d transitions were not observed. The luminescence spectra are of π→π* in origin. The bivalent iron is in high spin state at room temperature and upon cooling a gradual spin-transition is observed. Hydrogen-bonding, π···π, and anion···π interactions as well as water tetramer and pentamer are present among the compounds.

Chapter 7

Water-Chloride Ion Clusters in 4′-(2-Pyridyl)-2,2′:6′,2″-Terpyridine Bis-chelates of M(II) {M = Fe, Ni, Ru}

Abstract: The bis-complexes of **L3** having the formula, $[M(\mathbf{L3})_2]Cl_2 \cdot xH_2O$, where M = Ni (**1**), Fe (**2**), Ru (**3**) and x = 8, 9, 10 respectively, were synthesized. Complex **1** exhibits d-d and ILCT transitions respectively in the visible and UV regions. Complexes **2** and **3** exhibit MLCT and ILCT transitions respectively in the visible and UV regions and the d-d transitions were not observed. The emission spectra are of $\pi \rightarrow \pi^*$ character in **1-3**. The room temperature μ_{eff} values are consistent with the presence of 2 and 4 unpaired electrons in **1** and **2** respectively. Complex **2** shows gradual spin decay on cooling and **3** is diamagnetic. All the three complexes crystallized in triclinic $P\bar{1}$ *space group and* consists of an iso-structural $[M(\mathbf{L3})_2]^{2+}$ species, two Cl^- ions and water molecules of crystallization. In **1-3**, the $[M(\mathbf{L3})_2]^{2+}$ ions are arranged in a layer forming the hydrophobic regions and hydrogen bonded networking of the Cl^- ions and water molecules forming hydrophilic regions. The centro-symmetric repeating unit are of L5(2)5(3)8(2)4 pattern.

Chapter 7

Water-Chloride Ion Clusters in 4′-(2-Pyridyl)-2,2′:6′,2″-Terpyridine Bis-chelates of M(II) {M = Fe, Ni, Ru}

In this chapter, complexes of the type $[M(\mathbf{L3})_2]Cl_2 \cdot xH_2O$, where M = Ni (**1**), Fe (**2**), Ru (**3**) and x = 8, 9, 10 respectively, with the degree of hydration that depends upon the nature of the metal ion, were synthesized using the ligand **L3**. The results of the structural studies on **1**-**3** were described.

7.1 Experimental

7.1.1 Syntheses

4′-(2-Pyridyl)-2,2′:6′,2″-terpyridine (L3): Has been synthesized using the procedure described in Chapter 2.

$[Ni(L3)_2]Cl_2 \cdot 8H_2O$ (1): $NiCl_2 \cdot 6H_2O$ (19 mg, 0.080 mmol) and **L3** (50 mg, 0.160 mmol) were stirred in methanol (25 mL) for 1h. Reddish brown crystals of **1** were obtained, after four days from the undisturbed solution. Yield: 41 mg (57%). IR, (KBr, cm^{-1}): 1616 ($C{=}N_{py}$), 1602 ($C{=}N_{py}$), 1556. Anal. Calcd. for: $C_{40}H_{44}N_8NiO_8Cl_2$: C, 53.66; H, 4.91; N, 12.52. Found: C, 53.69; H, 4.93; N, 12.49%.

$[Fe(L3)_2]Cl_2 \cdot 9H_2O$ (2): Complex **2** was prepared using anhydrous $FeCl_3$, adopting the procedure described for **1**. Yield: 33 mg (45%). IR, (KBr, cm^{-1}): 1615 ($C{=}N_{py}$),

1600 (C=N_{py}), 1556. Anal. Calcd. for: $C_{40}H_{46}N_8FeO_9Cl_2$: C, 52.77; H, 5.06; N, 12.32. Found: C, 52.75; H, 5.11; N, 12.39%.

$[Ru(L3)_2]Cl_2 \cdot 10H_2O$ (3): $RuCl_2(DMSO)_4$ (20 mg, 0.041 mmol) and **L3** (26 mg, 0.083 mmol) were heated at reflux in ethanol (30 mL) for 30 min. The solvent was removed and the red-solid was washed thoroughly with hot benzene. The solid was dissolved in minimum amounts of acetonitrile and the solution was left undisturbed. The dark-red crystals obtained after a week were used for further studies. Yield: 18 mg (45%). IR, (KBr, cm^{-1}): 1618 (C=N_{py}), 1588 (C=N_{py}), 1559. Anal. Calcd. for: $C_{40}H_{48}N_8RuO_{10}Cl_2$: C, 49.35; H, 4.93; N, 11.51. Found: C, 49.50; H, 4.96; N, 11.38%.

7.2 Results and Discussion

7.2.1 Syntheses

Complexes of the type $[M(\mathbf{L3})_2]Cl_2 \cdot xH_2O$, where M = Ni (**1**), Fe (**2**), Ru (**3**) and x = 8, 9, 10 respectively, with the degree of hydration that depends upon the nature of the metal ion, were synthesized using the ligand **L3**. In the synthesis of **2**, the iron(III) has been converted to iron(II) in the presence of **L3**, could possibly be due to the solvent ethanol.

7.2.2 Optical Spectra and Magnetism

The UV-Vis spectra of **1**-**3**, were recorded in acetonitrile (Figure 1) and the data were provided in Table 1. Complex **1** exhibits d-d transitions in visible and intra-ligand charge transfer (ILCT) in UV regions. The $^3A_{2g} \rightarrow {}^3T_{2g}$ and $^3A_{2g} \rightarrow {}^3T_{1g}$(P) transitions, occur at 800 and 570 nm, respectively. But the transition, $^3A_{2g} \rightarrow {}^3T_{1g}$(F) was not observed which may be obscured by the intra-ligand bands. These are identical with that

observed for $[Ni(\mathbf{L3})_2](PF_6)_2 \cdot 2H_2O$, discussed in Chapter 5. The intra-ligand charge transfer transitions are of $\pi \rightarrow \pi^*$ and $n \rightarrow \pi^*$ (from 4′-(2-pyridyl)) in origin.[243]

The $[M(tpy)_2]^{2+}$ (M = Fe, Ru) complexes usually exhibit three types of electronic spectrum such as (i) intraligand $\pi \rightarrow \pi^*$ between 250–400 nm; (ii) MLCT absorptions in the visible region and (iii) weak d–d transitions at around 835 nm.[274-276].

In complexes **2** and **3** the peaks appearing in the range, 240–280 nm, are of $n \rightarrow \pi^*$ (from 4′-(2-pyridyl)) in origin.[274-276] The $\pi \rightarrow \pi^*$ transitions occur in the 285–365 nm region. The intensely purple-colored **2**, exhibit a MLCT band having a sharp peak centered at 570 nm, with a wide base along with shoulders at 490 and 630 nm, may be of vibrational structures.[274-276] Similarly in the red-colored **3**, the MLCT is at 490 nm with the shoulders at 445 and 570 nm. In both **2** and **3**, d-d transitions were not observed.

Table 1. UV-Visible Data[a]

Complex	λ_{max}, nm (ε, M^{-1} cm^{-1})
1	800(22), 570(15), 345(12035), 330(14790), 317(15195), 300(15900), 286(37250)
2	570(5210), 365(2275), 335(9425), 325(11140), 285(20360), 280(18835), 240(14985)
3	565(1845), 491(7600), 330(14120), 315(17680), 285(19210), 275(18955), 255(13455).

[a] In Acetonitrile

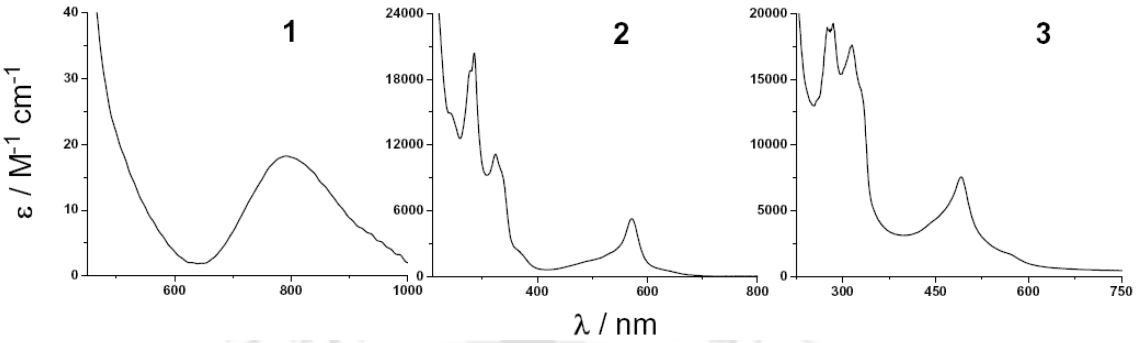

Figure 1. UV-Vis spectra of **1-3**.

The emission spectra of **1-3**, were recorded in acetonitrile with λ_{ex} = 345 nm (for **1**) and λ_{ex} = 315 nm (for **2** and **3**). As noted above, these λ_{ex} values correspond to the $\pi \rightarrow \pi^*$ transition and the emission observed in **1-3**, are of $\pi \rightarrow \pi^*$ in character. The emission (Figure 2) occur at 436, 472 nm (for **1**); 395 nm (for **2**) and 368 nm (for **3**).[255-259]

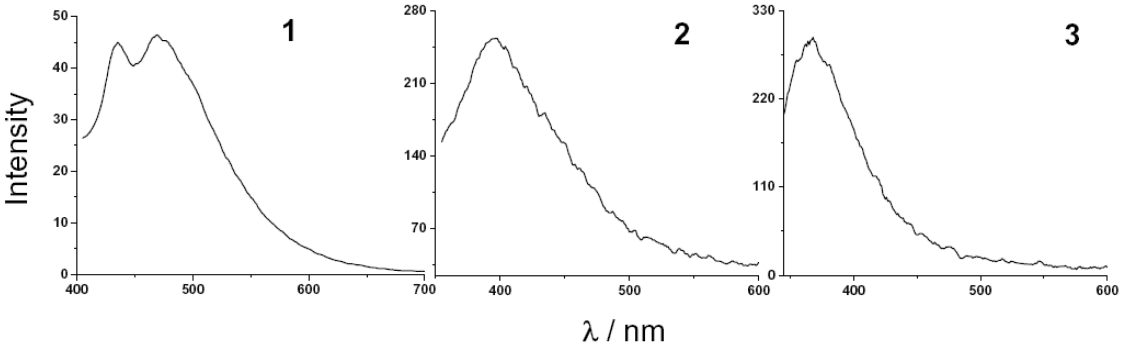

Figure 2. Emission spectra of **1-3**.

The μ_{eff} values calculated from the least square fitting of the initial magnetization curve (χ = M/H) of **1** is 3.47 B.M at room temperature. The value is consistent with that for the

presence of two unpaired electrons and is slightly higher than the $\mu_{s.o.}$ value. The bivalent ruthenium has a $5d^6$ configuration and is always exists in the low-spin state. Therefore, **3** has the low-spin $t_{2g}^6e_g^0$ electronic configuration and is diamagnetic in nature.[247]

The bivalent iron has a d^6 electronic configuration for the free ion and its octahedral complexes can exist in high-spin $t_{2g}^4e_g^2$ or low-spin $t_{2g}^6e_g^0$ configurations. The high-spin and low-spin states respectively show 4-electron paramagnetism and diamagnetism. However, polypyridyl complexes of iron(II) generally show temperature dependent spin cross-over phenomenon, that is conversion from paramagnetism to diamagnetism with the decrease of temperature.[247–249] Complex **2**, have a μ_{eff} value of 5.09 B.M. at room temperature and are slightly higher than the $\mu_{s.o.}$ value of 4.90 B.M. consistent with the high-spin state. A plot of temperature (300-50 K) *vs.* μ_{eff}, *vs.* χ_M and *vs.* $1/\chi_M$ is displayed in Figure 3. As the temperature is decreased, the μ_{eff} values decrease gradually. From the χ_M plot it is evident that the values increases and then decrease with a maximum in the temperature range 110–125 K.[277-280]

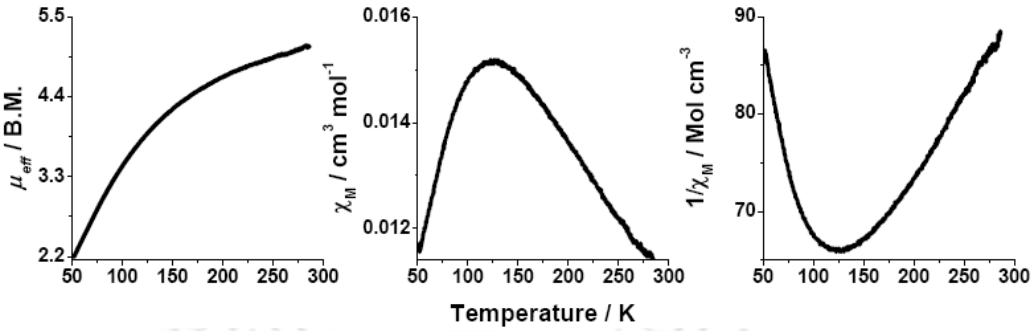

Figure 3. Magnetism in complex **2**.

7.2.3 Molecular Structure

The molecular structures of **1-3** were determined and the crystal data and the refinement parameters are listed in Table 2. The selected bond distances and bond angles are provided respectively in Table 3 and Table 4.

Table 2. Crystal Data and Refinement Parameters for **1-3**

	1	**2**	**3**
Empirical formula	$C_{40}H_{44}N_8NiO_8Cl_2$	$C_{40}H_{46}N_8FeO_9Cl_2$	$C_{40}H_{48}N_8RuO_{10}Cl_2$
Formula weight	894.42	909.45	972.67
Temperature	296(2)	296(2)	296(2)
Wavelength, Å	0.71073	0.71073	0.71073
Crystal system	Triclinic	Triclinic	Triclinic
Space group	*P*	*P*	*P*
a, Å	10.392(2)	10.323(1)	10.380(1)
b, Å	12.167(3)	12.022(1)	12.124(1)
c, Å	19.584(4)	19.485(1)	19.585(1)
α, deg	75.927(3)	77.727(1)	76.199(1)
β, deg	87.258(2)	88.335(1)	87.281(2)
γ, deg	66.652(2)	66.847(1)	66.625(1)
V, Å3	2201.9(8)	2168.5(1)	2193.9(1)
Z	2	2	2

D_{calc} (g cm^{-3})	1.350	1.353	1.496
μ, (mm–1)	0.565	0.535	0.543
[a]GOF on F^2	1.002	1.049	1.000
R [I>2σ(I)]	[b]R_1 = 0.0681,	[b]R_1 = 0.0625,	[b]R_1 = 0.0374,
	[c]wR_2 = 0.2131	[c]wR_2 = 0.1774	[c]wR_2 = 0.1133
R indices (all data)	[b]R_1 = 0.0682,	[b]R_1 = 0.0795,	[b]R_1 = 0.0374,
	[c]wR_2 = 0.2132	[c]wR_2 = 0.1929	[c]wR_2 = 0.1133

[a]GOF = $[\Sigma[w(F_0^2 - F_c^2)^2]/M - N]^{1/2}$ (M = number of reflections, N = number of parameters refined). [b]$R_1 = \Sigma ||F_0| - |F_c||/\Sigma|F_0|$. [c]$wR_2 = [\Sigma[w(F_0^2 - F_c^2)^2]/\Sigma[w(F_0^2)^2]]$.

Table 3. Selected Bond Distances (Å)

	1	**2**	**3**
M–N1	2.114(3)	1.979(2)	2.081(2)
M–N2	1.995(3)	1.877(2)	1.979(2)
M–N3	2.121(3)	1.982(2)	2.065(2)
M–N5	2.101(3)	1.973(2)	2.071(2)
M–N6	1.992(3)	1.876(2)	1.974(2)
M–N7	2.111(3)	1.982(2)	2.079(2)

Table 4. Selected Bond Angles (°)

	1	**2**	**3**
N2–Ni1–N6	178.20(12)	179.09(10)	179.25(8)
N1–Ni1–N3	155.83(12)	161.49(10)	157.66(9)
N5–Ni1–N7	155.98(12)	161.55(10)	157.48(9)
N1–Ni1–N2	78.06(12)	80.85(10)	78.69(8)
N2–Ni1–N3	77.82(12)	80.71(10)	78.98(8)
N5–Ni1–N6	78.11(12)	80.93(10)	78.89(8)
N6–Ni1–N7	77.87(12)	80.64(10)	78.66(8)
N1–Ni1–N5	94.36(12)	89.04(10)	95.90(8)
N1–Ni1–N6	103.34(12)	98.26(10)	101.76(8)
N1–Ni1–N7	90.50(12)	94.43(10)	90.34(8)
N2–Ni1–N5	100.71(12)	98.83(10)	100.49(8)
N2–Ni1–N7	103.31(12)	99.61(10)	101.95(8)

N3–Ni1–N5	88.62(12)	92.25(9)	88.77(8)
N3–Ni1–N6	100.75(12)	100.17(10)	100.57(8)
N3–Ni1–N7	96.49(12)	90.16(10)	93.64(8)

Complex **1-3** crystallized in triclinic *P* *space group and consists of a [M(*L3)2]$^{2+}$ species, two Cl^{-} ions and water molecules of crystallization. The [M(**L3**)$_2$]$^{2+}$ units are iso-structural in nature and perspective views in **2** and **3** is depicted in Figure 4 and 5 respectively.

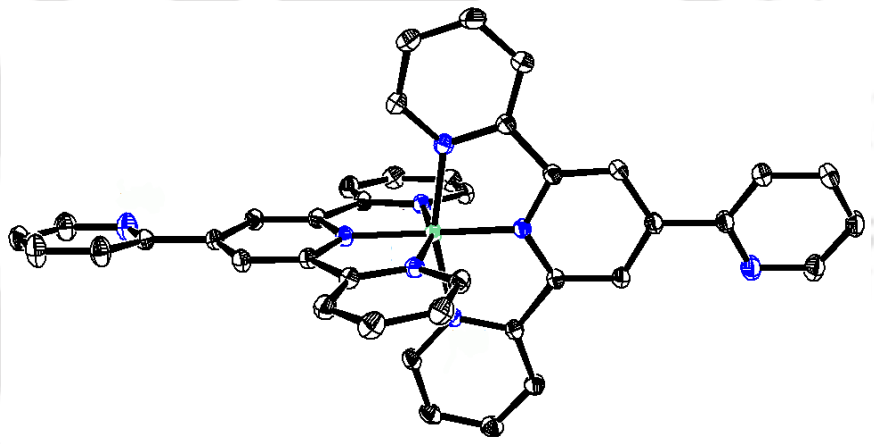

Figure 4. ORTEP of complex **2**.

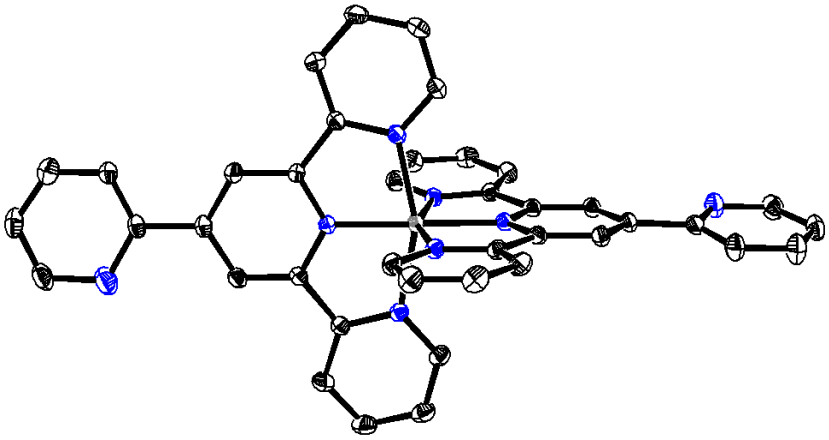

Figure 5. ORTEP of complex **3**.

In each of the bis-chelates, the bivalent metal ion is coordinated by the tridentate **L3** and has a distorted octahedral geometry having a *mer*-N_3N_3 chromophore. Overall, the chelate bite angles are in the range 77.8–80.9° while the other *cis* angles span a wider range, 88.6–103.4°. The intra-ligand *trans* angle, $N_{(X)}$–M–$N_{(X')}$ is 155.8–161.6° and deviates largely from linearity. While the inter-ligand *trans* angle made by the two Y-rings, N2–M–N6 is 178.2–179.3°. For a given metal ion, the M–$N_{(Y)}$ distance is shorter by about 0.10–0.13 Å than the M–$N_{(X)}$ distance. This trend, always observable in the transition metal complexes of terpyridines, has been ascribed to two factors: the efficient overlap of metal t_{2g} orbitals with the π* orbitals of the central pyridyl group and the geometrical constraints of the ligand, probably the former contributing more.[246, 268] The Z-rings deviate from planarity with respect to the Y-rings and is evident from the

torsional angles which are in the range 7.8–14.7°.The two MN_3 planes from each ligand intersects by 86.9–88.1°.

In **1-3**, packing diagram reveals that the $[M(\mathbf{L3})_2]^{2+}$ ions are arranged in a layer. These layers are separated by the layered structures made up of hydrogen bonded networking of the Cl^- ions and water molecules (shown in Figure 6 for **1**). Therefore, the layer of the $[M(\mathbf{L3})_2]^{2+}$ ions form the hydrophobic regions and network of the Cl^- ions and water molecules form the hydrophilic regions. The significant π···π interaction that occurs between the $[M(\mathbf{L3})_2]^{2+}$ ions are: C4···C16, 3.59(1) Å (**1**); C24···C36, 3.59(1) Å (**2**) and C32···C36, 3.60(1) Å (**3**). In addition, the C–H···π interaction *viz.,* C19–H19···C22 3.65(1) Å (**1**); C19–H19···C34 3.56(1) Å (**2**); and C39–H39···C14 3.65(1) Å (**3**) is also present.

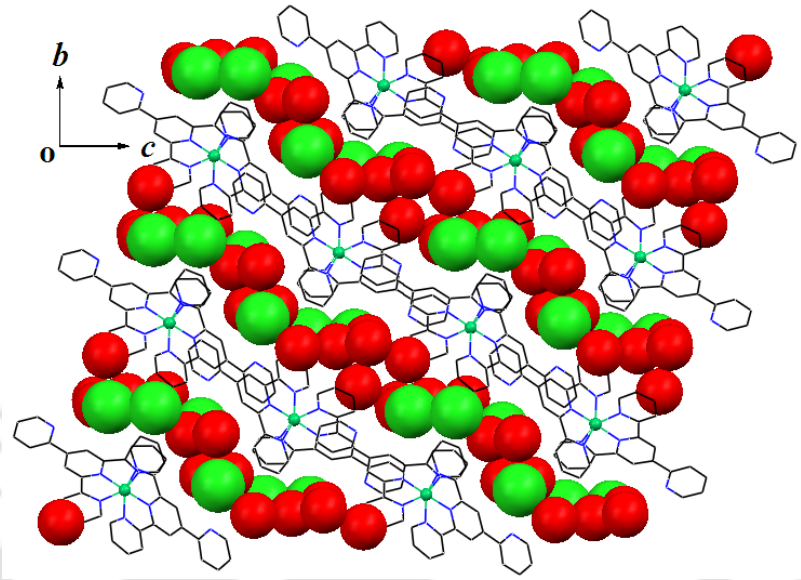

Figure 6. Packing diagram of **1**.

In **1** and **2**, one chloride ion is disordered and refined with partial site-occupancy-factors (Cl2 and Cl3), (0.47964 and 0.52036 in **1**) and (0.48540 and 0.51460 in **2**). The hydrophilic layers made up of the water-chloride ion 2D-network in **1**–**3**, are depicted in Figures 7 and 8.

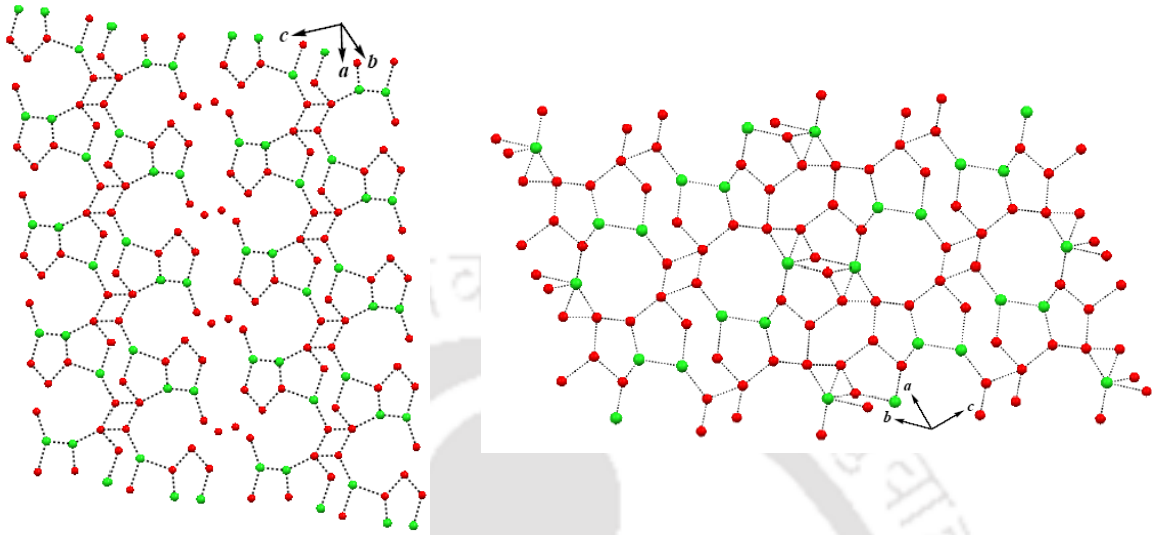

Figure 7. Hydrophilic layers depicting the water-chloride ion network in **1** and **2**

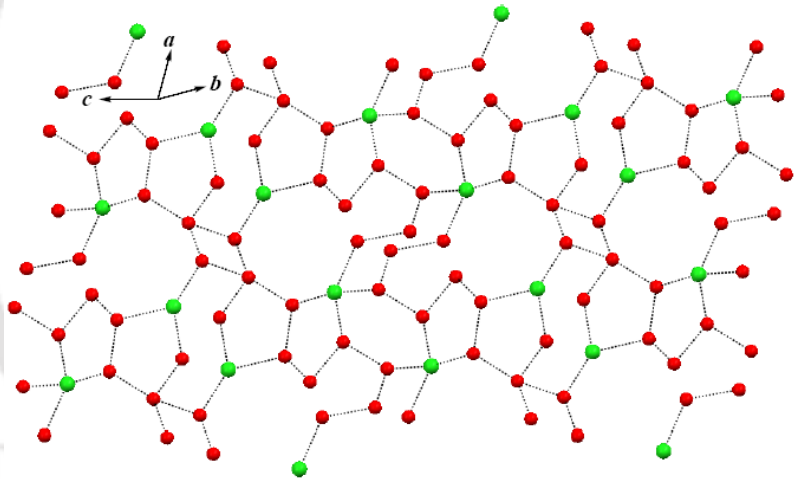

Figure 8. Hydrophilic layers depicting the water-chloride ion network in **3**.

The centro-symmetric repeating 2D-network in **1**–**3** is shown in Figure 9. These units contain a crown shaped O_6Cl_2 eight membered rings that accommodate the chloride ion refined with full weight and are separated by three water molecules. This eight membered ring is connected to a five-membered O_3Cl_2 (in **1**), O_4Cl (in **2** and **3**) ring through a O_2Cl unit generating a five-membered ring and to O_2 through O_2 units leading to a four-membered ring. As per Infantes *et al*., this has the L5(2)5(3)8(2)4 pattern.[322] In **1**,

O8 is a discrete water and is involved in C1–H1···O8 interaction only. The non-bonded contacts are listed in Table 5. It is pertinent to note that the studies water clusters is of great interest in recent time.[283-329]

Figure 9. Repeating Water-chloride ion cluster in **1**, **2**, and **3**.

Table 5. Selected Non-bonded Distances (Å) in **1-3**

	1		**2**		**3**
Cl1···O1	3.159(1)	Cl1···O1	3.015(1)	Cl1···O7	3.029(5)
Cl1···O6	3.133(1)	Cl1···O3	3.169(1)	Cl1···O8	3.146(5)
Cl1···O3	3.254(1)	O1···O2	2.910(1)	Cl1···O1	3.216(4)
O1···O5	2.862(1)	O2···O3	2.878(1)	O4···O8	2.817(6)

O5···O6	2.852(1)	O2···O7	2.931(1)	O4···O7	2.968(6)
Cl3···O3	2.932(1)	O6···O7	3.023(1)	O4···O3	2.977(5)
O2···O3	3.028(1)	Cl1···Cl2	3.185(1)	Cl2···O3	3.008(7)
O2···O4	3.015(1)	Cl2···O4	2.936(1)	O1···O3	2.919(6)
Cl2···O7	3.065(1)	O4···O5	2.930(1)	O1···O2	2.983(6)
Cl2···Cl3	3.023(1)	O5···O6	2.952(1)	O2···O6	3.023(6)
		O6···O9	2.802(1)	O6···O9	2.902(8)
		O8···O9	2.647(1)	O9···O10	2.769(13)
		O8···Cl3	3.265(1)	Cl2···O5	3.107(7)
		O6···Cl3	2.907(1)	Cl2···O6	3.009(5)

7.3 Conclusion

The *bis*-chelates of **L3** of the type $[M(\mathbf{L3})_2]Cl_2{\cdot}xH_2O$, where M = Ni (**1**), Fe (**2**), Ru (**3**) and x = 8, 9, 10 respectively were synthesized. Complex **1** exhibits d-d transitions and ILCT bands at visible and UV region respectively. In complex **2** and **3** the d-d transitions were not observed, and both exhibit MLCT and ILCT bands respectively in visible and UV region. The emission spectra are of $\pi\rightarrow\pi^*$ character in **1**-**3**. At room temperature, the μ_{eff} value of complex **1** is 3.47 B.M and complex **3** is diamagnetic. Complex **2** is high spin at room temperature with μ_{eff}, 5.09 B.M. and exhibits a gradual spin decay on cooling. All the complexes **1**-**3** crystallized in triclinic *P* *space group and consists of an* iso-structural $[M(\mathbf{L3})_2]^{2+}$ species, two Cl^- ions and water molecules of crystallization. The hydrophobic layers of $[M(\mathbf{L3})_2]^{2+}$ are generated through π···π stacking as well as C–H···π interactions and are separated by hydrophilic layers made up of hydrogen bonded 2D-network of the Cl^- ions and water molecules. The centro-symmetric repeating unit present in the 2D-network has a L5(2)5(3)8(2)4 pattern.

Summary of Part B

- 4′-(2-pyridyl)-2,2′:6′,2′′-terpyridine (**L3**) prepared using the procedure described **Part A**, has been utilized for studying the coordination chemistry of bivalent iron, nickel and ruthenium
- **L3** complexes of Fe(II) shows different protonation characteristics at the non-coordinated pyridine-N atom.
- **L3** is a useful motif for supramolecular architecture.

Abbreviations

a	Unit cell dimension a
b	Unit cell dimension b
c	Unit cell dimension c
D	density of the crystal
α	Interfacial angle α in a unit cell
β	Interfacial angle β in a unit cell
γ	Interfacial angle γ in a unit cell
Z	Unit cell formula units
λ	Wave length
ν	Wave number
μ	Absorption coefficient
ε	Molar extinction coefficient
τ	Geometric parameter applicable for five-co-ordinate structures as an index of the degree of trigonality between trigonal bipyramidal and rectangular pyramidal.
$\mu_{S.O.}$	Spin-only magnetic moment
μ_{eff}	Effective magnetic moment
χ	Magnetic Susceptibility
χ_M	Molar Susceptibility
H	Applied Magnetic Field
g	Lande splitting factor
A	Hyperfine splitting constant

References

1. Schiff, H. *Ann. Chem. Suppl.* **1864**, *3*, 343.
2. Schiff, H. *Ann. Chem.* **1869**, *150*, 193.
3. Schiff, H. *Ann. Chem.* **1869**, *151*, 186.
4. Sacconi, L. *Coord. Chem. Rev.*, **1966**, *1*, 126.
5. Yamada, S. *Coord. Chem. Rev.*, **1966**, *1*, 415.
6. Hobday, M. D.; Smith, T. D. *Coord. Chem. Rev.*, **1973**, *9*, 311.
7. Holm, R. H.; Everett, G. W.; Chakravorty, A. *Prog. Inorg. Chem.* **1966**, *7*, 83.
8. Holm, R. H.; O'Connor, M. J. *Prog. Inorg. Chem.*, **1971**, *14*, 214.
9. Toscano, P. J.; Marzilli, L. G. *Prog. Inorg. Chem.* **1984**, *31*, 105.
10. Alexander, V. *Chem. Rev.* **1995**, *95*, 273.
11. Fenton, D. E.; Okawa, H. *Chem. Ber.* **1997**,*130*, 433.
12. Collinson, S. R.; Fenton, D. E. *Coord. Chem. Rev.* **1996**, *148*, 19.
13. Fenton, D. E. *Pure Appl. Chem.* **1986**, *58*, 1437.
14. Atwood, D. A.; Harvey, M. J. *Chem. Rev.* **2001**, *101*, 37.
15. Che, C. -M.; Huang, J. -S. *Coord. Chem. Rev.* **2003**, *242*, 97.
16. Canali, L.; Sherrington, D. C. *Chem. Soc. Rev.* **1999**, *28*, 85.
17. Gibson, V. C.; Spitzmesser, S. K. *Chem. Rev.* **2003**, *103*, 283;
18. Britovsek, G. J. P.; Gibson, V. C.; Wass, D. F. *Angew. Chem. Int. Ed.* **1999**, *38*, 428.
19. Curtis, N. F. *Coord. Chem. Rev.* **1968**, *3*, 3.
20. Busch, D. H. *Science* **1971**, *171*, 241.
21. Nelson, S. M. *Pure Appl. Chem.* **1980**, *52*, 2461.
22. Okawa, H.; Furutachi, H.; Fenton, D. E. *Coord. Chem. Rev.* **1998**, *174*, 51.
23. Lindoy, L. F. *The Chemistry of Macrocyclic Ligand Complexes*, Cambridge University, Cambridge, UK, **1989**.
24. Lindoy, L. F. *Pure Appl. Chem.* **1989**, *61*, 1575.

25. Lindoy, L. F. in: Izatt, R. M.; Christensen, J. J. (Eds.) *Synthesis of Macrocycle: The Design of Selective Complexing Agents*, Wiley, New York, **1987**, p. 53.
26. Guerriero, P.; Tamburini, S. ; Vigato, P. A. *Coord. Chem. Rev*. **1995**, *139*, 17.
27. Kahn, O. *Adv. Inorg. Chem.* **1995**, *43*, 179.
28. Murray, K. S. *Adv. Inorg. Chem.* **1995**, *43*, 261.
29. Coper, S. R. (Ed.), *Crown Compounds: Toward Future Applications*, VCH Publisher Inc., New York, **1992**.
30. Melson, G. A. (Ed.), *Coordination Chemistry of Macrocyclic Compounds*, Plenium Press, New York, **1979**.
31. Martell, A.; Penitka, J.; Kong, D. *Coord. Chem. Rev*. **2001**, *216–217*, 55.
32. Beer, P. D.; Smith, D. K. *Prog. Inorg. Chem.* **1997**, *46*, 1.
33. McKee, V. *Adv. Inorg. Chem.* **1993**, *40*, 323.
34. Nelson, J.; McKee, V.; Morgan, G. *Prog. Inorg. Chem.* **1998**. *47*, 167.
35. Brooker, S. *Coord. Chem. Rev*. **2001**, *222*, 33.
36. Inone, Y.; Gokel, G. W. (Eds.), *Cation Binding by Macrocycles*, Marcel Dekker Inc., New York, USA, **1990**.
37. Branchi, A.; Bowman-James, K.; Garcia-España, E. (Ed.), *Supramolecular Chemistry of Anions*, Wiley-VCH, New York, USA, **1997**.
38. Amendola, V.; Fabbrizzi, L.; Mangano, C.; Pallavicini, P.; Poggi, A.; Taglietti, A. *Coord. Chem. Rev*. **2001**, *219–221*, 821.
39. Kaden, T. A. *Top. Curr. Chem*. **1984**, *121*, 157.
40. Hay, R. W. in: Kimura, E. (Ed.), *Current Topics in Macrocyclic Chemistry in Japan*, Hiroshima University, **1987**, p. 56.
41. Alcock, N. W.; Balakrishnan, K. P.; Moore, P.; Pike, G. A. *J. Chem. Soc., Dalton Trans*. **1987**, 889.
42. Arnold, K. A.; Echegoyen, L.; Fronczek, F. R.; Gandour, R. D.; Gatto, V. J.; White, D.; Gokel, G. W. *J. Am. Chem. Soc*. **1987**, *109*, 3716.
43. Fenton, D. E.; Rossi, G. *Inorg. Chim. Acta* **1985**, *98*, L29.

44. Gatto, V. J.; Gokel, G. W. *J. Am. Chem. Soc*. **1984**, *106*, 8240.

45. Adams, H.; Bailey, N. A.; Carlisle, W. D.; Fenton, D. E.; Rossi, G. *J. Chem. Soc., Dalton Trans.* **1991**, 1271.

46. Adams, H.; Bailey, N. A.; Dwyer, M. J. S.; Fenton, D. E.; Hellier, P. C.; Hempstead, P. D. *J. Chem. Soc., Chem. Commun*. **1991**, 1297.

47. Messerschmidt, A.; Rossi, A.; Ladenstein, R.; Hubber, R.; Bolognesi, M.; Gatti, G.; Marchesini, A.; Petruzelli, R.; Finazzi-Agro, A. *J. Mol. Biol*. **1989**, *206*, 5133.

48. Torzilli, M. A.; Colquhoun, S.; Kim, J.; Beer, R. H. *Polyhedron* **2002**, *21*, 705.

49. Costes, J. -P.; Dahan, F.; Fernandez, M. B. F; Garcia, M. I. F.; Deibe, A. M. G.; Sanmartin, J. *Inorg. Chim. Acta* **1998**, *274*, 73.

50. Root, C. A.; Hoeschele, J. D.; Cornman, C. R.; Kampf, J. W.; Pecoraro, V. L. *Inorg. Chem*. **1993**, *32*, 3855.

51. Sacconi, I. L.; Nannelli, P.; Campigli, U. *Inorg. Chem.* **1965**, *4*, 818.

52. Goto, M.; Ishikawa, Y.; Ishihara, T.; Nakatake, C.; Higuchi, T.; Kurosaki, H.; Goedken, V. L. *J. Chem. Soc., Dalton Trans.* **1998**, 1213

53. Nelson, S. M.; Esho, F. S.; Drew, M. G. B. *J. Chem. Soc., Dalton Trans.* **1982**, 407.

54. Constable, E. C.; Holmes, J. M. *Inorg. Chim. Acta* **1987**, *126*, 187.

55. Duncan, C. A.; Copeland, E. P.; Kahwa, I. A.; Quick, A.; Williams, D. J. *J. Chem. Soc., Dalton Trans.* **1997**, 917.

56. Hernández-Molina, R.; Mederos, A.; Dominguez, S.; Gili, P.; Ruiz-Pérez, C.; Castiñeiras, A.; Solans, X.; Lloret, F.; Real, J. A. *Inorg. Chem*. **1998**, *38*,5102.

57. Carlisle, W.D.; Fenton, D.E.; Mulligan, D.C.; Roberts, P.B.; Vigato P.A.; Tamburini, S. *Inorg. Chim. Acta* **1987**, *126*, 233.

58. Cheng, P.; Liao, D.; Yan, S.; Jiang, Z.; Wang, G.; Yao, X.; Wang, H. *Inorg. Chim. Acta* **1997**, *248*, 135.

59. Lewis, W. G.; Magallon, F. G.; Fokin, V. V.; Finn, M. G. *J. Am. Chem. Soc*. **2004**, *126*, 9152.

60. Troshin, P. A.; Troyanov, S. I.; Boiko, G. N.; Lyubovskaya, R. N.; Lapshin, A. N.; Goldshleger, N. F. *Fullerenes, Nanotubes and Carbon Nanostructures* **2004**, *12*, 413.

61. Grigg, R.; Donegan, G.; Gunaratne, H. Q. N.; Kennedy, D. A.; Malone, J. F.; Sridharan, V.; Thianpatanagul, S. *Tetrahedron* **1989**, *45*, 1723.

62. Percec, V.; Guliashvili, T.; Popov, A. V. *U.S. Pat. Appl. Publ.* **2005**, 55 pp.

63. Matyjaszewski, K.; Gaynor, S. G.; Paik, H-J.; Pintauer, T.; Pyun, J.; Qiu, J.; Teodorescu, M.; Xia, J.; Zhang, X. *PCT Int. Appl.* **2000**, 200 pp.

64. Xia, J.; Matyjaszewski, K. *Polymer Preprints* (ACS, Division of Polymer Chemistry) **1999**, *40*, 442.

65. Bell, T. W.; Hu, L. Y. *Tetrahedron Lett.* **1988**, *29*, 4819.

66. Tejel, C.; Ciriano, M. A.; del Rio, M. P.; van den Bruele, F. J.; Hetterscheid, D. G. H.; Tsichlis i Spithas, N.; de Bruin, B. *J. Am. Chem. Soc*. **2008**, *130*, 5844.

67. Lions, F.; Martin, K. V. *J. Am. Chem. Soc*. **1957**, *79*, 2733.

68. Creber, M. L.; Orrell, K. G.; Osborne, A. G.; Sik, V.; Coles, S. J.; Hibbs, D. E.; Michael, H. B. *Inorg. Chim. Acta* **2000**, *299*, 209.

69. Goe, G. L.; Keay, J. G.; Scriven, E. F. V.; Prunier, M. L.; Quimby, S. J. *PCT Int. Appl.* **1992**, 29 pp.

70. Goodwin, H. A.; Lions, F. *J. Am. Chem. Soc*. **1959**, *81*, 6415.

71. Goldsworthy, D. H.; Kite, K. *J. Organomet. Chem.* **1987**, *319*, 257.

72. Padhi, S. K.; Sahu, R.; Manivannan, V. *Polyhedron* **2008**, *27*, 805.

73. Song, J.; Shen, Q.; Xu, F.; Lu, X. *Tetrahedron* **2007**, *63*, 5148.

74. Ceder, R. M.; Muller, G.; Ordinas, M.; Ordinas, J. I. *Dalton Trans*. **2007**, 83.

75. Song, Y.; Xu, Z.; Sun, Q.; Su, B.; Gao, Q.; Liu, H.; Zhao, J. *J. Coord. Chem*. **2007**, *60*, 2351.

76. Regnier, T.; Lavastre, O. *Tetrahedron* **2006**, *62*, 155.

77. Bandini, M.; Luque, R.; Budarin, V.; Macquarrie, D. J. *Tetrahedron* **2005**, *61*, 9860.

78. Chen, J.; Cunico, R. F. *Tetrahedron Lett*. **2003**, *44*, 8025.

79. Vilaivan, T.; Winotapan, C.; Shinada, T.; Ohfune, Y. *Tetrahedron Lett*. **2001**, *42*, 9073.

80. Boduszek, B. *Polish J. Chem.* **2001**, *75*, 663.

81. Boduszek, B. *Phosphorus, Sulfur Silicon Relat. Elem.* **1996**, *113*, 209.

82. Menard, L.; Fontaine, L.; Brosse, J-C. *Reactive Polymers* **1994**, *23*, 201.

83. Harada, K.; Kaji, E.; Zen, S. *Chemical & Pharmaceutical Bulletin* **1980**, *28*, 3296.

84. Babler, J. H.; Invergo, B. J. *J. Org. Chem.* **1981**, *46*, 1937.

85. Dinizo, S. E.; Watt, D. S. *J. Am. Chem. Soc*. **1975**, *97*, 6900.

86. Chowdhury, H.; Bose, D.; Ghosh, R.; Rahaman, S. H.; Ghosh, B. K. *Ind. J. Chem.* **2004**, *43A*, 1239.

87. Alyea, E. C.; Jain, V. K. *Polyhedron* **1996**, *15*, 1723.

88. Johnson, D. W.; Mayer, H. K.; Minard, J. P.; Banaticla, J.; Miller, C. *Inorg. Chim. Acta* **1988**, *144*, 167.

89. Walther, D.; Herzog, V. *Z. fuer Chemie* **1981**, *21*, 195.

90. Robinson, M. A.; Curry, J. D.; Busch, D. H. *Inorg. Chem.* **1963**, *2*, 1178.

91. Kuhl, S.; Schneider, R.; Fort, Y. *Organometallics* **2003**, *22*, 4184.

92. Wang, Y.; Mi, A.; Jiang, Y. *Synthetic Commun.* **1992**, *22*, 265.

93. Pointeau, P.; Patin, H.; Mousser, A.; Le M., Jean Y. *J. Organomet. Chem*. **1986**, *312*, 263.

94. Standfest-Hauser, C. M.; Mereiter, K.; Schmid, R.; Kirchner, K. *Eur. J. Inorg. Chem.* **2003**, *10*, 1883.

95. Shell Internationale Research Maatschappij N. V. *Neth. Appl.* **1968**, 13 pp.

96. Annunziata, R.; Benaglia, M.; Caporale, M.; Raimondi, L. *Tetrahedron: Asymmetry* **2002**, *13*, 2727.

97. Rüelke, R. E.; Kaasjager, V. E.; Kliphuis, D.; Elsevier, C. J.; van Leeuwen, P. W. N. M.; Vrieze, K.; Goubitz, K. *Organometallics* **1996**, *15*, 668.

98. Rüelke, R. E.; Ernsting, J. M.; Spek, A. L.; Elsevier, C. J.; van Leeuwen, P. W. N. M.; Vrieze, K. *Inorg. Chem.* **1993**, *32*, 5769.

99. Cortes, R.; Lezama, L.; Ruiz de Larramendi, J. I.; Madariaga, G.; Mesa, J. L.; Zuniga, F. J.; Rojo, T. *Inorg. Chem*. **1995**, *34*, 778.

100. Stor, G. J.; van der Vis, M.; Stufkens, D. J.; Oskam, A.; Fraanje, J.; Goubitz, K. *J. Organomet. Chem.* **1994**, *482*, 15.

101. Ramesh, K.; Mukherjee, R. N. *Ind. J. Chem.* **1991**, *30A*, 1057.

102. Arriortua, M. I.; Insausti, M.; Cortes, R.; Larramendi, J. I. R. *Powder Diffraction* **1994**, *9*, 161.

103. Kamei, T.; Kishii, N.; Kobayashi, T.; Kurihara, K.; Matsuzawa, N.; Iwamoto, H.; Morita, H. *Jpn. Kokai Tokkyo Koho* **2000**, 22 pp.

104. Failla, S.; Finocchiaro, P. *Phosphorus, Sulfur Silicon Relat. Elem.* **1996**, *114*, 83.

105. Steevens, J. B.; Pandit, U. K. *Tetrahedron* **1983**, *39*, 1395.

106. Srivastava, S.; Singh, M. L.; Pandey, Y. *J. Ind. Chem. Soc.* **2004**, *81*, 590.

107. Kriza, A.; Pricop, L.; Meghea, A.; Stanica, N. *J. Ind. Chem. Soc.* **2001**, *78*, 448.

108. Zhou, X-H.; Wu, T.; Li, D. *Inorg. Chim. Acta* **2006**, *359*, 1442.

109. Charette, A. B.; Boezio, A. A.; Janes, M. K. *Org. Lett.* **2000**, *2*, 3777.

110. Khalaji, A. D.; Amirnasr, M.; Welter, R. *Acta Cryst.* **2006**, *E62*, m2950.

111. Khalaji, A. D.; Amirnasr, M.; Welter, R. *Anal. Sci.: X-Ray Structure Analysis Online* **2006**, *22*, x151.

112. Banerjee, S.; Lassahn, P-G.; Janiak, C.; Ghosh, A. *Polyhedron* **2005**, *24*, 2963.

113. Banerjee, S.; Ghosh, A.; Wu, B.; Lassahn, P-G.; Janiak, C. *Polyhedron* **2005**, *24*, 593.

114. Banerjee, S.; Gangopadhyay, J.; Lu, C-Z.; Chen, J-T.; Ghosh, A. *Eur. J. Inorg. Chem*. **2004**, *12*, 2533.

115. Louloudi, M.; Nastopoulos, V.; Gourbatsis, S.; Perlepes, S. P.; Hadjiliadis, N. *Inorg. Chem. Commun*. **1999**, *2*, 479.

116. Gourbatsis, S.; Plakatouras, J. C.; Nastopoulos, V.; Cardin, C. J.; Hadjiliadis, N. *Inorg. Chem. Commun*. **1999**, *2*, 468.

117. Gourbatsis, S.; Perlepes, S. P.; Butler, I. S.; Hadjiliadis, N. *Polyhedron* **1999**, *18*, 2369.

118. Gourbatsis, S.; Hadjiliadis, N.; Perlepes, S. P.; Garoufis, A.; Butler, I. S. *Transition Met. Chem.* **1998**, *23*, 599.

119. Oshima, S.; Hirayama, N.; Kubono, K.; Kokusen, H.; Honjo, T. *Anal. Chim. Acta* **2001**, *441*, 157.

120. Biel, J. H.; Hoya, W. K. *U.S. Pat. Appl. Publ.* **1965**, 5 pp.

121. Heterocyclic alkylenediimines and -diamines. (Lakeside Laboratories, Inc.). *G.B. Pat. Appl. Publ.* **1964**, 10 pp.

122. Iovel, I.; Golomba, L.; Popelis, J.; Grinberga, S.; Belyakov, S.; Lukevics, E. *Chem. Heterocycl. Comp*. **2002**, *38*, 1210.

123. Montalvo-Gonzalez, R.; Ariza-Castolo, A. *J. Mol. Struct*. **2003**, *655*, 375.

124. Rohovec, J.; Vojtisek, P.; Lukes, I. *Phosphorus, Sulfur Silicon Relat. Elem.* **1999**, *148*, 79.

125. Zheng, Hao; Sheng, Ying-Zhong; Gu, Hong-Wei; Pan, Yi; Gu, Wei-Jing. Wuji *Huaxue Xuebao* **1999**, *15*, 336.

126. Failla, S.; Finocchiaro, P.; Latronico, M.; Libertini, M. *Phosphorus, Sulfur Silicon Relat. Elem.* **1994**, *88*, 185.

127. El-Shafei, A. K.; Hassan, K. M. *Curr. Sci.* **1983**, *52*, 633.

128. Hess, U.; Thiele, R. *J. fuer Praktische Chemie* (Leipzig) **1982**, *324*, 385.

129. Holzbecher, Z.; Van Trung, H. *Collect. Czech. Chem. Commun*. **1976**, *41*, 1506.

130. Kramberger, L.; Lorencak, P.; Polanc, S.; Vercek, B.; Stanovnik, B.; Tisler, M.; Povazanec, F. *J. Heterocyclic Chem.* **1975**, *12*, 337.

131. Callander, S. E.; Roberts, E. R. *Biochim. Biophys. Acta* **1961**, *54*, 92.

132. Brzezinski, B.; Zundel, G. *Chem. Phys. Lett.* **1985**, *115*, 212.

133. Yurt, A.; Bereket, G.; Kivrak, A.; Balaban, A.; Erk, B. *J. Appl. Electrochem.* **2005**, *35*, 1025.

134. Mohamed, S. K. *Bulletin of the Faculty of Science, Assiut University, B: Chemistry* **1999**, *28*, 1.

135. Iovel, I.; Golomba, L.; Popelis, J.; Grinberga, S.; Lukevics, E. *Chem. Heterocycl. Comp*. **2003**, *39*, 49.

136. Hamed, M. M. *Can. J. Appl. Spectrosc*. **1991**, *36*, 1.

137. Tang, Bo; Zhang, G.; Han, F.; Chen, D.; Chen, Z.; Li, P. *Faming Zhuanli Shenqing Gongkai Shuomingshu* **2002**, 8 pp.

138. Kuduk-Jaworska, J. *Transition Met. Chem*. **1994**, *19*, 296.

139. Bala, M.; Sinha, A. I. P. *Asian J. Chem.* **1989**, *1*, 392.

140. Yanez, X.; Claver, C.; Castillon, S.; Fernandez, E. *Tetrahedron Lett*. **2003**, *44*, 1631.

141. Katagiri, N.; Kato, T.; Niwa, R. *J. Heterocyclic Chem.* **1984**, *21*, 407.

142. Capitan-Vallvey, L. F.; Salinas, F.; Jimenez, C.; Cuadros, L. *Can. J. Chem.* **1982**, *60*, 1706.

143. Nagy, S.; Neal-Hawkins, K. L. *U.S. Pat. Appl. Publ.* **2003**, 6 pp.

144. Phillips, J. P.; Keown, R. W.; Fernando, Q. *J. Org. Chem.* **1954**, *19*, 907.

145. Ishiyama, T.; Hartwig, J. *J. Am. Chem. Soc.* **2000**, *122*, 2043.

146. Troisi, L.; Granito, C.; Pindinelli, E.; Ronzini, L. *Heterocycles* **2007**, *71*, 1381.

147. Angurell, I.; Martinez-Ruiz, I.; Rossell, O.; Seco, M.; Gomez-Sal, P.; Martin, A.; Font-Bardia, M.; Solans, X. *J. Organomet. Chem*. **2007**, *692*, 3882.

148. Das, S.; Maloor, S. A.; Pal, S.; Pal, S. *Cryst. Growth Des*. **2006**, *6*, 2103.

149. Majumder, A.; Rosair, G. M.; Mallick, A.; Chattopadhyay, N.; Mitra, S. *Polyhedron* **2006**, *25*, 1753.

150. Gao, E-Q.; Bai, S-Q.; He, Z.; Yan, C-H. *Inorg. Chem*. **2005**, *44*, 677.

151. Sugiura, M.; Robvieux, F.; Kobayashi, S. *Synlett.* **2003**, *11*, 1749.

152. Park, M. S.; Jun, K.; Shin, S. R.; Oh, S. W.; Park, K. H. *J. Heterocyclic Chem.* **2002**, *39*, 1279.

153. Chatterjee, D.; Mukherjee, S.; Roy, B. C. *React. Kinet. Catal. Lett.* **2000**, *71*, 217.

154. Hillairet, C.; Michaud, G.; Sirol, S. *PCT Int. Appl.* **2007**, 59pp.

155. Duin, M. A.; Ernsting, J. M.; Elsevier, C. J. *Collect. Czech. Chem. Commun*. **2007**, *72*, 764.

156. Duran, M. L.; Romero, J.; Rodriguez, A.; Sousa, Y. *An. Quim. B: Quim. Inorg. Quim. Anal.* **1988**, *84*, 60.

157. Tyler, L. A.; Olmstead, M. M.; Mascharak, P. K. *Inorg. Chem.* **2001**, *40*, 5408.

158. Singh, K.; Singh, R.; Tandon, J. P. *Bull. Chem. Soc. Jpn*. **1988**, *61*, 4494.

159. Morgan, G. T; Burstall, F. H. *J. Chem. Soc.* **1932**, 20.

160. Morgan, G. T; Burstall, F. H. *J. Chem. Soc.* **1937**, 1649.

161. Constable, E. C. *Adv. Inorg. Chem. Radiochem.* **1986**, *30*, 69.

162. Jennette, K.; Lippard, S. J.; Vassiliades, G.; Bauer, W. *Proc. Natl. Acad. Sci. U. S. A.* **1974**, *71*, 3839.

163. Bonse, S.; Richards, J. M.; Ross, S. A.; Lowe, G.; Krauth-Siegel. R. L. *J. Med. Chem.* **2000**, *43*, 4812.

164. Long-Xuan, Z.; Moon, Y-S.; Basnet, A.; Kim, E-k.; Jahng, Y.; Park, J. G.; Jeong, T. C.; Cho, W-J.; Choi, S-U.; Lee, C. O.; Lee, S-Y.; Lee, C-S.; Lee, E-S. *Bioorg. Med. Chem. Lett.* **2004**, *14*, 1333.

165. Swiegers, G. F.; Malefetse, T. J. *Chem. Rev.* **2000**, *100*, 3483.

166. Hofmeier, H.; Schubert. U. S. *Chem. Soc. Rev.* **2004**, *33*, 373.

167. Chelucci, G. *Synth. Commun.* **1993**, *23*, 1897.

168. Uenishi, J.; Nishiwaki, K.; Hata, S.; Nakamura, K. *Tetrahedron Lett.* **1994**, *35*, 7973.

169. Chelucci, G.; Cabras, M. A.; Saba, A. *J. Mol. Catal. A.* **1995**, *95*, L7.

170. Leroy-Lhez, S.; Fages, F. *C. R. Chimie*, **2005**, *8*, 1204.

171. Ward, M. D. *Chem. Soc. Rev.* **1995**, *24*, 121.

172. Sauvage, J.-P.; Collin, J.-P.; Chambron, J.-C.; Guillerez, S.; Coudret, C.; Balzani, V.; Barigelletti, F.; De Cola, L.; Flamigni, L. *Chem. Rev.* **1994**, *94*, 993.

173. Thompson, A. M. W. C. *Coord. Chem. Rev.* **1997**, *160*, 1.

174. Thummel, R. P. *in*: Mccleverty, J. A.; Meyer, T. J. (Eds) *Comprehensive Coordination Chemistry II*. Elsevier, Oxford, **2004**, p. 41.
175. Kröhnke, F. *Synthesis* **1976**, 1.
176. Smith, C. B.; Raston, C. L.; Sobolev, A. N.; *Green Chem*. **2005**, *7*, 650.
177. Hou, L.; Li, D.; Shi, W-J.; Yin, Y-G.; Ng, S. W. *Inorg. Chem.* **2005**, *44*, 7825.
178. Arm, K. J.; Leslie, W.; Williams, J. A. G. *Inorg. Chim. Acta* **2006**, *359*, 1222.
179. Feng, H.; Zhou, X-P.; Wu, T.; Li, D.; Yin, Y-G.; Ng, S. W. *Inorg. Chim. Acta* **2006**, *359*, 4027.
180. Shi, W-J.; Hou, L.; Li, D.; Yin, Y-G. *Inorg. Chim. Acta* **2007**, *360*, 588.
181. Gou, L.; Wu, Q-R.; Hu, H-M.; Qin, T.; Xue G-L.; Yang, M-L.; Tang, Z-X. *Polyhedron* **2008**, *27*, 1517.
182. Hou, L.; Li, D.; Yin, Y-G.; Ng, S. W. Acta. Cryst. 2005, E61, m21.
183. Hou, L.; Li, D.; Ng, S. W. Acta. Cryst. 2005, E61, m404.
184. Padhi, S. K.; Saha, D.; Sahu, R.; Subramanian, J.; Manivannan, V. *Polyhedron* **2008**, *27*, 1714.
185. Cave, G. W. V.; Raston, C. L. *Chem. Commun.* **2000**, 2199.
186. Cave, G. W. V.; Raston, C. L. *J. Chem. Soc., Perkin Trans.* **2001**, *1*, 3258.
187. Goodall, W.; Williams, J. A. G. *J. Chem. Soc., Dalton Trans.*, **2000**, 2893.
188. Constable, E. C.; Housecroft, C. E.; Neuburger, M.; Schaffner, S.; Schaper, F. *Inorg. Chem. Commun*. **2006**, *9*, 433.
189. Persaud, L.; Barbiero, G. *Can. J. Chem.*, **1991**, *69*, 315.
190. Hegde, V.; Jahng, Y.; Thummel, R. P.; *Tetrahedron Lett.* **1987**, *28*, 4023.
191. Constable, E. C.; Thompson, A. M. W. C. *J. Chem. Soc. Dalton Trans*. **1992**, 2947;
192. Constable, E. C.; Housecroft, C. E.; Neuburger, M.; Schaffner, S.; Schaper, F. *Inorg. Chem. Commun*. **2006**, *9*, 616.
193. Wang, J.; Hanan, G. S. *Synlett.* **2005**, *8*, 1251.
194. Shirai, H.; Hanabusa, K.; Takahashi, Y.; Mizobe, F.; Hanada, K. *PCT Int. Appl.* **1994**, 54 pp.

195. Beves, J. E.; Constable, E. C.; Housecroft, C. E.; Kepert, C. J.; Neuburger, M.; Price, David J.; Schaffner, S. *CrystEngComm*, **2007**, 1073.

196. Beves, J. E.; Constable, E. C.; Housecroft, C. E.; Neuburger, M.; Schaffner, S. *CrystEngComm*, **2008**, 1073.

197. Winter, A.; Schubert, U. S. *Macromol. Chem. Phys*. **2007**, *208*, 1956.

198. Davidson, G. J. E.; Loeb, S. J. *Dalton Trans.* **2003**, 4319.

199. Constable, E. C.; Dunphy, E. L.; Housecroft, C. E.; Kylberg, W.; Neuburger, M.; Schaffner, S.; Schofield, E. R.; Smith, C. B. *Chem. Eur. J.* **2006**, *12*, 4600.

200. Constable, E. C.; Schofield, E. *Chem. Commun*. **1998**, 403.

201. Constable, E. C.; Housecroft, C. E.; Neuburger, M.; Phillips, D.; Raithby, P. R.; Schofield, E.; Sparr, E.; Tocher, D. A.; Zehnder, M.; Zimmermann, Y. C. *Dalton* **2000**, 2219.

202. Pitarch Lopez, J.; Kraus, W.; Reck, G.; Thuenemann, A.; Kurth, D. G. *Inorg. Chim. Acta* **2005**, *358*, 3384.

203. Constable, E. C.; Thompson, A. M. W. C. *Dalton Trans* **1994**, 1409.

204. Beves, J. E.; Dunphy, E. L.; Constable, E. C.; Housecroft, C. E.; Kepert, C. J.; Neuburger, M.; Price, D. J.; Schaffner, S. *Dalton Trans.* **2008**, 386.

205. Mayer, C. R.; Dumur, F.; Miomandre, F.; Dumas, E.; Devic, T.; Fosse, C.; Secheresse, F. *New J. Chem.* **2007**, *31*, 1806.

206. Beves, J. E.; Constable, E. C.; Housecroft, C. E.; Kepert, C. J.; Price, D. J. *CrystEngComm* **2007**, 456.

207. Figgemeier, E.; Constable, E. C.; Housecroft, C. E.; Zimmermann, Y. C. *Langmuir* **2004**, *20*, 9242.

208. Figgemeier, E.; Merz, L.; Hermann, B. A.; Zimmermann, Y. C.; Housecroft, C. E.; Guentherodt, H. J.; Constable, E. C. *J. Phys. Chem. B* **2003**, *107*, 1157.

209. Rymmai, E. K.; Rao, K. *Ind. J. Chem.* **2003**, *42A*, 1892.

210. Chichak, K.; Jacquemard, U.; Branda, N. R. *Eur. J. Inorg. Chem.* **2002**, *2*, 357.

211. Sun, S-S.; Silva, A. S.; Brinn, I. M.; Lees, A. J. *Inorg. Chem*. **2000**, *39*, 1344.

212. Sun, S-S.; Lees, A. J. *Inorg. Chem.* **2001**, *40*, 3154.

213. Hutchison, K.; Morris, J. C.; Nile, T. A.; Walsh, J. L.; Thompson, D. W.; Petersen, J. D.; Schoonover, J. R. *Inorg. Chem*. **1999**, *38*, 2516.

214. Chichak, K.; Branda, N. R. *Chem. Commun*. **1999**, *6*, 523.

215. Metcalfe, C.; Spey, S.; Adams, H; Thomas, J. A. *Dalton Trans*. **2002**, 4732.

216. Jahug, Y.; Moon, S. W.; Thummel, R. P. *Bull. Kor. Chem. Soc.* **1997**, *18*, 174.

217. Indumathy, R.; Radhika, S.; Kanthimathi, M.; Weyhermuller, T.; Nair, B. U. *J. Inorg. Biochem*. **2007**, 434.

218. Masuhara, N.; Hayami, S.; Motokawa, N.; Shuto, A.; Inoue, K.; Maeda, Y. *Chem. Lett*. **2007**, 90.

219. Kurth, D. G.; Lopez, J. P.; Dong, W-F. *Chem. Commun*. **2005**, 2119.

220. Hayami, S.; Hashiguchi, K.; Juhasz, G.; Ohba, M.; Okawa, H.; Maeda, Y.; Kato, K.; Osaka, K.; Takata, M.; Inoue, K. *Inorg. Chem*. **2004**, *43*, 4124.

221. Priimov, G. U.; Moore, P.; Helm, L.; Merbach, A. E. *Inorg. React. Mech.* **2001**, *3*, 1.

222. Govindaswamy, P.; Kollipara, M. R. *J. Coord. Chem.* **2006**, *59*, 663.

223. Paul, J.; Spey, S.; Adams, H.; Thomas, J. A. *Inorg. Chim. Acta* **2004**, *357*, 2827.

224. Moya, S. A.; Pastene, R.; Pardey, A. J.; Baricelli, P. *Bol. Soc. Chil. Quim.* **1996**, *41*, 251.

225. Moya, S. A.; Pastene, R.; Sartori, R.; Dixneuf, P.; Le Bozec, H. Fac. *J. Braz. Chem. Soc*. **1995**, 29.

226. Priimov, G. U.; Moore, P. *Inorg. React. Mech*. **2003**, 5, 21.

227. Beves, J. E.; Constable, E. C.; Housecroft, C. E.; Neuburger, M.; Schaffner, S. *Inorg. Chem. Commun*. **2007**, *10*, 1185.

228. Noshiranzadeh, N.; Ramazani, A.; Morsali, A.; Hunter, A. D.; Zeller, M. *Inorg. Chim. Acta* **2007**, *360*, 3603.

229. Noshiranzadeh, N.; Ramazani, A.; Morsali, A.; Hunter, A. D.; Zeller, M. *Inorg. Chem. Commun*. **2007**, *10*, 738.

230. Lopez, J. P.; Kraus, W.; Reck, G.; Thuenemann, A.; Kurth, D. G. *Inorg. Chem. Commun.* **2005**, *8*, 281.
231. Zhang, S-S.; Zhan, S-Z.; Li, M.; Peng, R.; Li, D. *Inorg. Chem* **2007**, *46*, 4365.
232. Hou, L.; Li, D.; Ng, S. W. *Acta Cryst.* **2004**, *E60*, m1734.
233. Zhang, C-F.; Huang, H-X.; Liu, B.; Chen, M.; Qian, D.-J. *J. Lumin.* **2008**, *128*, 469.
234. Granifo, J.; Garland, M. T.; Baggio, R. *Inorg. Chem. Commun*. **2004**, *7*, 77.
235. Liu, B.; Huang, H-X.; Zhang, C-F.; Chen, M.; Qian, D-J. *Thin Solid Films* **2008**, *516*, 2144.
236. Constable, E. C.; Housecroft, C. E.; Thompson, A. C.; Passaniti, P.; Silvi, S.; Maestri, M.; Credi, A. *Inorg. Chim. Acta* **2007**, *360*, 1102.
237. Evans, I. P.; Spencer, A.; Wilkinson, G. *J. Chem. Soc., Dalton Trans.* **1973**, 205.
238. Sheldrick, G. M. SADABS, University of Göttingen, Göttingen, Germany, (**1996**).
239. SMART and SAINT, Siemens Analytical X-ray Instruments Inc., Madison, WI, (**1996**).
240. Sheldrick, G. M. SHELXS-97 and SHELXL-97, University of Göttingen, Göttingen, Germany, (**1997**).
241. Nakamoto, K. *Infrared and Raman Spectra of Inorganic and Coordination Compounds*. Part B, fifth ed., Wiley, New York, **1997**.
242. Folgado, J. V.; Martinez-Tamayo, E.; Beltran-Porter, A.; Beltran-Porter, D.; Fuertes, A.; Miravitlles, C. *Polyhedron* **1989**, *8*, 1077.
243. Lever, A. B. P. *Inorganic Electronic Spectroscopy*, Elsevier, Amsterdam, **1986**.
244. Drago, R. S. *Physical Methods for Chemists*, 2nd ed., Saunders College Publishers, New York, **1992**.
245. Hathaway, B. J.; Billing, D. E. *Coord. Chem Rev*. **1970**, *5*, 143.
246. Figgins, P. E.; Busch, D. H. *J. Phys. Chem.* **1961**, *65*, 2236.
247. O'Connor, C. J. *Prog. Inorg. Chem*. **1982**, *29*, 203.
248. Kahn, O. *Molecular Magnetism*, Wiley-VCH, **1993**.

249. Arcon, D.; Prassides, K. *Structure and Bonding*, *vol. 100*, Springer, Berlin, **2001**, p. 129.

250. Tubbs, K. J.; Szajna, E.; Bennet, B.; Halfen, J. A.; Watkins, R. W.; Arif, A. M.; Berreau, L. M. *J. Chem. Soc., Dalton Trans*. **2004**, 2398.

251. Cockle, S. A. *J. Biochem*. **1974**, *137*, 587.

252. Chandra, S.; Gupta, L. K. *Spectrochim. Acta: A* **2005**, *62*, 1102.

253. Arulsamy, N.; Hodgson, D. J. *Inorg. Chem.* **1994**, *33*, 4531.

254. Adams, H.; Shongwe, M. S.; Al-Bahri, I.; Al-Busaidi, E.; Morris, M. J. *Acta Cryst*. **2005**, *C61*, m497.

255. Field, J. S.; Haines,R. J.; Jr., L. P. Ledwaba; McGuire,R.; Murno, O. Q.; Low, M. R.; McMillin, D. R. *Dalton Trans.* **2007**, 192.

256. Moore, J. J.; Nash, J. J.; Fanwick, P. E.; McMillin, D. R. *Inorg. Chem.* **2002**, *41*, 6387.

257. Yersin, H.; Donges, D. *Top. Curr. Chem*. **2001**, 81.

258. DeArmond, M. K.; Hills, J. E.; *J. Chem. Phys*., **1971**, *54*, 2247.

259. Rivera, E. J.; Figueroa, C.; Colón, J. L.; Grove, L. J.; Connick, W. B. *Inorg. Chem*. **2007**, *46*, 8569.

260. Baidya, N.; Olmstead, M.; Mascharak, P. K. *Inorg. Chem*. **1991**, *30*, 929.

261. Champouret, Y. D. M.; Maŕechal, J.-D.; Dadhiwala, I.; Fawcett, J.; Palmer, D.; Singh, K.; Solan, G. A. *Dalton Trans*. **2006**, 2350.

262. Cortes, R.; Arriortua, M. I.; Rojo, T.; Solanst, X.; Beltran, D. *Polyhedron* **1986**, *5*, 1987.

263. Calatayud, M. L.; Sletten, J.; Julve, M.; Castro, I. *J. Mol. Struct.* **2005**, *741*, 121.

264. Constable, E. C.; Phillips, D.; Raithby, P. R. *Inorg. Chem. Commun*. **2002**, *5*, 519.

265. Baggio, R.; Garland, M. T.; Perec, M. *Inorg. Chim. Acta*, **2000**, *310*, 103.

266. Manzano, B. R.; Jalon, F. A.; Ortiz, I. M.; Soriano, M. L.; Gomez de la Torre, F.; Elguero, J.; Maestro, M. A.; Mereiter, K.; Claridge, T. D. W. *Inorg. Chem.* **2008**, *47*, 413.

267. Childs, B. J.; Craig, D. C.; Scudder, M. L.; Goodwin, H. A. *Aust. J. Chem.*, **1999**, *52*, 673.

268. Baker, A. T.; Craig, D. C.; Rae, A. D. *Aust. J. Chem.*, **1995**, *48*, 1373.

269. Cortes, R.; Lezama, L.; Larramendi, J. I. R.; Insausti, M.; Folgado, J. V.; Madariagab, G.; Rojo, T. *J. Chem. Soc. Dalton Trans*. **1994**, 2573.

270. Priimov, G. U.; Moore, P.; Maritim, P. K.; Butalanyi, P. K.; Alcock, N. W. *J. Chem. Soc., Dalton Trans*. **2000**, 445.

271. Alonso, C.; Ballester, L.; Gutiérrez, A.; Perpiñán, M. F.; Sánchez, A. E.; Azcondo, M. T. *Eur. J. Inorg. Chem.* **2005**, 486.

272. Constable, E. C.; Lewis, J.; Liptrot, M. C.; Raithby, P. R. *Inorg. Chim. Acta*, **1990**, *178*, 47.

273. Zaccheddu, M.; Filippi, C.; Buda, F. *J. Phy. Chem. A* **2008**, *112*, 1627.

274. Krumholz, P. *Inorg. Chem.* **1964**, *4*, 612.

275. Braterman, P. S.; Song, J-I. *Inorg. Chem.***1991**, *31*, 555.

276. Ruminski, R. R.; Petersen, J. D. *Inorg. Chim. Acta*, **1985**, *97*, 129.

277. Holland, J. M.; McAllister,J. A.; Kilner, C. A.; Thornton-Pett, M.; Bridgeman, A. J.; Halcrow, M. A. *J. Chem. Soc*., *Dalton Trans*., **2002**, 548.

278. Elhaïk, J.; Money, V. A.; Barrett, S. A.; Kilner, C. A.; Evans; I. R.; Halcrow, M. A. *Dalton Trans*., **2003**, 2053.

279. Money, V. A.; Elhaïk, J.; Evans; I. R.; Halcrow, M. A.; Howard, J. A. K. *Dalton Trans*., **2004**, 65.

280. Money, V. A.; Elhaïk, J.; Halcrow, M. A.; Howard, J. A. K. *Dalton Trans*., **2004**, 1516.

281. Schottel, B. L.; Chifotides, H. T.; Dunbar, K. R. *Chem. Soc. Rev.* **2008**, *37*, 68.

282. Hay, B. P.; Bryantsev, V. S. *Chem. Commun* .**2008**, 2417.

283. Papoian, G. A.; Ulander, J.; Eastwood, M. P.; Luthey-Schulten, Z.; Wolynes, P. G. *Proc. Natl. Acad. Sci. U. S. A.* **2004**, *101*, 3352.

284. Yoshizawa, M.; Kusukawa, T.; Kawano, M.; Ohhara, T.; Tanaka, I.; Kurihara, K.; Niimura, N.; Fujita, M. *J. Am. Chem. Soc.* **2005**, *127*, 2798.

285. Butchard, J. R.; Curnow, O. J.; Garrett, D. J.; Maclagan, R. *Angew. Chem. Int. Ed.* **2006**, *45*, 7550.

286. Thallapally, P. K.; Lloyd, G. O.; Atwood, J. L.; Barbour, L. J. *Angew. Chem., Int. Ed.* **2005**, *44*, 3848.

287. Lakshminarayanan, P. S.; Suresh, E.; Ghosh, P. *Angew. Chem., Int. Ed.* **2006**, *45*, 3807.

288. Yuge, T.; Tohnai, N.; Fukuda, T.; Hisaki, I.; Miyata, M. *Chem. Eur. J.* **2007**, *13*, 4163.

289. Oxtoby, N. S.; Blake, A. J.; Champness, N. R.; Wilson, C. *Chem. Eur. J.* **2005**, *11*, 4643.

290. Sansam, B. C. R.; Anderson, K. M.; Steed, J. W. *Cryst. Growth Des.* **2007**, *7*, 2649.

291. Kang, S. O.; Powell, D.; Day, V. W.; Bowman-James, K. *Cryst. Growth Des.* **2007**, *7*, 606.

292. Shi, X. F.; Zhang, W. Q. *Cryst. Growth Des.* **2007**, *7*, 595.

293. Stahly, G. P. *Cryst. Growth Des.* **2007**, *7*, 1007.

294. Jiang, G. Q.; Bai, J. F.; Xing, H.; Li, Y. Z.; You, X. Z. *Cryst. Growth Des.* **2006**, *6*, 1264.

295. Upreti, S.; Datta, A.; Ramanan, A. *Cryst. Growth Des.* **2007**, *7*, 966.

296. Karabach, Y. Y.; Kirillov, A. M.; da Silva, M.; Kopylovich, M. N.; Pombeiro, A. J. L. *Cryst. Growth Des.* **2006**, *6*, 2200.

297. Infantes, L.; Motherwell, S. *CrystEngComm* **2002**, *4*, 454.

298. Bond, A. D. *CrystEngComm* **2007**, *9*, 833.

299. Infantes, L.; Fabian, L.; Motherwell, W. D. S. *CrystEngComm* **2007**, *9*, 65.

300. Jin, Y.; Che, Y. X.; Batten, S. R.; Chen, P.; Zheng, J. M. *Eur. J. Inorg. Chem.* **2007**, 1925.

301. N. K. Keutsch, R. J. Saykally, *Proc. Natl. Acad. Sci. USA* **2001**, *98*, 10533.

302. Raghuraman,K.; Katti, K. K.; Barbour, L. J.; Pillarsetty, N.; Barnes, C. L.; Katti, K. V. *J. Am. Chem. Soc*. **2003**, *125*, 6955.

303. Lakshminarayanan, P. S.; Suresh, E.; Ghosh, P.; *J. Am. Chem. Soc*. **2005**, *127*, 13132.

304. Zuhayra, M.; Kampen, W. U.; Henze, E.; Soti, Z.; Zsolnai, L.; Huttner, G.; Oberdorfer, F. *J. Am. Chem. Soc*. **2006**, *128*, 424.

305. Janiak, C.; Scharmann, T. G.; Mason, S. A. *J. Am. Chem. Soc*. **2002**, *124*, 14010.

306. MacGillivray, L. R.; Atwood, J. L. *J. Am. Chem. Soc*. **1997**, *119*, 2592.

307. Blanton, W. B.; Gordon-Wylie, S. W.; Clark, G. R.; Jordon, K. D.; Wood, J. T.; Geiser, U.; Collins, T. J. *J. Am. Chem. Soc*. **1999**, *121*, 3551.

308. Atwood, J. L.; Barbour, L. J.; Ness, T. J.; Raston, C. L.; Raston, P. L. *J. Am. Chem. Soc*. **2001**, *123*, 7192.

309. Ludwig, R. *Angew. Chem. Int. Ed.* **2001**, *40*, 1808.

310. Ugalde, J. M.; Alkorta, I.; Elguero, J. *Angew. Chem. Int. Ed.* **2000**, *39*, 717.

311. Ghosh, S. K.; Bharadwaj, P. K. *Inorg. Chem*. **2004**, *43*, 5180.

312. Moorthy, J. N.; Natarajan, R.; Venugopalan, P. *Angew. Chem. Int. Ed*. **2002**, *41*, 3417.

313. Custelcean, R.; Afloroaei, C.; Vlassa, M.; Polverejan, M. *Angew. Chem. Int. Ed*. **2000**, *39*, 3094.

314. Ma, B.-Q.; Sun, H.-L.; Gao, S. *Angew. Chem. Int. Ed*. **2004**, *43*, 1374.

315. Rodriguez-Cuamatzi, P.; Vargas-Diaz, G.; Höpfl, H. *Angew. Chem. Int. Ed*. **2004**, *43*, 3041.

316. Sreenivasulu, B.; Vittal, J. J. *Angew. Chem. Int. Ed*. **2004**, *43*, 5769.

317. Ghosh, S. K.; Ribas, J.; Fallah, M. S. E.; Bharadwaj, P. K. *Inorg. Chem*. **2005**, *44*, 3856.

318. Ghosh, S. K.; Bharadwaj, P. K. *Inorg. Chem*. **2005**, *44*, 5553.

319. Lakshminarayanan, P. S.; Kumar, D. K.; Ghosh, P. *Inorg. Chem*. **2005**, *44*, 7540.

320. Henry, M.; Taulelle, F.; Loiseau, T.; Beitone, L.; Férey, G. *Chem. Eur. J.* **2004**, *10*, 1366.
321. Liu, Q.-Y.; Xu, L. *CrystEngComm* **2005**, *7*, 87.
322. Infantes, L.; Chisholm, J.; Motherwell, S. *CrystEngComm* **2003**, *5*, 480.
323. Ma, B.-Q.; Sun, H.-L.; Gao, S. *Chem. Commun*. **2005**, 2336.
324. Ma, B.-Q.; Sun, H.-L.; Gao, S. *Chem. Commun*. **2004**, 2220.
325. Doedens, R. J.; Yohannes, E.; Khan, M. I. *Chem. Commun*. **2002**, 62.
326. Barbour, L. J.; Orr, G.W.; Atwood, J. L. *Chem. Commun*. **2000**, 859.
327. Henry, M. *ChemPhysChem* **2002**, *3*, 607.
328. Weinhold, F. *J. Chem. Phys*. **1998**, *109*, 367.
329. Supriya, S.; Manikumari, S.; Raghavaiah, P.; Das, S. K. *New J. Chem.* **2003**, *27*, 218.

List of Publications

1. Padhi, S. K.; Manivannan, V. *Inorg. Chem.* **2006**, *45*, 7994-7996.
2. Padhi, S. K.; Manivannan, V. *Polyhedron*, **2007**, *26*, 1619-1624.
3. Padhi, S. K.; Manivannan, V. *Polyhedron*, **2007**, *26*, 3092-3096.
4. Padhi, S. K.; Sahu, R.; Manivannan, V. *Polyhedron*, **2008**, *27*, 805-811.
5. Padhi, S. K.; Saha, D.; Sahu, R.; Subramanian, J.; Manivannan, V. *Polyhedron*, **2008**, *27*, 1714-1720.
6. Padhi, S. K.; Sahu, R.; Manivannan, V. *Polyhedron,* **2008**, *27*, 2221-2225.